Final Report to

NAVAL TRAINING SYSTEMS CENTER
12350 Research Parkway
Orlando, FL 32826-3224

DISPLAY PROJECTOR TECHNOLOGY

VIA SINGLE CRYSTAL FACEPLATE TECHNOLOGY

Contract N61339-91-C-0052

Presented to: Richard Hebb, Code 253

Prepared by:

TRIDENT INTERNATIONAL, INC.
Central Florida Research Park
32511 D Progress Drive
Orlando, FL 32826
407-282-3344
Fax 407-282-3343

September, 1993

Table of Contents

SECURITY CLASSIFICATION OF THIS PAGE

REPORT DOCUMENTATION PAGE

1a. REPORT SECURITY CLASSIFICATION Unclassified	1b. RESTRICTIVE MARKINGS
2a. SECURITY CLASSIFICATION AUTHORITY	3. DISTRIBUTION/AVAILABILITY OF REPORT Approved for Public Release Distribution is Unlimited
2b. DECLASSIFICATION/DOWNGRADING SCHEDULE	
4. PERFORMING ORGANIZATION REPORT NUMBER(S)	5. MONITORING ORGANIZATION REPORT NUMBER(S)
6a. NAME OF PERFORMING ORGANIZATION Trident International, Inc. 6b. OFFICE SYMBOL (If applicable)	7a. NAME OF MONITORING ORGANIZATION Naval Training Systems Center Sensor Simulation Branch, Code 263
6c. ADDRESS (City, State, and ZIP Code) 3251 D Progress Drive Orlando, FL 32826	7b. ADDRESS (City, State, and ZIP Code) 12350 Research Parkway Orlando, FL 32826-3224
8a. NAME OF FUNDING/SPONSORING ORGANIZATION Naval Air Systems Command 8b. OFFICE SYMBOL (If applicable)	9. PROCUREMENT INSTRUMENT IDENTIFICATION NUMBER N61339-91-C-0052
8c. ADDRESS (City, State, and ZIP Code)	10. SOURCE OF FUNDING NUMBERS PROGRAM ELEMENT NO. / PROJECT NO. / TASK NO / WORK UNIT ACCESSION NO.

11. TITLE (Include Security Classification)
Display Projector Technology via Single Crystal Faceplate Technology

12. PERSONAL AUTHOR(S)
Tucker, A. and Kindl, H. J.

13a. TYPE OF REPORT	13b. TIME COVERED	14. DATE OF REPORT (Year, Month, Day)	15. PAGE COUNT
Final	FROM Nov. 90 TO Aug. 93	93 September 29	

16. SUPPLEMENTARY NOTATION
Final Report Single Crystal Faceplate Evaluation

17. COSATI CODES			18. SUBJECT TERMS (Continue on reverse if necessary and identify by block number)
FIELD	GROUP	SUB-GROUP	Video Projectors, Single Crystal Phosphor, CRTs, Flight Simulators

19. ABSTRACT (Continue on reverse if necessary and identify by block number) Single crystal phosphor faceplates are epitaxial phosphors grown on crystalline substrates with the potential for high light output, resolution and extended operational life. Single crystal phosphor faceplate industrial technology in the United States is capable of providing faceplates appropriate to the projection industry up to four (4) inches in diameter.

This contract continued the evaluation of the use of single crystal phosphor faceplates integrated into CRTs and incorporated into projection display systems. Previous government contractual evaluation of 3" SCFP CRTs (green) lent encouragement to the potential for development of red and blue single crystal faceplate based CRTs; thus, forming the basis for fabrication of a high brightness, long life projection display system for use in government flight simulators.

While satisfactory spectral responses were attained for the red and blue colors, mechanical assembly problems with Ce:Bel (blue) precludes its use as a light source.

Abstract continued on reverse side -

20. DISTRIBUTION/AVAILABILITY OF ABSTRACT ☐ UNCLASSIFIED/UNLIMITED ☒ SAME AS RPT. ☐ DTIC USERS	21. ABSTRACT SECURITY CLASSIFICATION Unclassified
22a. NAME OF RESPONSIBLE INDIVIDUAL Richard C. Hebb, Code 263	22b. TELEPHONE (Include Area Code) 407-280-4578 22c. OFFICE SYMBOL NTSC/Code 253

DD FORM 1473, 84 MAR 83 APR edition may be used until exhausted. All other editions are obsolete

Unclassified
SECURITY CLASSIFICATION OF THIS PAGE

★U.S. Government Printing Office: 1985-607-047

1.0 Introduction

Three single crystal faceplates were to be integrated into Cathode Ray Tube (CRT) envelopes with the intent of evaluating the light output from Ce:YAG (Green), modified Ce:Gd,YAG (Orange), Ce:BEL (Blue). These CRT's were to be mounted in the projection test bed developed under Contract N61339-90-C-0047 and furnished G.F.P. to Trident International, Inc. for use and delivery during this contract.

Three 3 inch diameter Ce:YAG faceplates were supplied as GFP from previous contract N61339-90-C-0047. One of these three was to be used for construction of a CRT, the remaining two were to be used for coating tests. During the processing of the CRT's one of the crystals was destroyed. The other two single crystal faceplates were incorporated in test CRT's. An additional Ce:Gd,YAG (Red shifted green) faceplate of 1.5 inches diameter and two Ce:BEL (Blue) crystals of 0.75 inch diameter were obtained from Allied Signal, Inc. by Trident.

Investigations were made to provide optimum optical coupling of the CRT light output into a projection lens. Index matching heat dissipation fluids were used. A wide angle lens was selected and supplied by the contractor. Filtering of the light output of the Ce:YAG, Ce:Gd,YAG and Ce:BEL faceplates was investigated for use in producing green, red and blue light outputs suitable for a full color video projector.

The green (Ce:YAG) and the red shifted (Ce:Gd,YAG) single crystal CRTs were tested, evaluated and demonstrated in the high performance video projection test bed developed under contract N61339-90-C-0047. The blue (Ce:BEL) crystal was not incorporated into a CRT successfully, but tests were performed on them (Ce:BEL) in a demountable vacuum chamber and with an ultraviolet laser to indicate efficiency (lumens/watt) and color spectrum emission. The projection testbed will be delivered with one green (Ce:YAG) 3" CRT installed.

2.0 Background

Under contract 61339-90-C-0047 an evaluation of single crystal faceplate performance when mounted (integrated) on a cathode ray tube was completed.

Delays in the assembly of the CRTs were encountered; however, initial test results were sufficiently encouraging to warrant proceeding with and evaluating equivalent red and blue faceplates with the goal of generating a full color projected picture. The data obtained was to establish the feasibility of producing a high brightness, long life video projection system for government simulator applications.

The construction of two 3" diameter green (Ce:YAG) CRT's by Hughes Display Products allowed Trident to perform tests on these units under various conditions. Early in the test program cooling was deemed necessary to produce the brightness goals desired. A liquid cooling chamber was designed and adapted to the CRT.

Problems with sealing the SCFP's to the glass proved to be troublesome and were not solved with the Ce:BEL (Blue) crystal material.

Ce:YAG was modified to red shift its spectral luminescence in the form of a 1.5" CRT. The test bed projector was used to evaluate these CRT's.

3.0 Objectives

3.1 Fabrication of red and blue single crystal faceplate cathode ray tubes.

3.2 To evaluate interference coatings to improve optical transmission and anti-reflection capabilities.

3.3 To test filters to shift and utilize the desired spectral output of the crystal faceplates to produce color images.

3.4 To test light output and resolution obtainable from projection test bed developed under Contract 61339-90-C-0047.

3.5 To deliver test bed and remaining CRTs.

4.0 Manufacturing Attempts and Test of Ce:BEL (Blue)

Three Ce:BEL crystal faceplates were made by Allied Signal Corp. for Trident International, Inc. in small 3/4" diameter x .1" thickness. Two Ce:BEL crystals were delivered to Hughes Display Products to assemble in a working CRT for testing by Trident. On 15 June 93 Trident was notified that the first CRT utilizing the Ce:BEL faceplate had failed. It is very difficult to frit seal the small (3/4") Ce:BEL crystal to the larger glass bulb and appears to be impractical. The fractured pieces were mailed to Trident for evaluation. Trident utilized a 2 watt argon laser to perform tests on the fractured Ce:BEL crystal pieces to determine the color temperature and destructibility of the material. Although the laser was capable of reaching very high spot power densities, no noticeable change occurred in the crystal. The color of the light output on the chromatic scale was X=.150, Y=.130. Allied Signal Corp. agreed to deliver Trident one remaining Ce:BEL crystal. It was then decided, because the power density of the laser in comparison with electron beam power could not be readily correlated, to ask Thomas Electronics, Inc. to mount the crystal in their demountable vacuum chamber for testing.

Mr. Thomas St. John and Mr. A. R. Tucker of Trident International, Inc. traveled to Thomas Electronics' facility in Wayne, NJ to run the tests. Thomas Electronics was very cooperative and aluminized the Ce:BEL crystal and placed it in the chamber. Testing revealed the crystal in the vacuum could not dissipate the heat and rapid thermal saturation became immediately apparent. The crystal was allowed to cool for 80 minutes and retested in short current applications allowing the Ce:BEL to cool between measurements. The results indicate that the high temperatures reached in the first attempt did no damage to the crystal.

The test set-up at Thomas was capable of 28 kv @ .600 ma. The crystal had to be held by two clips in the vacuum chamber which apparently caused asymmetrical heat conduction. The crystal broke during a power application of 28 kv @ .450 ma. It was noted that the aluminization was being precipitated off the crystal at those power levels and temperatures. Light outputs projected by Allied Signal, Inc. of up to 1.2 lumens per watt could not be verified.

It has not been determined if the Ce:BEL is the desired chemical composition to produce the optimum blue faceplate at this time. It has not been determined if the CE:BEL can be grown in large enough crystals to be useful or if the structure is stable enough to withstand the mechanical and thermal stresses. The expansion coefficient of Ce:BEL (blue) crystal has not been measured adequately and attempts to seal with gradient frit-to-glass techniques have not been successful to date.

Several attempts have been made to frit seal bond the Ce:BEL (Blue) faceplate onto a ceramic ring which is itself bonded to the glass bulb. On each occasion an apparent expansion rate mismatch occurs between the Ce:BEL faceplate and the ceramic ring.

In order to accelerate the Ce:BEL SCFP evaluation we attempted to replace the frit seal area with a vacuum grade epoxy (Torr Seal epoxy made by Varian Company). The advantage of using this epoxy is that it removes the expansion rate mismatch differentials by joining at room temperature, not 450 degrees C. This material is used for vacuum applications at 10% Torr and below. It is bakeable to 150 degrees C and has a dielectric strength compatible to the frit it replaces. The expansion rate of the Torr Seal epoxy is significantly different from the expansion rate of the Ce:BEL faceplate and ceramic ring; but, joining and operation of these parts at room temperature eliminates the development of thermally induced expansion stresses. The remaining Ce:BEL: crystal fractured before this seal could be tried. No successful blue (Ce:BEL) CRT was made.

5.0 Tests of Blue Single Crystal Faceplates

The cathodoluminescence of Ce:BEL was characterized in a thin wafer of a Czochralski boule prepared from a melt of 0.5% cerium content. Ce:BEL proved to be an excellent blue phosphor with a peak fluorescence at 485 nm and a fluorescence bandwidth of 80 nm (Fig. #1). Thus, there is significant light energy at the extremely blue wavelength, 445 nm. The measured cathodoluminescent efficiency of the available crystal was 0.1 lumen/watt, weighted according to the C.I.E. photoptic curve. It was found that annealing at 1150 degrees C in a reducing atmosphere of 10% hydrogen in argon doubles the efficiency of Ce:BEL to 0.2 lumens/watt (Fig. #2). Annealing also changes the appearance of the crystals from an orange color to transparent. It was also found that the light output of Ce:BEL does not saturate up to an electron beam power of 19 watt/cm squared if adequately cooled.

Mass spectroscopy of the CE:BEL crystal revealed a cerium content of 3.9 x 10 to the eighteenth power atoms/cc, as compared with 23 x 10 to the eighteenth power atoms/cc for YAG. If cerium content of CE:BEL can be increased to the level of cerium in YAG, this six-fold increase in concentration could increase the C.I.E. weighted efficiency of CE:BEL to 1.2 lumens/watt. Since the refractive indices of CE:BEL are about the same value as the refractive index of YAG, reticulation or stippling should yield an increase in external efficiency.

Attempts to incorporate Ce:BEL (Blue) .75" crystals failed by cracking during bakeout or shortly thereafter. No successful blue CRT has been constructed. Blue (CE:BEL) crystal fragments were placed in a vacuum demountable chamber at Thomas Electronics, Inc. and tested. The light output was an excellent blue (420 nm), but because the crystal could not be cooled in the vacuum chamber, saturation was rapidly reached. By pulsing the current and allowing the crystal to cool between tests additional data was obtained (See Figs. #3, 4 and 5).

Methods of matching the CE:BEL crystals' expansion coefficient with the frit seal to a glass envelope or possibly a metal to glass seal need to be tried. Ce:BEL (blue) efficiencies indicated by Allied Signal, Inc.s' study for Trident International, Inc. dated Feb. 1992,), Enclosure #12.1) indicate up to 1.2 lumens per watt are possible. Other blue generating phosphors need to be tested to fully evaluate their possibilities.

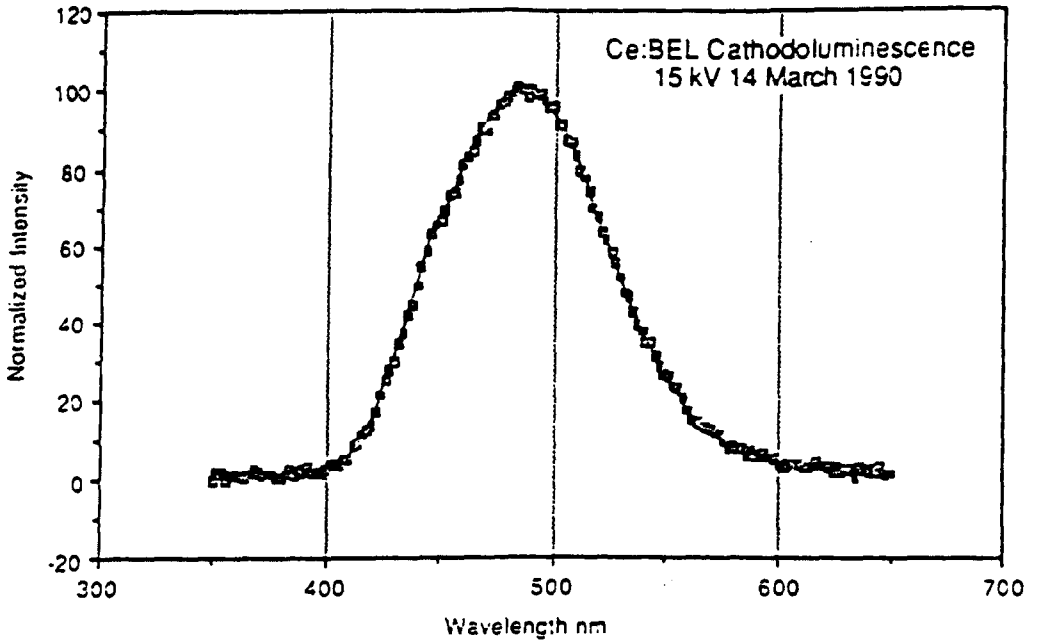

Fig. 1 Cathodoluminescence spectrum of Ce:BEL.

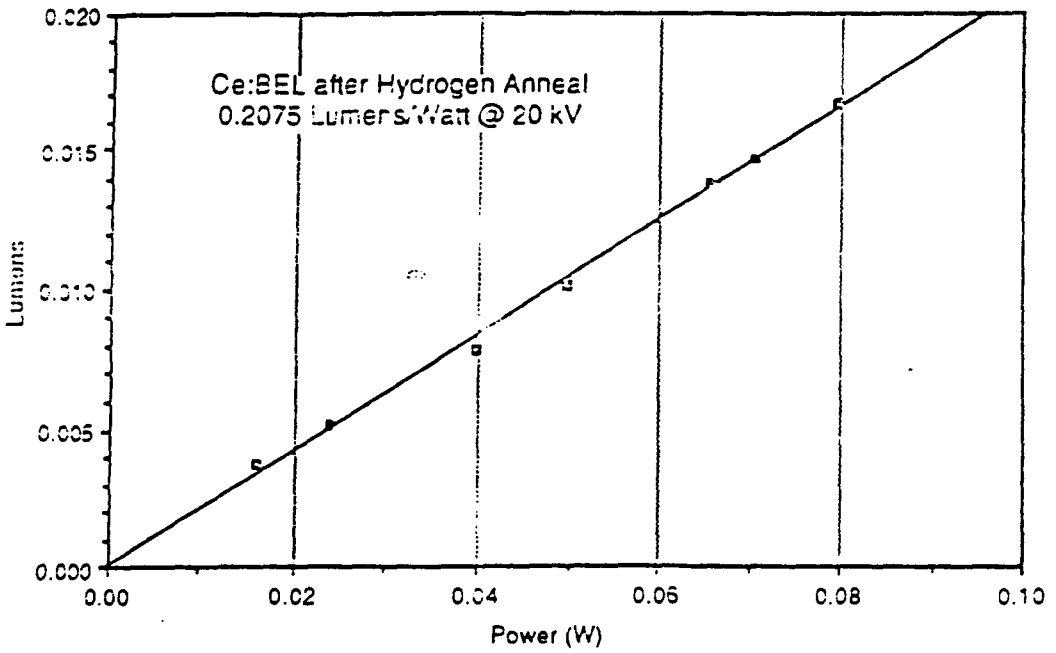

Fig. 2 Cathodoluminescent efficiency of Ce:BEL after hydrogen anneal.

CE: BEL
EPITAXIAL CRYSTAL TESTS
(UNMOUNTED)

June, 29, 1993
IMAGE SIZE (.5 X .5) INCHES

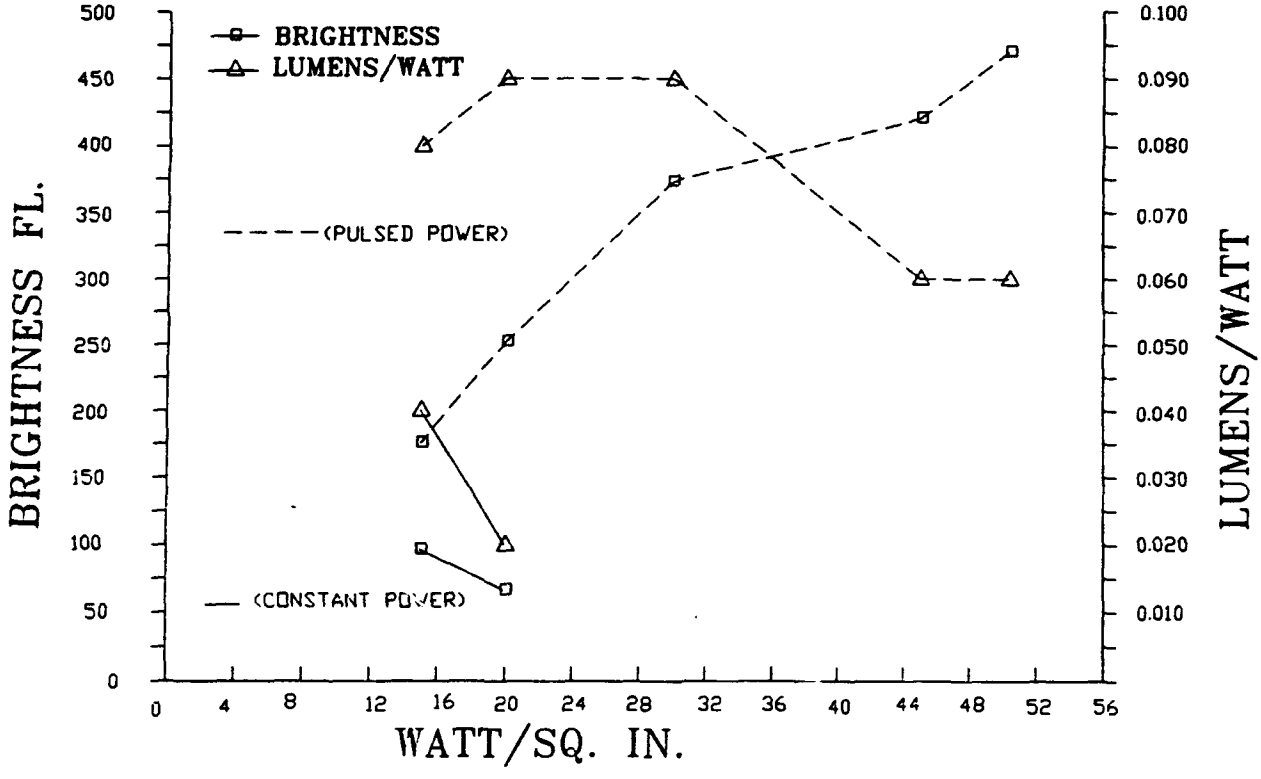

Figure 3

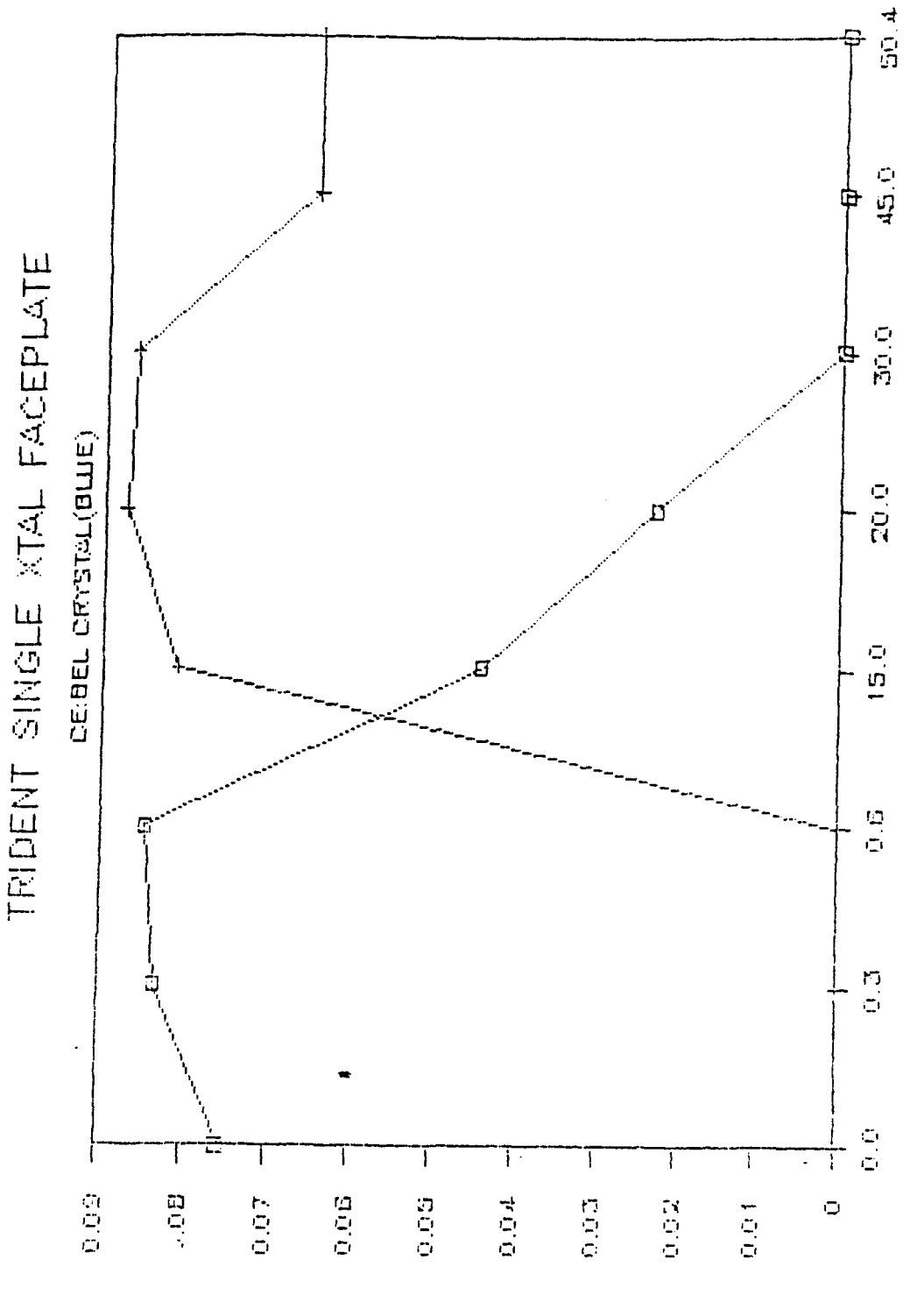
TRIDENT SINGLE XTAL FACEPLATE
CE:BEL CRYSTAL(BLUE)
LUMENS PER WATT
0.09
.08
0.07
0.06
0.05
0.04
0.03
0.02
0.01
0
0.0
0.3
0.6
15.0
20.0
30.0
45.0
50.4
WATTS/SQ.INCH
CONTINUOUS POWER
+ PULSED POWER

FIGURE 4

DATA TAKEN AT THOMAS ELECTRONICS, INC. FROM CE:BEL CRYSTALS

29-JUNE-93 CE.BEL CRYSTAL NO.2

CRYSTAL FACEPLATE(NOT MOUNTED)									
IMAGE SIZE(SQ.".5 X .5)	0.25	0.25	0.25	0.25	0.25	0.25	0.25	0.25	
IMAGE SIZE(SQ.CM.)	0.64	0.64	0.64	0.64	0.64	0.64	0.64	0.64	
SQ.FEET	0.0017	0.0017	0.0017	0.0017	0.0017	0.0017	0.0017	0.0017	
PHOSPHOR TYPE(COLOR)BLUE									
SCAN AREA,INCHES	.5 X.5	.5 X.5	.5 X.5	.5 X.5	.5 X.5	.5 X.5	.5 X.5	.5 X.5	
MOD.AREA(PEAK POWER) IMAGE SIZE(SQ.INCHES)TEST	0.250	0.250	0.250	0.250	0.250	0.250	0.250	0.250	
SQ.FEET,TEST	0.0017	0.0017	0.0017	0.0017	0.0017	0.0017	0.0017	0.0017	
COOLING (TEMP.F)	70								
HIGH VOLTAGE (KV.)	25	25	25	25	25	25	25	28	
BEAM CURRENT(AMPS.)TEST#1	0.007	0.05	0.1	0.15	0.2	0	0	0	
WATTS TO TARGET	0.175	1.25	2.5	3.75	5	0	0	0	
BEAM CURRENT(AMPS.)TEST#2	0	0	0	0.15	0.2	0.3	0.45	0.45	
WATTS TO TARGET	0	0	0	3.75	5	7.5	11.25	12.6	
SWEEP FREQ.	15750/30	15750/30	15750/30	15750/30	15750/30	15750/30	15750/30	15750/30	
SPOT SIZE(LINE WIDTH)	FOCUSED								
W/SQ.IN.	0.0	0.3	0.6	15.0	20.0	30.0	45.0	50.4	
BRIGHTNESS FL. TEST#1	7.60	60.0	122.0	96.0	66.0	0.0	0.0	0.0	(CRYSTAL OVERHEATED,SATURATED)
BRIGHTNESS FL. TEST#2	0	0	0	175	252	373	420	470	(PULSED POWER-UNTIL CRYSTAL CRACKED)
LIGHTOUTPUT(LUMENS)TEST#1	0.01	0.10	0.21	0.17	0.11	0.00	0.00	0.00	
LIGHTOUTPUT(LUMENS)TEST#2	0.00	0.00	0.00	0.30	0.44	0.65	0.73	0.82	
LUMENS PER WATT, TEST#1	0.08	0.00	0.08	0.04	0.02				
LUMENS PER WATT, TEST#2				0.08	0.09	0.09	0.06	0.06	(STARTED TO HEAT)

COMMENTS:

SAMPLE AL.LAYER EVAPORATING AS MORE POWER APPLIED
TEMP.OF CRYSTAL IN VACUUM CHAMBER MUST BE VERY HIGH
NO WAY OF MEASURING
ALLOWED CRYSTAL TO COOL 80 MIN.THEN PULSED CURRENT TO CRYSTAL
TO SEE EFFECT OF THERMAL QUENCHING.(SEE GRAPH)

Ce:BEL Test Data
Refer to paragraph "A"

Figure 5

6.0 Tests of Red Single Crystal Faceplates

The fluorescent spectrum of cerium in single crystal faceplates may be shifted toward the red from the green by incorporating gadolinium and grown to Ce:(Y,Gd) on YAG. The spectral peak is approximately 50 um toward the red (580 um) compared to 535 um of green Ce:YAG. LIght output at the desired red peak of 650 um is 31% of the spectral peak compared to 19% for Ce:YAG. Using absorption filters such as Schott OG 570 (See Fig. #6) will produce adequate red energy to generate the 29% of total energy of white to produce a white image. A 1.5" SCFP CRT was manufactured by Hughes Display Products from crystals furnished by Trident International, Inc. grown by Allied Signal, Inc. This CRT was tested by Trident International, Inc. The test results as shown in Figs. #7, 8 and 9). The CRT failed during tests, but sufficient data was obtained to determine its relative efficiency and color spectrum. The failure was not related to the crystal composition and the CRT construction techniques developed in 3" green Ce:YAG faceplates and successfully integrated onto a CRT will be used in further manufacturing.

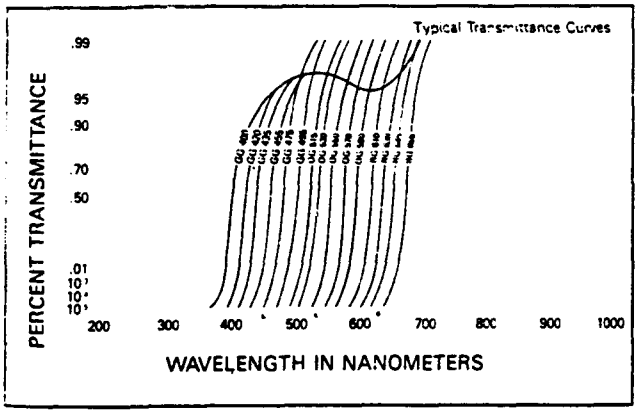

Yellow, Orange and Red Sharp Cut-Off Glass Filters

Schott Glass Type	$\frac{\Delta\lambda}{\Delta T}$	Correction Factor (t_1/t_2)	PRODUCT NUMBER
GG 400	0.07	0.91	03 FCG 057
GG 420	0.07	0.91	03 FCG 059
GG 435	0.07	0.91	03 FCG 061
GG 455	0.08	0.915	03 FCG 063
GG 475	0.09	0.915	03 FCG 065
GG 495	0.10	0.915	03 FCG 067
OG 515	0.11	0.915	03 FCG 083
OG 530	0.12	0.915	03 FCG 085
OG 550	0.13	0.915	03 FCG 087
OG 570	0.14	0.915	03 FCG 089
OG 590	0.15	0.915	03 FCG 098
RG 610	0.16	0.915	03 FCG 101
RG 630	0.17	0.915	03 FCG 103
RG 645	0.17	0.915	03 FCG 105
RG 665	0.17	0.915	03 FCG 107

$\frac{\Delta\lambda}{\Delta T}$ is the temperature coefficient of half-power point position shift, in nm/°C. See text.

Figure #6

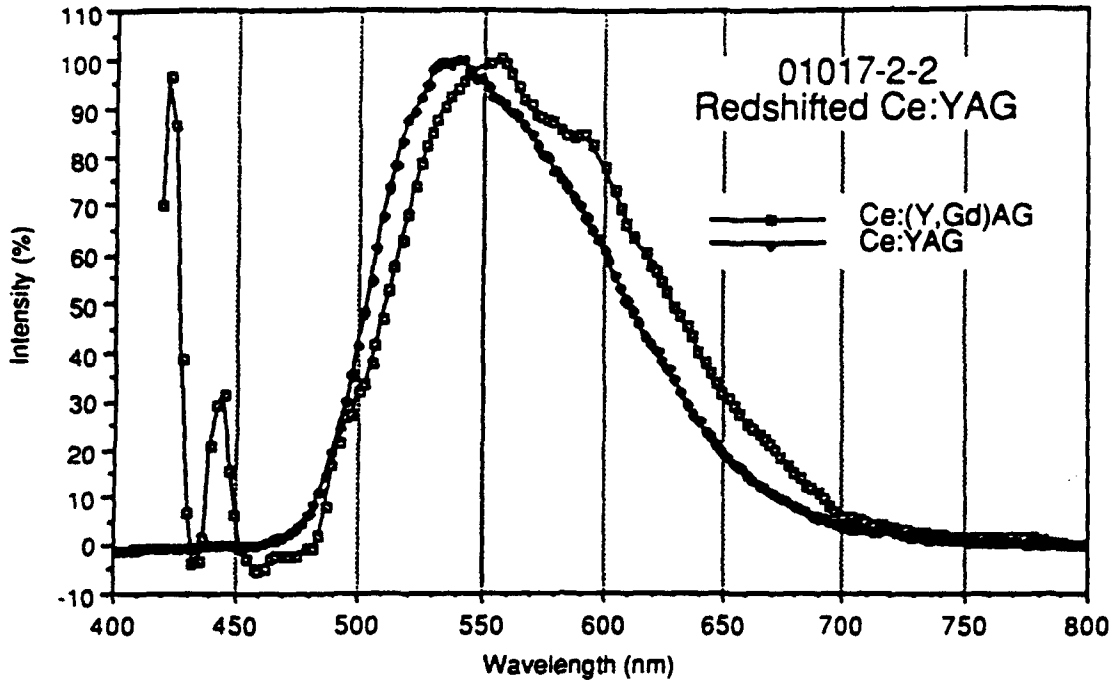

Fig. 7 Cathodoluminescent spectrum of a Ce:$Y_2Gd_1Al_5O_{12}$ phosphor layer grown on a YAG substrate.

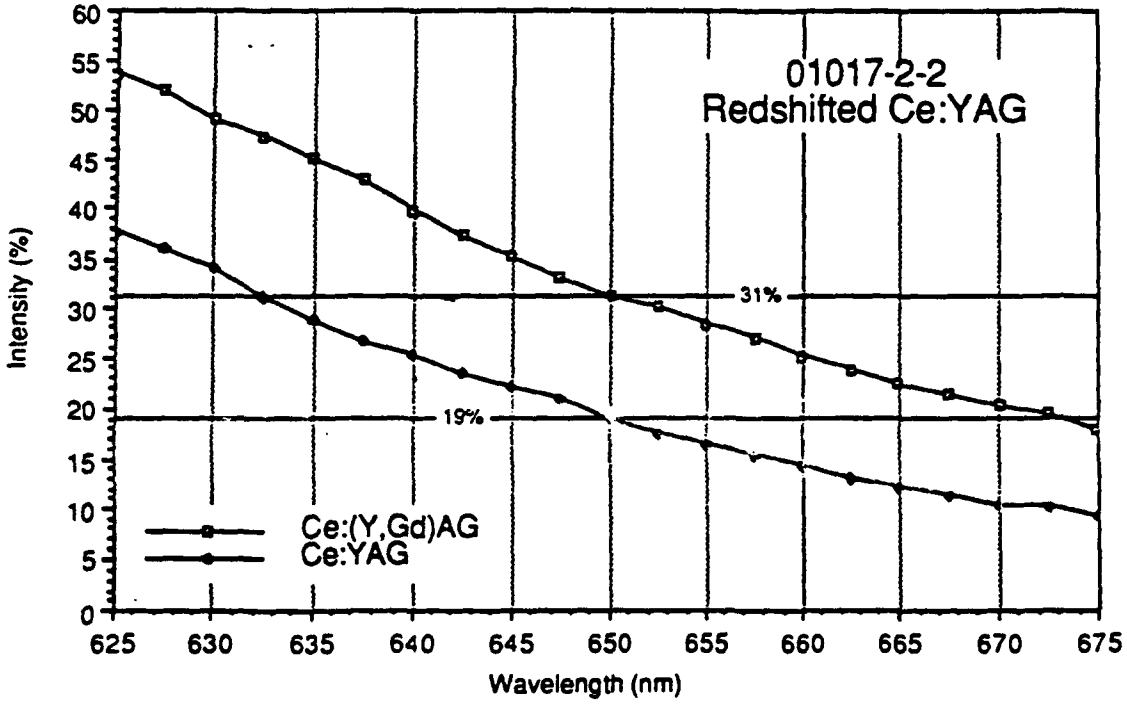

Fig. 8 Cathodoluminescent spectrum (detail) of a Ce:$Y_2Gd_1Al_5O_{12}$ phosphor layer grown on a YAG substrate.

Red Shifted Ce:Y,Gd,YAG 1.5" Single Crystal Faceplate CRT
#11-114-2-1 Test Date 17 August 1992

Raster Size .6417 sq in (.9055" X .7087")
Aluminized, Non-Reticulated

High Volt (KV)	Beam "I" (ma)	Light Output (fl)	Power (W)	Lumens	L/W	Coolant Temp o/F
30.28	.048	269	1.45	1.1987	.82	78
30.34	.051	304	1.547	1.3547	.87	78
30.34	.055	359	1.67	1.6	.96	78
30.35	.062	465	1.88	2.0	1.1	78
30.36	.085	786	2.58	3.5	1.36	78
30.36	.124	1294	3.76	5.76	1.53	78
30.37	.193	2190	5.86	9.76	1.66	78
30.38	.301	3540	9.14	15.77	1.72	78
30.38	.445	5310	13.5	23.66	1.75	78
30.39	.408	4980	12.4	22.2	1.79	78
30.42	.503	6170	15.32	27.5	1.79	79
30.42	.557	6780	16.97	30.16	1.78	79
30.43	.685	8050	20.95	35.9	1.71	81
30.43	.754	8700	12.00	38.77	1.68	82
30.44	.142	1600	4.30	7.13	1.65	82
30.47	.700	8200	21.00	36.54	1.74	83
30.46	1.08	11240	30.46	50.	1.64	83

Figure 9

7.0 Test Results of Deliverable Monochrome Projector (Green)

The raster lire width measurement was measured by projecting on a screen. The green (CE:YAG) SCFP projector had an HD6 (U.S. Precision, Inc.) wide angle lens installed and a square image projected. The image size on the SCFP CRT was 1.626" square. The projected image was 28.625".

$$\frac{28.625"}{1.626"} = 17.6 \text{ X magnification}$$

The line width at various beam currents and high voltages were measured. Faceplate brightness was taken using a Tektronix luminous probe J6523 1 degree spot brightness meter. The CRT brightness was measured through the lens looking at the CRT. This measurement does include all the losses of the lens, X-ray glass, fluid and YAG faceplate. Measurements were then taken at the screen. A standard magnesium flashed block was used at the screen surface to measure foot lamberts. The test results are shown in Figs. 10 through 13. Considerable crystal edge illumination was noted and also there was noticeable halation on the highlights. The test setup did not have liquid coupling to the lens but did have fluid to the X-ray window. The lens was coated for first surface reflections, but the X-ray window was not.

The graphs in Figures 10 and 11 were derived from data shown on Page 17, Figures 12 and 13. The test results shown by Figure 12 were run to measure spot (line width) growth at constant power with high voltage change. The line width decreased from .0046" to .0034" with high voltage increase from 20 kv to 30 kv indicating improved resolution possible with higher anode voltages. The line width measurements were taken by projecting the image on a screen to enable the individual scan lines to be observed. A micrometer was used to measure from skirt to skirt. Several lines were measured in the center of the image. This method will give larger line width readings than those normally quoted when a slit scanner is used. Measurements shown in Figure 13 were an attempt to verify losses through the optical system. Discrepancies occur because of the poor measurement ability in taking the faceplate brightness through the projection optics. The Tektronix one (1) degree spot brightness probe's subtense is not accurate under these conditions, but the screen measurements are correct.

Example pertaining to data in Figure 13:

The transmission should be as follows:

(HD6 lens .91)(X-ray glass .894)(Fluid .99) = Total .8054

F:1 lens efficiency .2

113.80 lu at the CRT face should generate 3.5 fl at the screen. (113.8)(.8054)(.2) = 18.60 divided by screen area 5.3166 sq.ft. = 3.5 fl.

CE: YAG SINGLE CRYSTAL FACEPLATE RESOLUTION (LINE WIDTH) VERSUS H.V. @ CONSTANT POWER

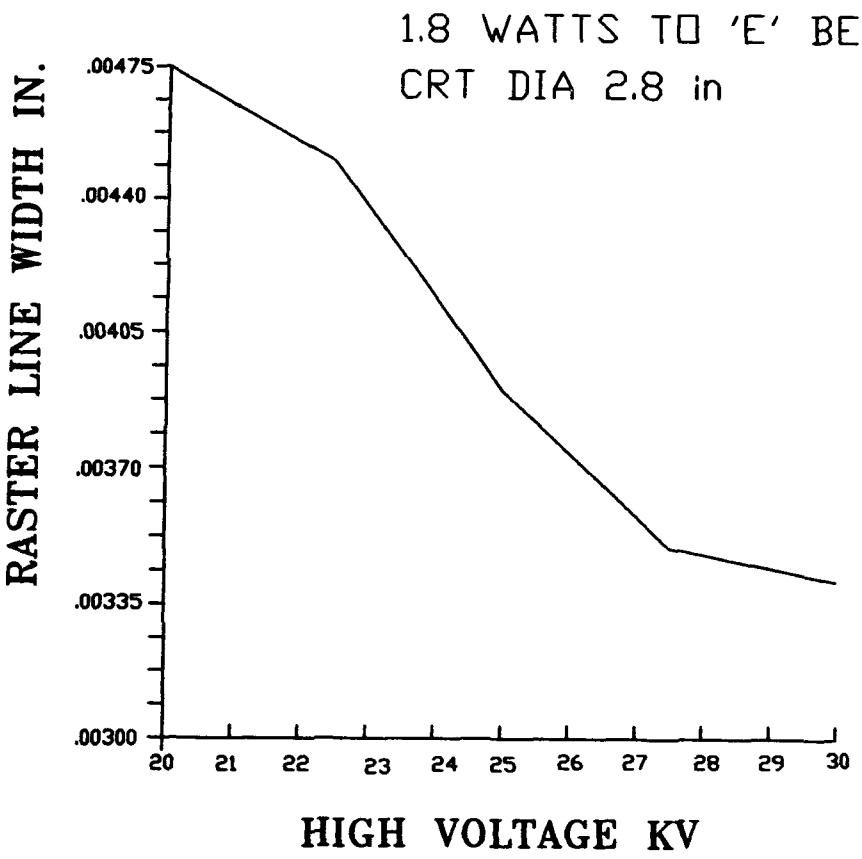

Figure 10

CE: YAG SINGLE CRYSTAL FACEPLATE CRT MOUNTED IN TRIDENT TEST BED PROJECTOR

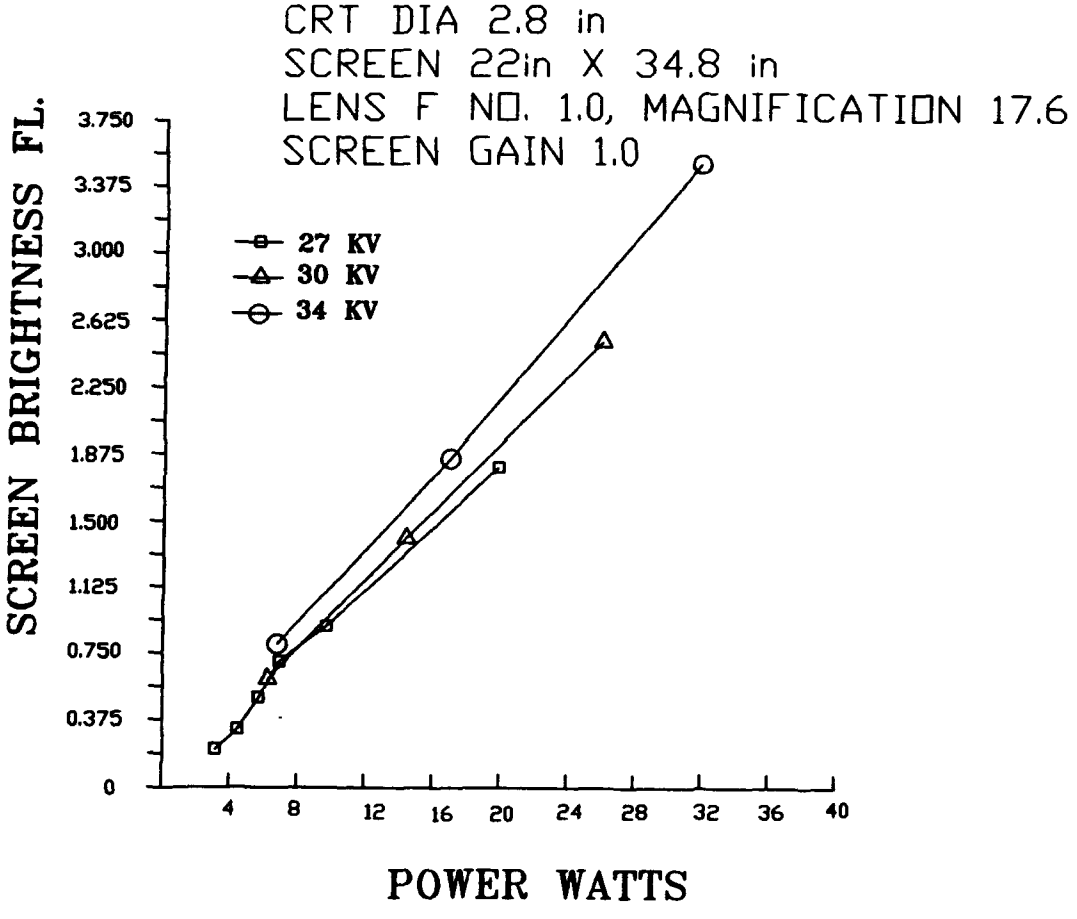

Figure 11

Ce:YAG Single Crystal Faceplate Resolution (Line Width)
Versus High Voltage @ Constant Power
Epitaxial Thickness 17 um

Watts	Beam Current	H.V. (kv)	Line Width @ Screen	Line Width @ CRT
1.8	.09 ma	20	.081"	.0046"
1.8	.08 ma	22.5	.079"	.0045"
1.8	.072 ma	25	.068"	.0039"
1.8	.065 ma	27.5	.060"	.0035"
1.8	.060 ma	30	.059"	.0034"

Figure 12

Ce:YAG Single Crystal Faceplate CRT Mounted in Trident
Test Bed Projector
CRT Crystal #10212-1-2 3"
Epitaxial Thickness 17 um

Brightness Measurements

Faceplate Image Size: 1.25" Wide x 1.98" High
2.475 sq. in. .0172 sq. ft.
Screen Image Size: 22" Wide x 34.8" High
5.3166 sq. ft.

H.V. (kv)	Faceplate Lumens*	Watts	Faceplate Brightness (fl)	Lu/W**	Screen Brightness	Screen Lumens*
27	6.88	3.10	400	2.22	.21 FL	1.11 Lu
27	10.32	4.43	600	2.33	.32 FL	1.70 Lu
27	16.03	5.67	932	2.83	.50 FL	2.66 Lu
27	22.36	6.92	1300	3.23	.70 FL	3.72 Lu
27	29,24	9.69	1700	3.01	.90 FL	4.78 Lu
27	58.48	19.84	3400	2.95	1.80 FL	9.56 Lu
30	19.51	6.21	1134***	3.14	.60 FL	3.19 Lu
30	45.50	14.40	2645***	3.25	1.40 FL	7.44 Lu
30	81.30	26.10	4726***	3.11	2.50 FL	13.29 Lu
34	25.90	6.80	1511***	3.80	.80 FL	4.25 Lu
34	59.80	17.00	3488***	3.52	1.85 FL	9.80 Lu
34	113.80	32.00	6616***	3.55	3.50 FL	18.60 Lu

* Lumen calculation: Brightness X sq. ft. screen image area
** Lu/W calculation: Lumens divided by watts
*** Calculated number based on optical efficiency of .1635

Figure 13

8.0 Study of Optical Coupling and Anti-Reflective Coatings

A study was contracted from Optical Research Associates in Pasadena, CA. (Enclosure #12.2), to determine the optical effects of using single crystal faceplates for CRT's in projection. The study compared the effects of the high refractive index of YAG crystal (1.832) to the existing glass faceplate (1.537) used in powder phosphor CRT's.

The goals were to minimize losses at the refractive index change boundaries and minimizing the incident reflected ray causing halation effects and to determine the optimum index matching fluid as well as optically coupling the faceplate to the optical system.

Trident International, Inc. has used liquid optical coupling in its high power, high resolution projectors for many years. The practicability of this cooling and coupling approach has been proven.

To accommodate the increased "light piping" (total internal reflection due to the critical angle effects), a thicker liquid chamber with black walls (See Fig. #14) is recommended to minimize internal scattering and contrast reduction. Interference coatings at the first highly concave element of the projection lens will aid in collection of energy from the SCFP CRT. Figure #1 in Optical Research Associate's study shows such a lens.

Graphs showing selected absorption filters to trim the spectral output of Ce:YAG, Ce:Gd,YAG and Ce:BEL single crystal faceplates and peak output versus NTSC standard points are shown in Figures 15 through 18 from tests taken by Trident International, Inc.

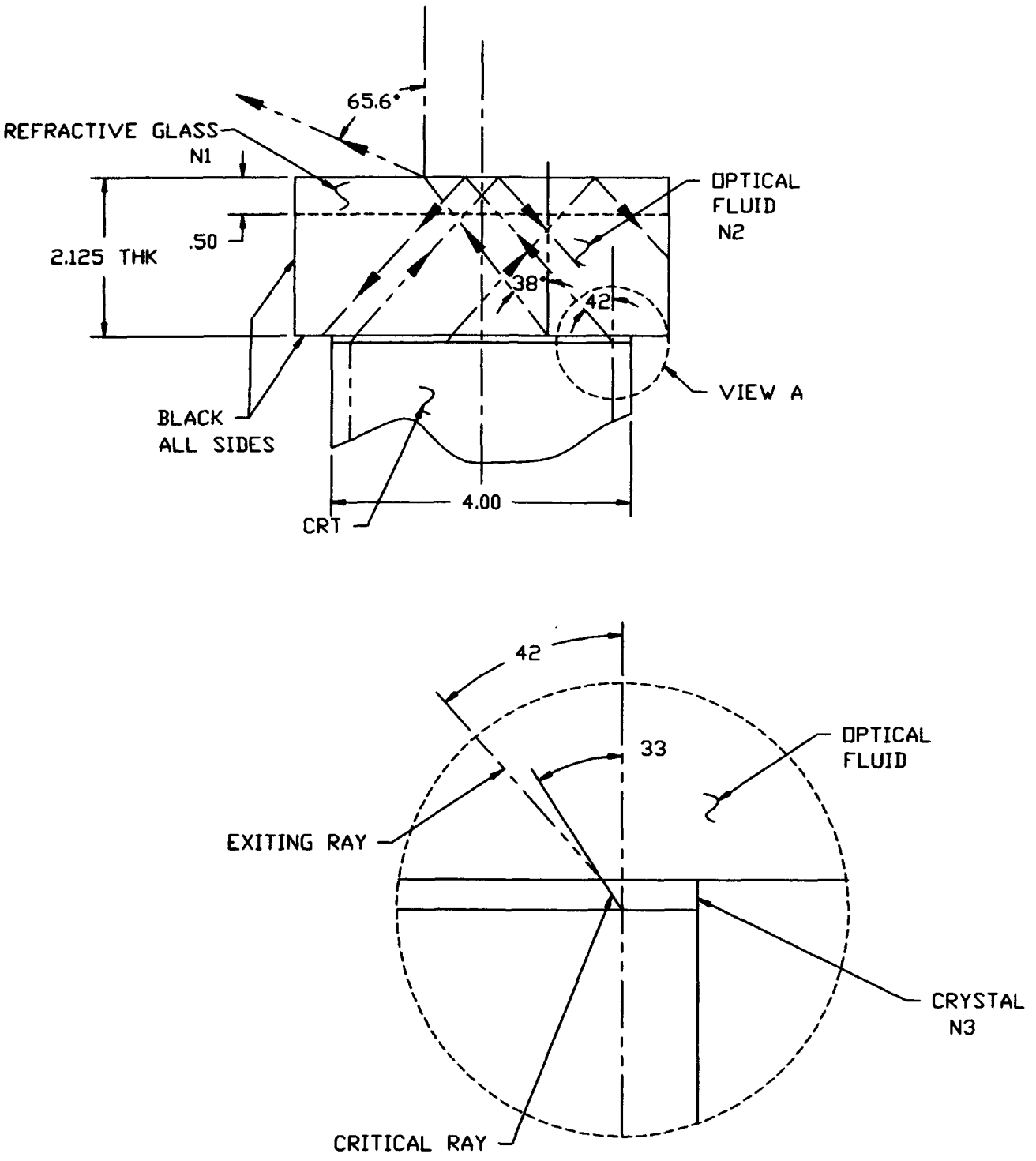

FIG. 2: LIQUID CHAMBER
N1 = N2 = 1.48; N3 = 1.84

Figure 14

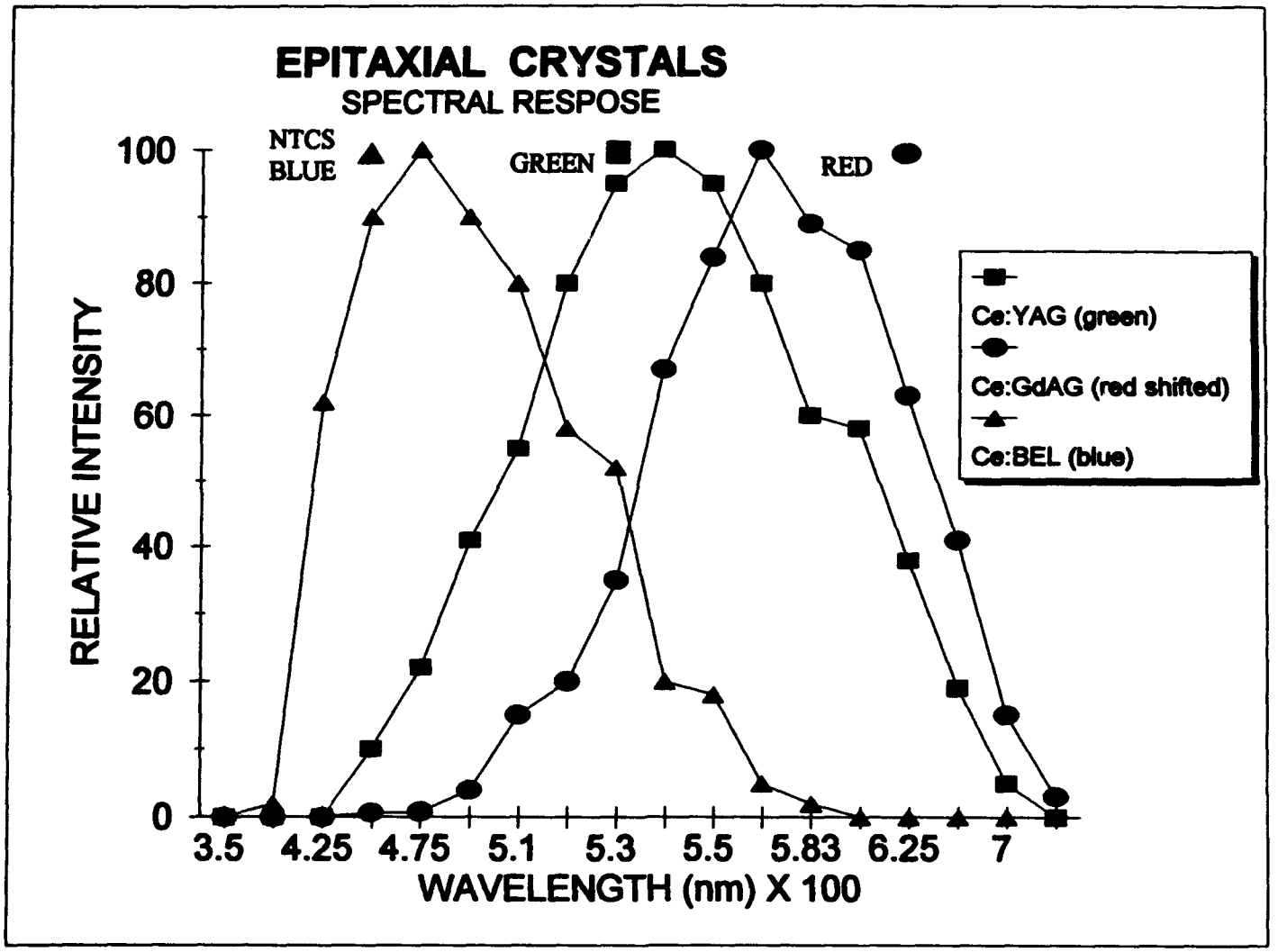
EPITAXIAL CRYSTALS
SPECTRAL RESPOSE
NTCS BLUE
GREEN
RED
100
80
60
40
20
0
RELATIVE INTENSITY
3.5
4.25
4.75
5.1
5.3
5.5
5.83
6.25
7
WAVELENGTH (nm) X 100
Ce:YAG (green)
Ce:GdAG (red shifted)
Ce:BEL (blue)

Figure 15

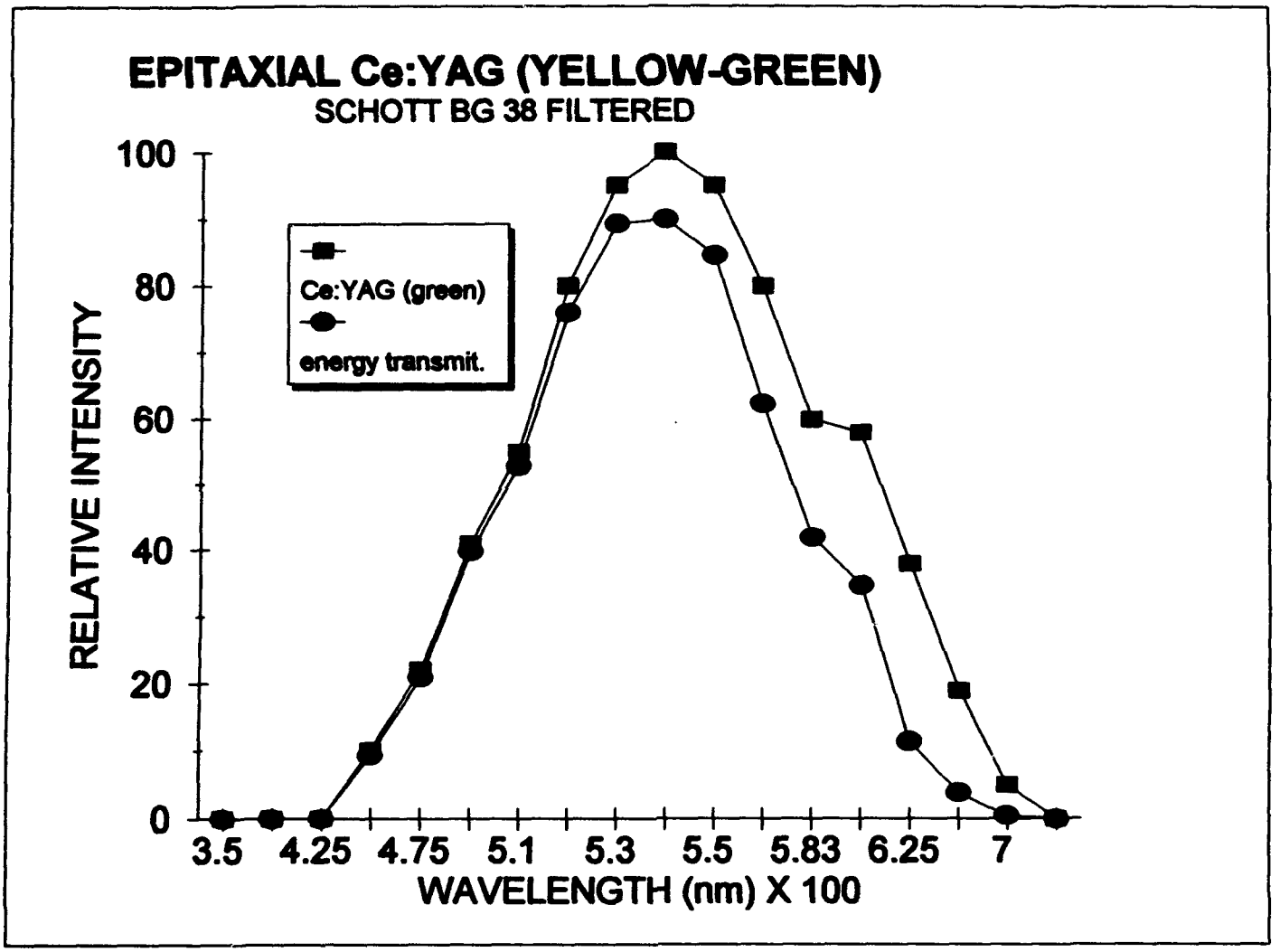
EPITAXIAL Ce:YAG (YELLOW-GREEN)
SCHOTT BG 38 FILTERED
RELATIVE INTENSITY
100
80
60
40
20
0
Ce:YAG (green)
energy transmit.
3.5
4.25
4.75
5.1
5.3
5.5
5.83
6.25
7
WAVELENGTH (nm) X 100

Figure 16

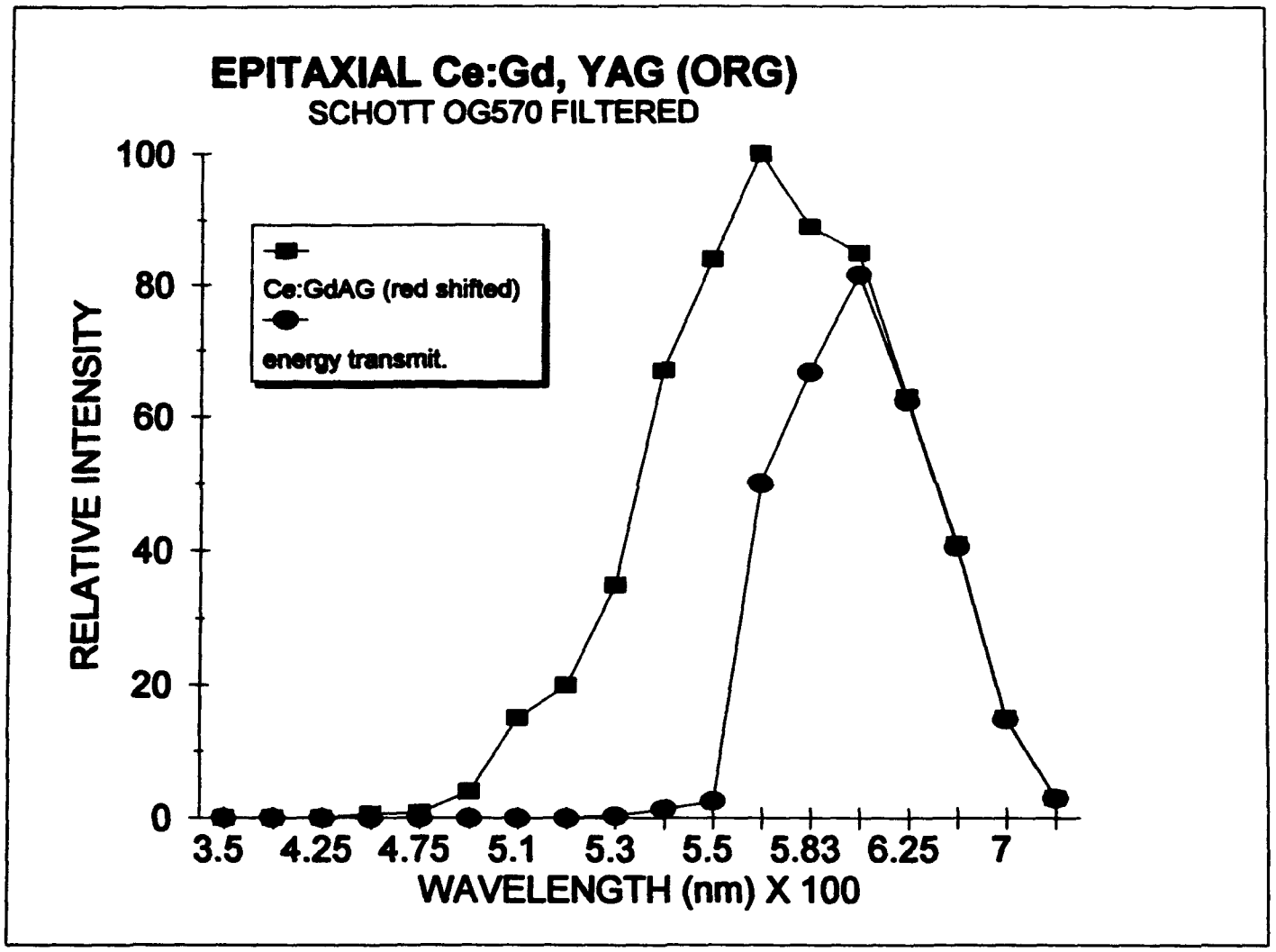
EPITAXIAL Ce:Gd, YAG (ORG)
SCHOTT OG570 FILTERED
RELATIVE INTENSITY
100
80
60
40
20
0
Ce:GdAG (red shifted)
energy transmit.
3.5
4.25
4.75
5.1
5.3
5.5
5.83
6.25
7
WAVELENGTH (nm) X 100

Figure 17

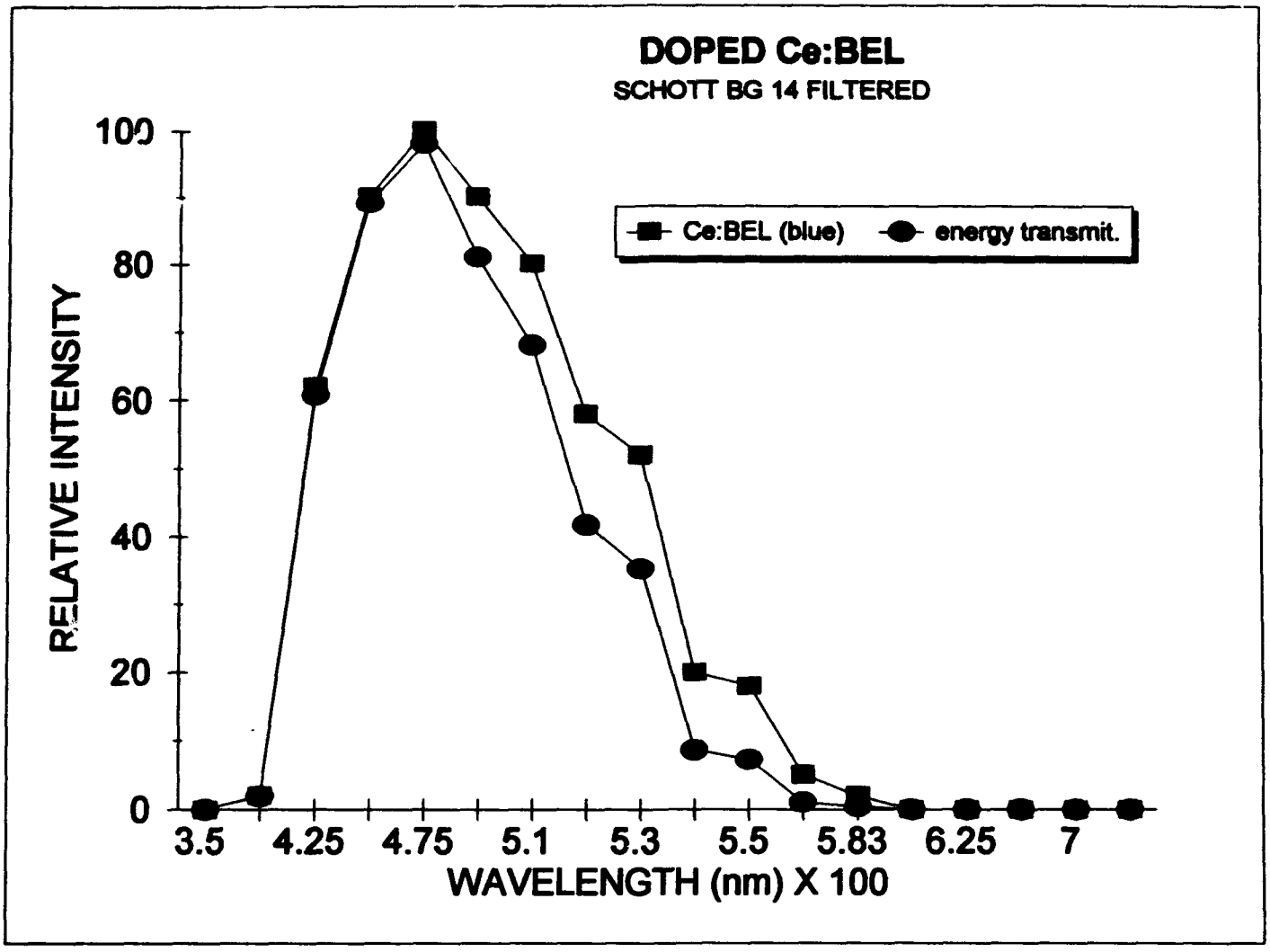
DOPED Ce:BEL
SCHOTT BG 14 FILTERED
Ce:BEL (blue)
energy transmit.
RELATIVE INTENSITY
100
80
60
40
20
0
3.5
4.25
4.75
5.1
5.3
5.5
5.83
6.25
7
WAVELENGTH (nm) X 100

Figure 18

9.0 Comparison of a Contemporary Powder Phosphor Versus Single Crystal Faceplate CRT Projectors

The following is an analysis and a comparison of the power requirements of a contemporary powder phosphor versus single crystal faceplate CRT projector with a 2046 faceplate lumen output as a constant.

A. A typical powder phosphor projector using a CRT with a 6.15" X 4.87" raster (so called 9" CRT) has the following:

31.68 sq.in. area or .022 sq.ft. per tube.

High voltage is 35 kv at an average beam current of 1.5 ma per tube.

The Trident projector is capable of reaching approximately three times the average power in small scene highlights. Using the powder phosphor efficiencies of 23 to 30 lu/watt green, 13 to 15 lu/W red and 6 to 8 lu/W blue

			Watts	Lumens
Green	P53	23 Lu/w	52.5	1207
Red	P22R	13 Lu/w	52.5	682.5
Blue	P22B	8 Lu/w	52.5	420

To obtain white balance the energy needs to be distributed as follows:

59%	Green	1207 lu	52.5 Watts
26%	Red	532 lu	41.0 Watts
15%	Blue	307 lu	38.4 Watts
	Total	2046 Lu	132.0 Watts

or white efficiency of 15.5 lumen/watt. If we use an F:1 lens system, the optical efficiency will be:

F:1 lambertion cone = 20% of energy collected.

A typical coated lens will have a transmission of 88% or (.2)(T.88) = .1760.
The light available at the screen with average power will be 2046 lu (.1760) = 361 lumens. The peak brightness that is usually quoted on CRT projectors then can approach 1,000 lumens equivalent brightness (2.88 X 361 lumens).

B. Using the efficiencies of single crystal faceplate CRT's determined by testing and reported in Allied Signal's report to Naval Training Systems Center Contract N61339-90-C-0046, August, 1991 and AT&T Bell Laboratories' Report AFWAL-TR-84-1185, dated July, 1984 and Trident International, Inc.'s report under Contract N61339-90-C-0047 and tests run during this contract, we can assume that reasonable efficiency expectations are:

Ce:YAG (Green) 4 - 5 lu/W
Ce:Gd,Ag (Red) 2.5 - 3.5 lu/W
Ce:BEL (Blue) .7 - 1.2 lu/W;

therefore, to generate the equivalent light output we need:

	Efficiency	Watts	Lumens
Green	@4.5 lu/w	268	1207
Red	3 lu/w *	177	532
Blue	1 lu/w	307	307
		752	2046

(* includes absorption filter)

This above comparison concludes that 2.72 lumens per watt for white balance in single crystal faceplate efficiency versus 15.5 lumens per watt for powder phosphor efficiency.

The possible advantage that single crystal faceplate CRT;s would have is their ruggedness against electron beam damage and practically infinite particle resolution versus powder phosphor grain size. Any image that is repeatedly scanned over the same screen area will cause reduction of light output in powder phosphor within a few hours particularly at the phosphor loading used in high power projectors. This is particularly true if the deflection system uses calligraphic or stroke writing to generate small bright lines or spots.

To generate the higher electron beam power necessary to overcome the 5.5 to 1 difference in efficiencies, the electron beam spot size will increase. To conserve resolution the high voltage to beam current ratio would have to be changed; such as, 50 kv vs 25 kv. The increase in high voltage will require additional X-ray shielding as well as increasing the absorption properties of the optical system.

Nothing in the above discussion precludes the use of single crystal faceplate projectors in lower light output application where images require prolonged stationary lines or spots; such as, maps, rail routes, communication lines or status boards of reasonable dimensions.

10.0 Conclusions

A. Powder phosphor faceplates are approximately five (5) times more efficient per input power than Ce:YAG single crystal faceplates.

B. Single crystal faceplates appear impervious to high beam power densities when adequately cooled.

C. Manufacturing problems associated with integrating single crystal faceplates onto CRT envelopes are not solved to the extent that practical fabrication processes are available. While some success was achieved with the Ce:YAG (Green), integration for the Ce:BEL was not achieved. Extensive materials and manufacturing process research would be necessary prior to any further initiatives in the projector application area.

D. The electron beam power requirements to produce equivalent light output to a powder phosphor based CRT system are so great that the electron beam spot size resulting from the high power input will limit the resolution on the maximum available faceplate size; therefore, the 1,000 line resolution specification cannot be met at required brightness levels.

E. Satisfactory spectral responses are attainable in all three colors (red, green and blue); however, mechanical problems with Ce:BEL currently preclude its use as a light source.

F. Early data taken indicating the ability to obtain high levels of brightness without saturation and coulombic destruction of the phosphor was confirmed; however, scaling of the power required for obtaining desired light output resulted in an unacceptable loss in resolution due to electron beam spot size growth.

11.0 Recommendations

In view of the problems remaining to be solved and the limited potential for their solution, further development effort on application of Single Crystal Faceplates to projection cathode ray tubes is not recommended.

12.0 Enclosures

12.1 Single Crystal Phosphor Faceplates for High Resolution, High Intensity Cathode Ray Tubes by Allied-Signal, Inc., Morristown, NJ., P.O. #9166 for Trident International, Inc.

12.2 The Study of the Performance of a YAG Faceplate, dated February 3, 1992, by Optical Research Associates, Pasadena, CA. for Trident International, Inc.

Final Report

SINGLE CRYSTAL PHOSPHOR FACEPLATES FOR HIGH RESOLUTION, HIGH INTENSITY CATHODE RAY TUBES

Purchase Order No. 9166

Submitted By

Applied Physics Laboratory
ALLIED-SIGNAL INC.
Research and Technology
P.O. Box 1021
Morristown, New Jersey 07962-1021

Submitted To:
Trident International Inc.
Central Florida Research Park
3290 Progress Drive Suite 155
Orlando, Florida 32826

Allied Signal

Single Crystal Phosphor Faceplates for High Resolution High Intensity Cathode Ray Tubes

a study for

Trident International, Inc.
Central Florida Research Park
3290 Progress Drive, Suite 155
Orlando, Florida 32826

by

D.M. Gualtieri
Allied-Signal, Inc.
Research and Technology
P.O. Box 1021
Morristown, NJ 07962-1021

February 1992

TABLE OF CONTENTS

Single Crystal Phosphor Faceplates for High Resolution High Intensity Cathode Ray Tubes

a study for

Trident International, Inc.
Central Florida Research Park
3290 Progress Drive, Suite 155
Orlando, Florida 32826

by

D.M. Gualtieri
Allied-Signal, Inc.
Research and Technology
P.O. Box 1021
Morristown, NJ 07962-1021

February 1992

1.0.0 INTRODUCTION

Conventional CRT faceplates are formed by the deposition of phosphor powder on the inside of a glass envelope of limited thermal conductivity. The image resolution and power capabilities of these faceplates are limited, and many applications now require CRT performance at the limits of phosphor faceplate technology. For example, sunlight-readable head-up displays (HUDs) for aircraft require a brightness of 10,000 foot-lamberts, a performance just achieved by conventional CRTs in stroke mode, and a factor of ten beyond that achieved in raster mode. The resolution of conventional faceplates is limited by phosphor particle size to twenty micrometers. High intensity operation is limited by a decomposition threshold of about 1 watt/cm^2. The phosphor particles will actually melt at about 5 watts/cm^2. High intensity operation also limits phosphor lifetime by a process called coulombic degradation. This failure mode reduces the intensity of P53, a standard phosphor, to 50% of its initial value after an electron dosage of 140 coulombs/cm^2. This leads to a CRT lifetime in a high luminance application of about 1000 hours under the best conditions.

Garnets are crystalline materials with many technologically useful properties. Garnets are oxides of the general composition $R_3T_5O_{12}$ (R and T are large and small metal or metalloid elements) which are resistant to chemical attack and high temperatures. There is much diversity in garnet composition since R and T can be combinations of one or several elements cohabiting a crystal sublattice, and R and T range over much of the Periodic Table. As an example, the yttrium in $Y_3Al_5O_{12}$ (YAG) can be partially replaced with neodymium to form the useful laser crystal Nd-YAG. YAG is used not only as a laser material, but as a substrate for the deposition of other garnet compositions. In particular, YAG doped with rare-earth elements, when grown as epitaxial layers on YAG substrates, is a cathodoluminescent material. Such layers can be used as phosphor faceplates in cathode ray tubes with significant advantages over standard, powder phosphor, faceplates. The single crystal nature of such epitaxial faceplates allows a higher resolution, and the intimate thermal contact between the epitaxial phosphor and the thermally conductive substrate allows operation of cathode ray tubes at power levels which would destroy a conventional powder phosphor.

Epitaxial phosphors are fluorescent crystalline layers which are grown on crystalline substrates. The usual case is homoepitaxial growth, in which a fluorescent ion is substituted for another ion in a host composition epitaxially grown onto a substrate of the host composition. An example is Ce:YAG epitaxially grown on YAG substrates, where cerium is incorporated into the layer on yttrium sites. The more unusual case is heteroepitaxy, in which a layer is grown on a substrate of different crystal structure; for example, zinc sulphide deposited on sapphire. Since electrons penetrate only a few microns into epitaxial phosphors, the epitaxial layer need not be very thick, 5-20 microns are usually sufficient. Epitaxial layers can be grown on top of other epitaxial layers to form penetration phosphors, in which different colors are excited at different anode potentials.

Epitaxial phosphor faceplates (EPF) have several significant advantages, which are summarized below:

1) *Ultra-High Resolution.* Resolution is limited only by electron beam size.

2) *Fast Decay Time.* Fluorescence decay of Ce:YAG (10 nsec), a standard epitaxial phosphor, is an order of magnitude faster than conventional powder phosphors.

3) *High Power Operation.* Epitaxial phosphors will not decompose at high power levels. There is no "burn". Thermal quench temperature is much higher than for powder phosphors.

4) *Superior Ageing Characteristics.* No coulombic degradation.

5) *Superior Mechanical Properties.* Single crystals have high strength. Faceplates resist scratching.

Since epitaxial phosphors are single crystals with no granulation, resolution is limited only by the dimension of the electron beam. Prof. Albert Crewe of the Fermi Institute, University of Chicago, has tested a Ce:YAG epitaxial phosphor faceplate fabricated by Allied-Signal, Inc. in a high resolution electron microscope and found no granulation to 0.1 μm spot size. This Ce:YAG epitaxial phosphor faceplate was further tested to a current density of 1000 A/cm^2 at 5 kV without permanent damage. M.W. van Tol and J. van Esdonk operated epitaxial phosphor faceplates at power levels of 10 W/cm^2 [1]. J.M. Robertson and M.W. van Tol tested epitaxial phosphor faceplates of Ce:YAG,

Tb:YAG, and Eu:YAG at power levels to 10^4 W/cm^2 [2]. They found that Ce:YAG is linear to the highest power levels, but that the light output of Tb:YAG and Eu:YAG saturates at power levels above 1 W/cm^2. Thus, Ce:YAG is preferred as a high intensity monochrome phosphor. The saturation in Tb:YAG arises from excited state absorption and cross-relaxation processes and it is a general feature of many phosphors, for example Mn:$BaAl_{12}O_{19}$ [3,4]. AT&T Bell Laboratories has developed a modified terbium composition, $Tb_{0.2}Y_{0.1}Lu_{2.7}Al_3Ga_2O_{12}$, with improved saturation characteristic [5]. Such a phosphor has shown a peak line brightness of 28,000 fL at a 25,000 inch/sec writing speed when excited with a 25 kV, 2 mA beam. This is equivalent to 594 lumens in a 2.75 inch diagonal raster.

Levy and Yaffe have shown that the thermal quenching temperature of Ce:YAG is about 400°C, and that a decrease in light output is first evident at 200°C [6]. They determined that it is safe to operate an EFP at thermal gradients up to 150°C/inch, and that a three inch diameter epitaxial phosphor faceplate can be operated at 25 watts excitation with no cooling. Since the thermal conductivity of YAG is high, forced-air cooling is very effective at higher excitation levels. Forced-air cooling can extract about 60% of the heat, radiation can dissipate about 20% of the heat, and conduction down the neck can dissipate the remaining 20%. Coulombic degradation does not occur in epitaxial phosphor faceplates, whereas 0.5 W/cm^2 is the conventional limit for projection CRTs. Operation of P53 at 0.5 W/cm^2 results in an extremely short lifetime.

The fluorescent spectrum of cerium in garnet crystals is a function of the atomic spacing in the crystal which is reflected in the lattice constant. It is possible to red-shift the green emission of Ce:YAG by incorporation of gadolinium. In the extreme case, Ce:$Gd_3Al_5O_{12}$ can be grown as the analog of Ce:$Y_3Al_5O_{12}$, and the spectral peak is shifted almost 50 nm towards the red. A blue-shift is possible, by using a small rare-earth ion in place of yttrium, but the magnitude of such a blue-shift is not sufficient to produce much energy at blue wavelengths suitable for color CRTs. Although other activators in YAG, notably thulium, are blue emitters, cerium seems to be the only activator which will not saturate at high power levels. Two blue cerium emitters, Ce:$La_2Be_2O_5$ (Ce:BEL) and Ce:Y_2SiO_5 (cerium orthosilicate), are candidates for blue faceplates. Ce:Y_2SiO_5 has emission extending below blue, so that much of its light output is not visible. Its performance in CRTs has been investigated by AT&T Bell Laboratories and elsewhere, and saturation has been observed in this phosphor. Ce:BEL, however, emits prominently in the blue, and does not appear to saturate. Thus, Ce:$Gd_3Al_5O_{12}$ (Ce:GdAG, red), Ce:$Y_3Al_5O_{12}$ (Ce:YAG, green), and Ce:$La_2Be_2O_5$ (Ce:BEL, blue), appear to be an appropriate trio of epitaxial phosphors for a high intensity color projection display. Figure 1.0.0.1 shows the spectra of these phosphors.

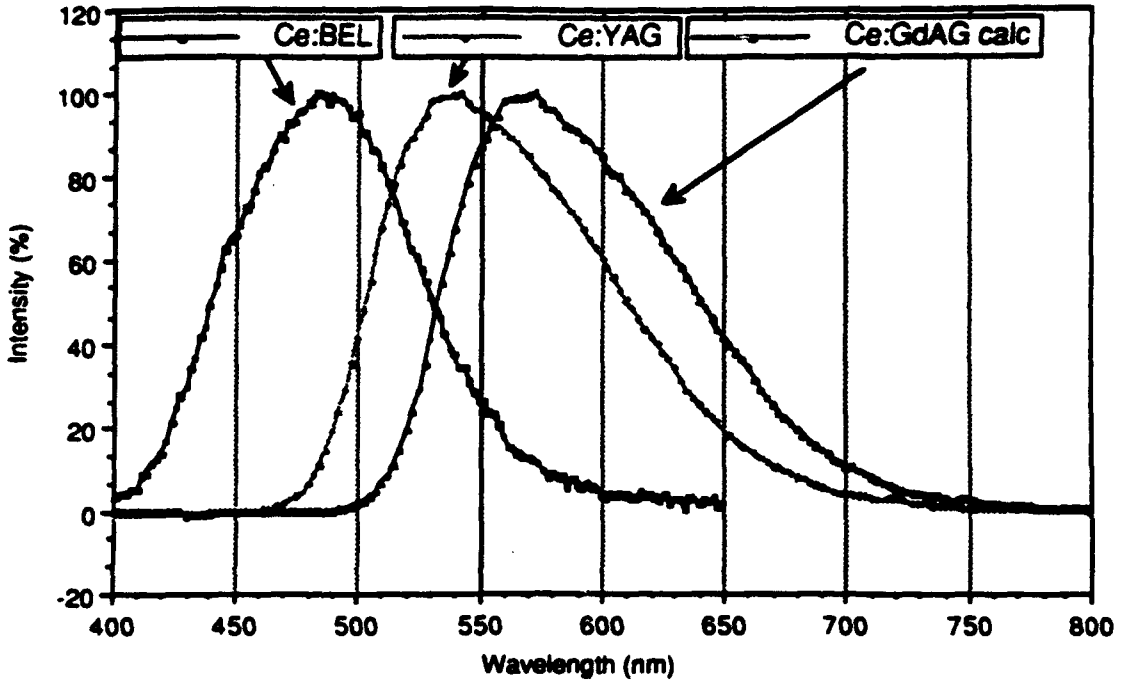

Fig. 1.0.0.1 Spectra of Ce:BEL (blue), Ce:YAG (green) and Ce:GdAG (red) phosphors.

2.0.0 PROCESS

Table 2.0.0.1 shows the major stages of the process for the production of epitaxial phosphor faceplates.

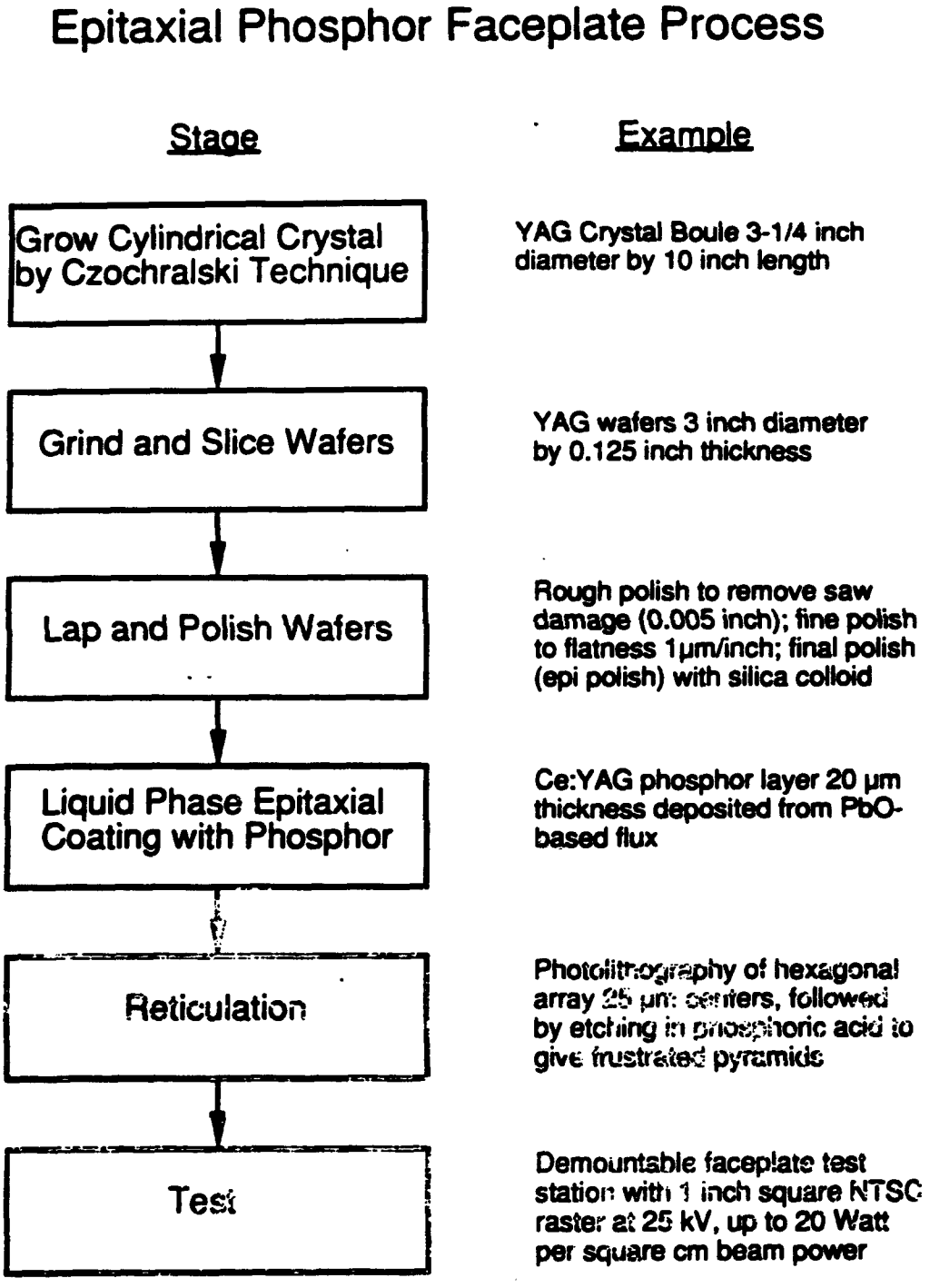

Table 2.0.0.1. Major stages of the process for the production of epitaxial phosphor faceplates.

2.1.0 Crystal Growth Process of Substrate Wafers

There are presently two processes which are suitable for the growth of the substrate wafers used in epitaxial phosphor faceplates. These are the Czochralski method, which has produced large single crystals of YAG up to three inches in diameter; and the Heat Exchanger Method. The Heat Exchanger Method (HEM™) is being used for the commercial production of 10-inch diameter sapphire crystals of very high quality. It is possible to grow sapphire by HEM free of scattering centers for stringent optical applications. HEM is used also for commercial production of multi-crystalline silicon ingots for photovoltaic and optical applications. Titanium-doped sapphire (Ti:Sapphire) boules are grown routinely for cw and pulsed laser applications. A number of mixed oxides, fluorides and compound semiconductors has also been grown by HEM.

2.1.1 Undoped Crystal Boule

Substrate wafer crystal for epitaxial phosphor faceplates of YAG have been produced up to three inches in diameter by the Czochralski process. In the Czochralski process, a melt is produced in a crucible by induction heating. A "seed" crystal is dipped into the melt and withdrawn with rotation at a slow rate as the melt is cooled. This produces solidified crystal on the seed with the same crystallographic orientation as the seed. Usually crystal weight is used as a process variable to control the growth in a feedback loop.

There are difficulties involved in the growth of large diameter Czochralski crystals. The crystal is in contact with the liquid melt, and in the case of YAG it is actually immersed in liquid. This leads to considerable thermal stress on the crystal which can cause cracking. Also, scale-up from one diameter to a larger diameter is troublesome, since the exact parameters for stable crystal growth depend critically on the thermal environment of the crystal. There is a steep "learning curve."

In the HEM method, he crucible with the seed positioned at the bottom is loaded with a material charge and placed on top of a heat exchanger. After evacuation, heat is supplied by the graphite heater and the material charge is melted. The seed is prevented from melting by forcing gaseous helium through the heat exchanger.Growth is started after sufficient meltback of the seed is achieved by increasing the flow of helium and thereby decreasing the heat exchanger temperature. The liquid temperature gradients are controlled by the furnace temperature, while the temperature gradient in the solid is controlled by the heat exchanger temperature. Crystal growth is achieved by controlling the heat input as well as the heat extraction. After solidification is complete, the gas flow through the heat exchanger is decreased to equilibrate the temperature throughout the crystal during the annealing and cooldown stage.

HEM is the only crystal growth process in which both the heat input and heat extraction are controlled. The heat flow is set up such that the heat input is from the sides and top of the crucible and the heat extraction is primarily through the heat exchanger at the bottom of the crucible. Under these conditions a convex solid-liquid interface is set up so that core-free crystals can be grown. The convexity of the solid-liquid interface can be controlled by changing the ratio of heat input and heat extraction. The independent liquid and solid temperature gradients are achieved without movement of the crucible, heat zone or crystal. After the crystal is grown, it is still in the heat zone and can be cooled at a controlled rate to relieve solidification stresses. This unique capability allows the growth of

sapphire up to 32 cm diameter and weighing about 50 kg without cracking due to thermal stresses associated with such large sizes.

A distinguishing feature of HEM, as compared with the Czochralski, top-seeded process, is that the solid-liquid interface is submerged beneath the surface and is surrounded by the melt. Under these conditions the thermal and mechanical perturbations are damped out by the surrounding molten mass before reaching the interface. This results in uniform temperature gradients at the interface. In the Czochralski process, growth occurs at the melt surface where the local gradients vary sufficiently to cause solidification and remelting of the crystal. Precise control of the furnace and heat exchanger temperatures, combined with minimized thermal perturbations resulting from the submerged interface, gives HEM an advantage over the Czochralski techniques for growing high-quality crystals.

In HEM growth, after the crystal is grown, the temperature of the furnace is reduced to just below the solidification temperature and the helium flow is reduced at a desired rate. The whole crystal can, therefore, be brought to high temperatures to anneal the solidification stresses, followed by uniform cooling at a controlled rate to room temperature. Because *in situ* annealing is part of the solidification cycle, HEM can reduce the defect density. Further the last and most impure material to solidify is along the crucible walls, where it can be removed. These features of HEM produce uniform, growth and the only sapphire free of light scatter. In the case of sapphire and silicon, it has been demonstrated that once crystal growth parameters are established, large crystals can be grown. The HEM has been adapted for the growth of Ti:Al_2O_3. HEM is cost competitive with Czochralski. The furnace is uncomplicated, automated, and well insulated, which results in low equipment, labor and energy costs.

2.1.2 Doped Crystal Boule

Single crystal boule may be produced with the activator ion grown into the crystal. There are both advantages and disadvantages to this technique. The principal advantage is that the subsequent deposition of the phosphor by liquid phase epitaxy is not required. The disadvantages relate to the difficulty in achieving as high an activator concentration as desired, maintaining the proper charge state of the activator, and the usually lower growth rate required for doped crystals.

One of the problems with doped crystals is the segregation coefficient of dopant in the host crystal. The segregation coefficient is the ratio of the concentration of a species in the crystal to that in the melt. If the segregation coefficient is low, there is a gradation in dopant concentration along the length of the crystal and it is necessary to grow crystals at low growth rates in order to maintain high quality. These problems are minimized as the segregation coefficient is higher and essentially there are minimal problems when the segregation coefficient is unity. For example, the segregation coefficient of Ti in Al_2O_3 and Nd in YAG is rather low, approximately 0.16. The growth of Nd-doped YAG for laser applications proceeds at about one-fifth the rate as for undoped YAG.

Ce-doped BEL has been produced in boule form, so that subsequent epitaxy of a phosphor layer is not required, but an anneal in a hydrogen atmosphere is required to bring the cerium into its reduced Ce^{3+} charge state. Likewise, the blue phosphor Ce:Y_2SiO_5 has been produced by AT&T Bell Laboratories as doped boule one-inch in diameter.

Researchers from Hitachi Chemical Co. [17] have reported growth of the similar crystal Ce:Gd_2SiO_5 in diameters to two-inch.

2.1.3 Current Size Limitations

The Czochralski method has produced YAG crystal up to three inches in diameter. Experience indicates that four inch crystal is a possibility, but only by a flat interface technique pioneered at Allied-Signal. However, a considerable development effort would be required to attain a process for the Czochralski growth of four inch YAG.

The Heat Exchanger Method (HEM™) is being used for the commercial production of 10-inch diameter sapphire crystals of very high quality. The growth of YAG crystal to this diameter appears possible. These melting point of YAG (1950°C) is lower than that for Al_2O_3 (2040°C): therefore, current HEM™ furnaces are adequate for growing this crystal. In the case of sapphire (Al_2O_3) crystals grown by HEM™, the processing is carried out under vacuum; however, it is expected that even though the host phosphor materials may be stable under vacuum, it may be necessary to control the atmosphere during growth of doped crystals. The candidate phosphor materials are compatible with using a molybdenum crucible and graphite resistance heat zone of the HEM™ furnace so that these crystals can be grown with existing HEM™ furnaces. In the case of BEL, it would be necessary to set up additional safety procedures for handling BeO raw material and BEL crystals because of their toxic nature.

2.2.0 Optical Fabrication of Wafer Faceplates

Fabrication of wafer faceplates from crystal boule is accomplished by standard techniques available in most optical shops. This involves centerless grinding of the crystal boule to diameter, xray orientation, wafer slicing with an ID saw, lapping and polishing. The requirement of the final polish is severe. This "epi" grade polish involves the use of a chemical-mechanical colloidal silica polish on a soft pad to produce a surface free of defects which would interfere with the subsequent epitaxial phosphor growth stage.

2.2.1 Grind and Slice Wafers

The crystal boule is first ground to the required diameter using a centerless grinding technique. After alignment of the crystal by xray diffraction, wafers are sliced by the type of saw ("ID" saw) used in processing of semiconductor wafers.

2.2.2 Lap and Polish

The sliced wafers are polished using finer grit until the saw damage has been removed (about 0.005 inch in the case of YAG) and the required flatness of about 1 μm/inch has been achieved. A final polish ("epi" polish) is done with a colloidal silica suspension to achieve a polish beyond an optical polish into the regime of a polish on an atomic scale.

2.2.3 Current Size Limitations

Since the semiconductor industry is now fabricating wafers up to ten and twelve inches in diameter, it is concluded that wafer fabrication will not constrain the development of large diameter single crystal faceplates.

2.3.0 Liquid Phase Epitaxy Process

The following is a general procedure for the growth of epitaxial layers of Ce:YAG on YAG substrates. A YAG wafer, prepared by the processes in the previous sections, is carefully cleaned and mounted in a substrate holder which allows rotation and translation. Epitaxy is achieved by dipping the substrate into a platinum crucible holding the molten constituent oxides of the Ce:YAG composition in the proportions listed in Table 2.3.0.1.

Table 2.3.0.1. Melt for the growth of epitaxial layers of Ce:YAG on YAG substrates at 980 °C. Note that cerium oxide, the dopant, is not included in the mole fraction calculation.

Oxide	Mole Fraction	Moles	Grams
PbO	0.90282	3.44684	769.299
Al_2O_3	0.01737	0.06632	6.762
B_2O_3	0.07524	0.28724	19.998
Y_2O_3	0.00457	0.01745	3.941
CeO_2		0.00581	1.000
	1.00000	3.82367	801.000

The platinum crucible, 3-inches high by 2.25-inch diameter for epitaxial growth on one-inch diameter wafers, is placed in a vertical furnace. These powders are heated to 1050 °C, a temperature well above the melting point of the mixture, and allowed to "soak" for 24 hours. The melt is stirred for one hour at 1050 °C and 200 rev/min just before each layer growth. After stirring, the melt is cooled to the growth temperature of about 980°C in 45 minutes (melt saturation occurs at about 990°C).

The YAG faceplate wafers are thermally equilibrated above the melt surface for ten minutes, dipped to the melt surface, and rotated at 200 rev/min. for about ten minutes. The Ce:YAG epitaxial phosphor layer grows at a rate of about 1.5 μm/min. After growth, the substrate with the epitaxial layer is raised above the melt, and the residual flux is spun-off by rapid rotation of 500 rev/min. Removal of the faceplate from the furnace to room temperature proceeds over the course of 90 minutes. This slow exit rate prevents thermal shock and cracking of the wafers. This entire process is done in a class 100 laminar flow hood. Remaining traces of solidified growth solution on the wafers are removed in a 40% solution of nitric acid at 90 °C. Layer thickness is measured by weight, using a density of 4.565 g/cc, the density of pure $Y_3Al_5O_{12}$. Optical thickness measurement is not possible since there is no refractive index difference between the layer and the substrate.

2.3.1 Equipment

Fig. 2.3.1.1 shows the equipment involved in the liquid phase epitaxy process. There are motor assemblies to "dip" and rotate the wafers in the solution, but the major

piece of equipment is the large-bore vertical tube furnace which heats and maintains the solution at about 1100°C ± 1°C.

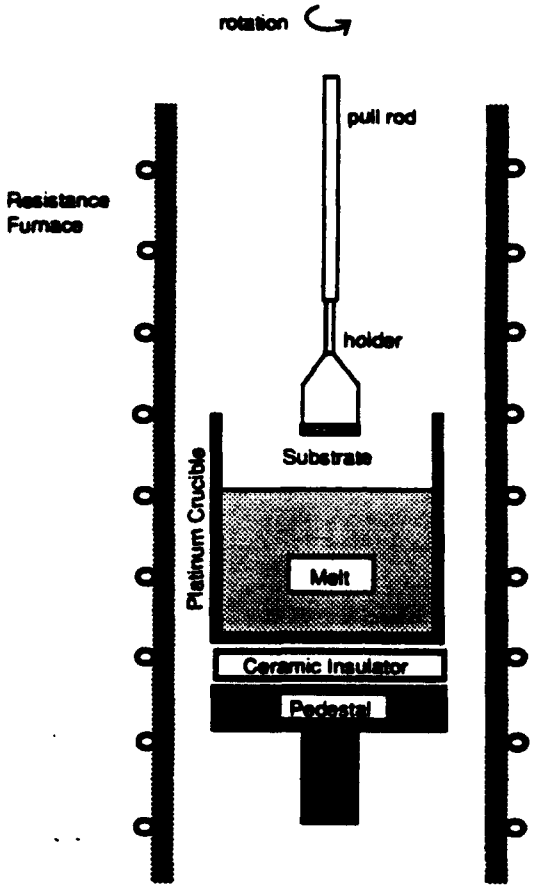

Fig. 2.3.1.1. Schematic diagram of system for liquid phase epitaxial growth of single crystal phosphors of Ce-YAG on YAG substrates.

2.3.2 Current Size Limitations

Liquid phase epitaxy is routinely carried out for wafers up to three inches in diameter in the preparation of magneto-optical materials. These wafers, however, are thin (0.020 inch) compared with YAG faceplate wafers (0.125 inch). Generally, a slower withdrawal rate from the epitaxy furnace is required for these thick wafers. Liquid phase epitaxy has been demonstrated on four-inch diameter by 0.020 inch thick wafers. There appears to be no fundamental size limitation for the liquid phase epitaxy process.

2.4.0 Photoreticulation

The major factor limiting the external efficiency of Ce:YAG phosphors is the high refractive index of the YAG substrate (1.84), which allows only rays less than a critical angle of 33° to be emitted from the faceplate. The remaining rays are waveguided to the

edges, so that only 16% of the cathodoluminescence is emitted from the faceplate. Higher external efficiencies can be expected from Ce:YAG through reticulation, a texturing of the epitaxial phosphor into structures which will focus the cathodoluminescence towards the observer. Non-reticulated epitaxial phosphors have low external efficiencies, since the cathodoluminescence is waveguided by the high refractive index of YAG to the edge of the faceplate.

P.F. Bongers, et al., [12] have etched grooves in the phosphor to increase the external efficiency. D.M. Gualtieri, et al. [13] have used a faceted epitaxial layer for the same purpose. D.T.C. Huo and T.W. Hou [14], have used photolithographic techniques to pattern a Ce:YAG epitaxial phosphor faceplate with an array of rectangular mesas. They were able to increase the external efficiency by a factor of three. A truncated cone geometry can increase the external efficiency by a factor of 5.5, if such a shape can be formed in the phosphor layer. Such reticulation will not limit the faceplate resolution if a small mesa size is used. The reticulation concept is shown schematically in fig. 2.4.0.1

Non-reticulated faceplates of Ce:YAG have an NTSC raster efficiency at 25 kV of 1.9 - 2.0 lumens/watt, when measured in our characterization station, so that at a beam power of 10 watts/cm^2 an NTSC raster of 2.75-inch diagonal on a *non-reticulated* Ce:YAG faceplate will have a luminance of 450 lumens. The best *reticulated* faceplate was found to give 5.38 lumens/watt at a beam power of 5 watt/cm^2. A beam power of 16 watt/cm^2 will be required for 2000 lumen output at such an efficiency. Fig. 2.4.0.2 shows the results of cathodoluminescent measurements on a reticulated faceplate.

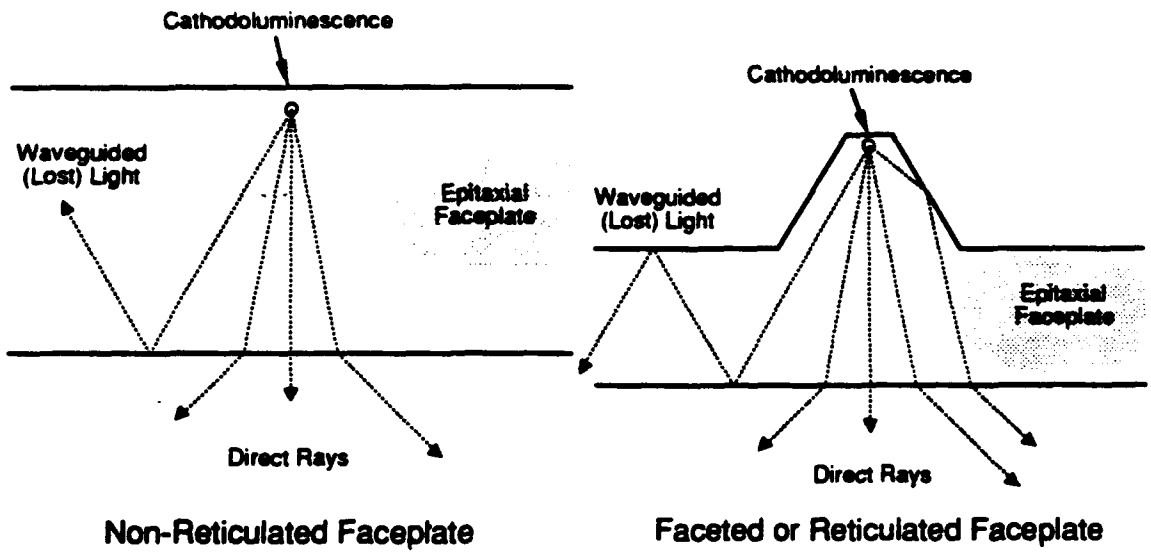

Fig. 2.4.0.1. Schematic illustration of waveguiding effect in epitaxial faceplates, and the role of reticulation in directing light into the critical cone.

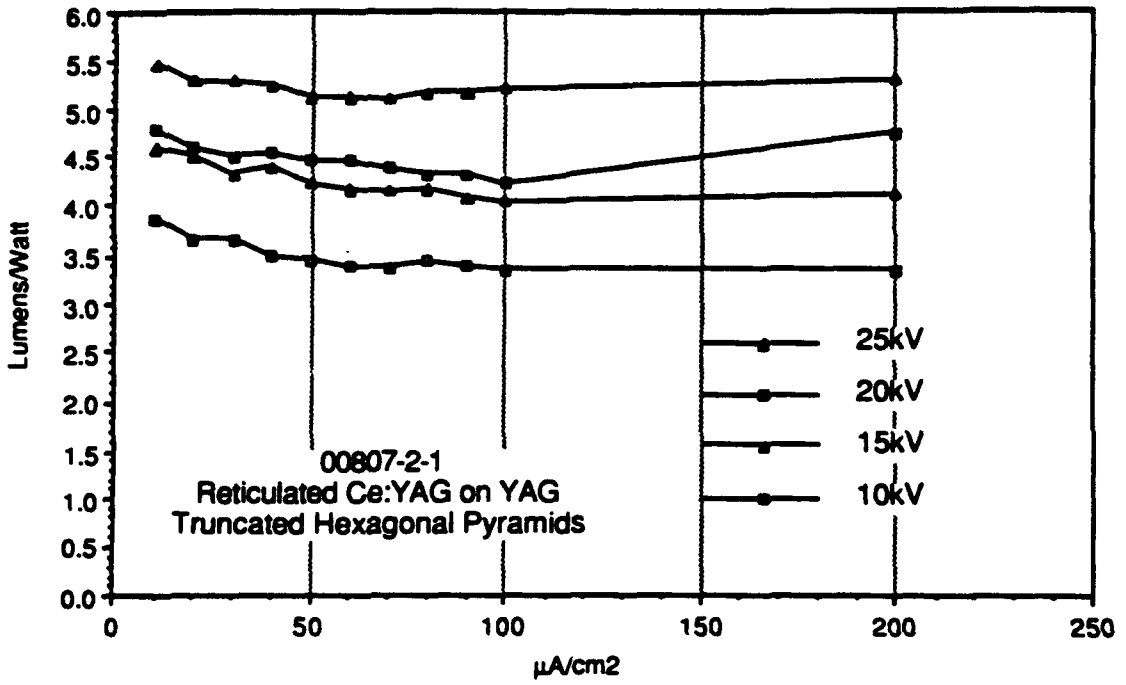

Fig. 2.4.0.2. Cathodoluminescent measurements on a reticulated faceplate.

2.4.1 Equipment

Photoreticulation is done by techniques common to fabrication of semiconductor devices. A mask aligner of micron resolution is required, typically a contact printer as distinct from a projector. A typical resist coater/developer/stripper line is required. Either a metallizer, such as an electron beam evaporator, or a plasma reactor for silica deposition are required to coat the wafers with an acid resisting mask for the etching stage. A phosphoric acid etcher is required. All this equipment must be sited in a class 100 clean room.

2.4.2 Current Size Limitations

Since the semiconductor industry is now fabricating wafers up to ten and twelve inches in diameter, it is concluded that this processing step will not constrain the development of large diameter single crystal faceplates.

3.0.0 FACEPLATE AND PHOSPHOR MATERIALS

3.1.0 Cerium Activators

Cerium seems to be the only activator which will not saturate at high power levels. Two blue cerium emitters, Ce:$La_2Be_2O_5$ (Ce:BEL) and Ce:Y_2SiO_5 (cerium orthosilicate), are candidates for blue faceplates. Ce:Y_2SiO_5 has emission extending below blue, peaking at about 390 nm, so that much of its light output is not visible. A similar phosphor Ce:Gd_2SiO_5 has a better spectral overlap with the visible, peaking at 430 nm. The performance of Ce:Y_2SiO_5 has been investigated by AT&T Bell Laboratories and elsewhere, and saturation has been observed in this phosphor. Ce:BEL, however, emits prominently in the blue, and does not appear to saturate. Thus, Ce:$Gd_3Al_5O_{12}$ (Ce:GdAG, red), Ce:$Y_3Al_5O_{12}$ (Ce:YAG, green), and Ce:$La_2Be_2O_5$ (Ce:BEL, blue), appear to be an appropriate trio of epitaxial phosphors for a high intensity color projection display.

3.2.0 Red Phosphors

3.2.1 Ce:(Y,Gd)AG on YAG

It is possible to epitaxially grow a red-shifted garnet composition on YAG wafer substrates. This garnet composition, Ce:$Y_2Gd_1Al_5O_{12}$, is strained with respect to the YAG wafer, and its red-shift is only about a third as large as that of Ce:$Gd_3Al_5O_{12}$. This composition has a lattice constant (measured perpendicularly at the (444) reflection) about 0.4% greater than YAG, which is just under the typical facet limit of 0.5%. Figs. 3.2.1.1 and 3.2.1.2 show cathodoluminescence measurements for this composition. There is a red-shift of 20 nm, and, most importantly, almost a two-fold increase in the luminance at the red wavelength of 650 nm. The light output at 650 nm was 31% of the spectral peak for this composition, as compared to 19% for Ce:YAG. The cerium emission in the fully substituted garnet, $Gd_3Al_5O_{12}$, would exhibit a larger red-shift, but it cannot be grown as an epitaxial layer on YAG.

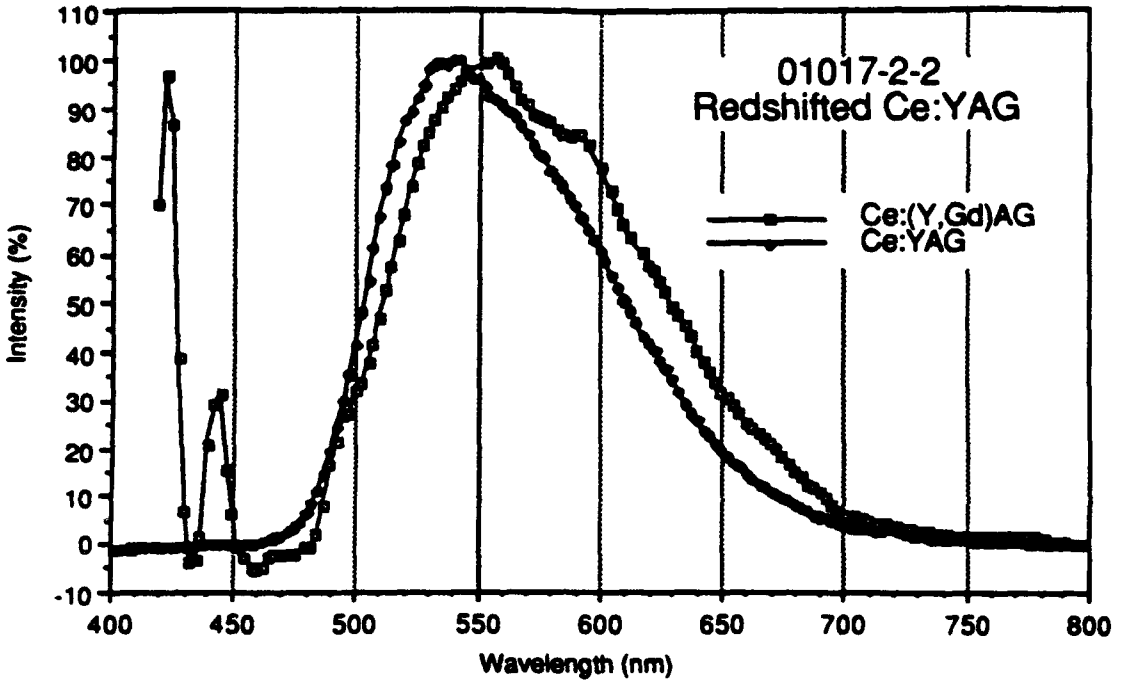

Fig. 3.2.1.1 Cathodoluminescent spectrum of a Ce:$Y_2Gd_1Al_5O_{12}$ phosphor layer grown on a YAG substrate.

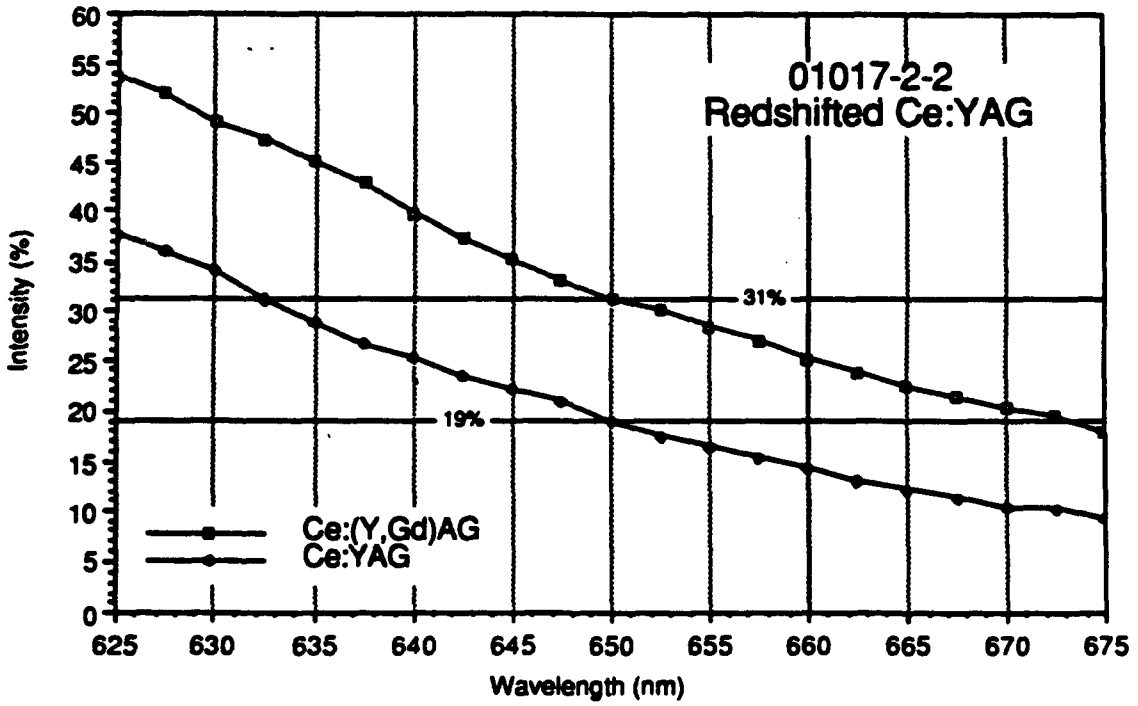

Fig. 3.2.1.2. Cathodoluminescent spectrum (detail) of a Ce:$Y_2Gd_1Al_5O_{12}$ phosphor layer grown on a YAG substrate.

3.2.2 Ce:GdAG on GdAG

Epitaxial layers of Ce:$Gd_3Al_5O_{12}$ could be grown on $Gd_3Al_5O_{12}$, and they would be good red faceplates in color projection systems since they would have a red-shift of about 50 nm.

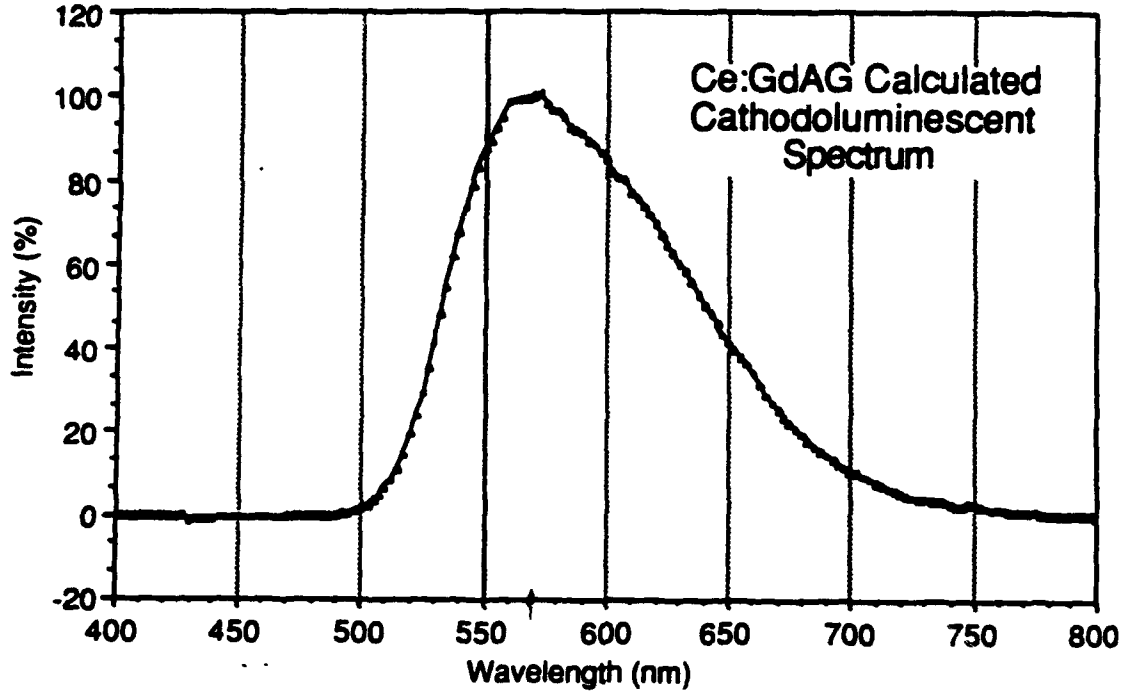

Fig. 3.2.2.1. Calculated spectrum of Ce:$Gd_3Al_5O_{12}$.

3.3.0 Green Phosphors

3.3.1 Ce:YAG

Cerium YAG is the material of choice for green epitaxial phosphors. Its cathodoluminescent spectrum appears as fig. 3.3.1.1.

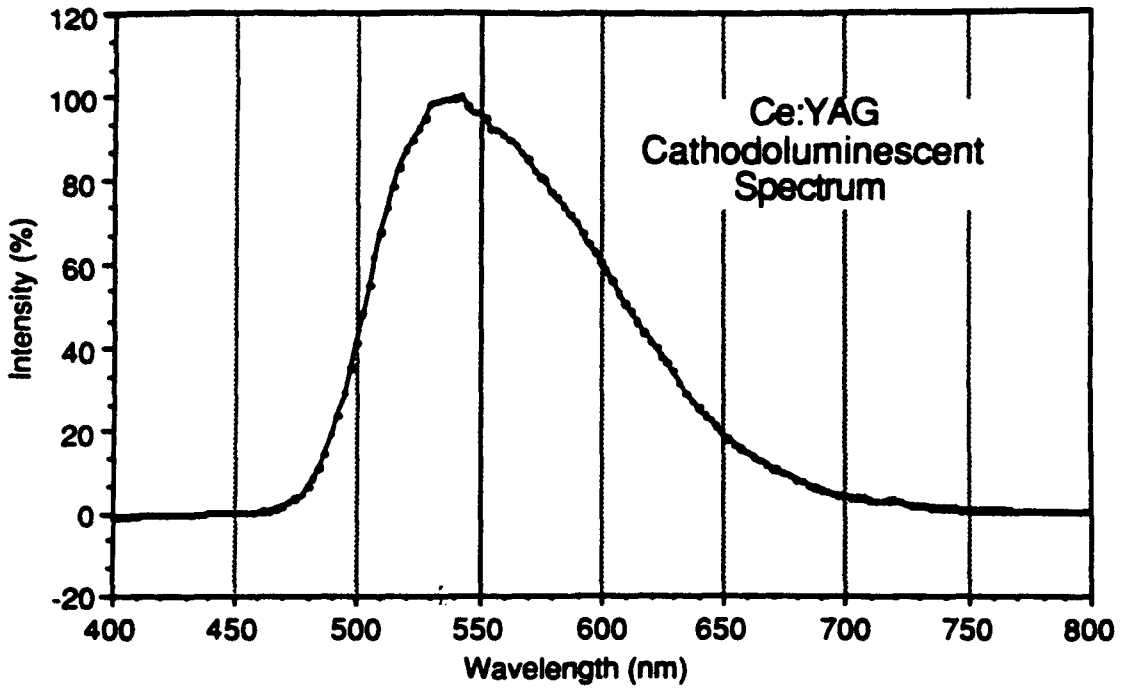

Fig. 3.3.1.1. Spectrum of Ce:$Y_3Al_5O_{12}$.

Non-reticulated faceplates of Ce:YAG have an NTSC raster efficiency at 25 kV of 1.9 - 2.0 lumens/watt, when measured in our characterization station, so that at a beam power of 10 watts/cm^2 an NTSC raster of 2.75-inch diagonal on a *non-reticulated* Ce:YAG faceplate will have a luminance of 450 lumens. The best *reticulated* faceplate was found to give 5.38 lumens/watt at a beam power of 5 watt/cm^2. A beam power of 16 watt/cm^2 will be required for 2000 lumen output at such an efficiency.

3.4.0 Blue Phosphors

3.4.1 Ce:BEL

The cathodoluminescence of Ce:BEL was characterized in a thin wafer of a Czochralski boule prepared from a melt of 0.5% cerium content [16]. Ce:BEL proved to be an excellent blue phosphor with a peak fluorescence at 485 nm and a fluorescence bandwidth (FWHM) of 80 nm (fig. 3.4.1.1). Thus, there is significant light energy at the extremely blue wavelength 445 nm. The measured cathodoluminescent efficiency of the available, as-grown Czochralkski crystal was 0.1 lumen/watt, weighted according to the C.I.E. photoptic curve. It was found that annealing at 1150 °C in a reducing atmosphere of 10% hydrogen in argon doubles the efficiency of Ce:BEL to 0.2 lumens/watt (fig. 3.4.1.2). Annealing also changes the appearance of the crystals from an orange color to transparent. It was also found that the light output of Ce:BEL does not saturate up to an electron beam power of 19 watt/cm^2.

Mass spectroscopy of the Ce:BEL crystal revealed a cerium content of 3.9×10^{18} atoms/cc, as compared with 23×10^{18} atoms/cc for YAG. If the cerium content of Ce:BEL can be increased to the level of cerium in YAG, this six-fold increase in concentration could increase the C.I.E. weighted efficiency of Ce:BEL to 1.2 lumens/watt. Since the refractive indices of Ce:BEL are about the same value as the refractive index of YAG, reticulation will yield the same increase in external efficiency.

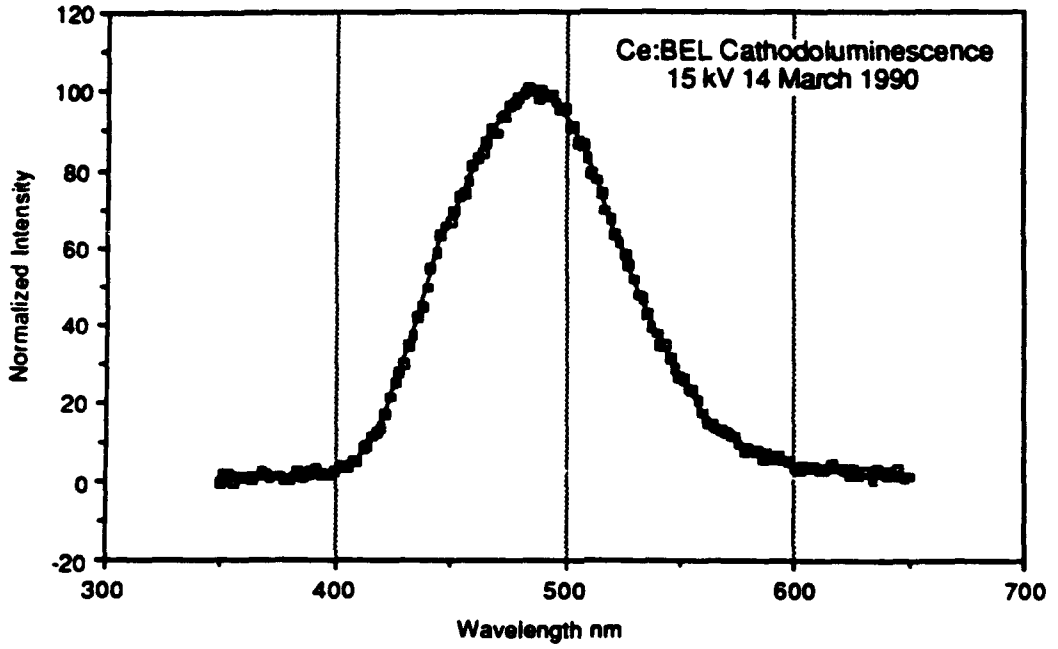

Fig. 3.4.1.1. Cathodoluminescence spectrum of Ce:BEL.

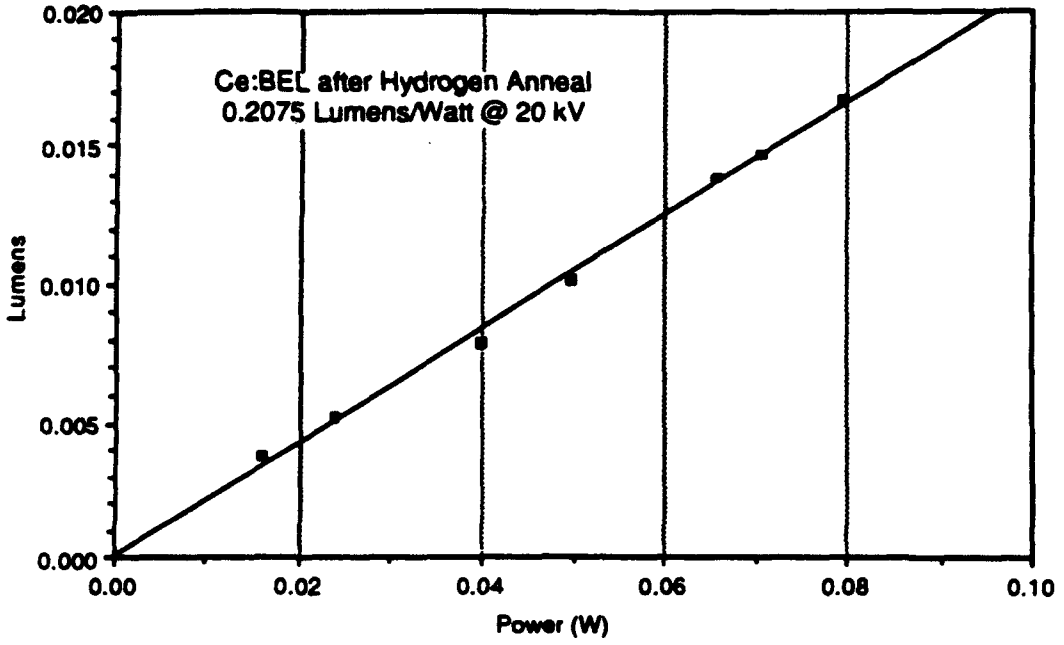

Fig. 3.4.1.2. Cathodoluminescent efficiency of Ce:BEL after hydrogen anneal.

3.4.2 Ce:Y_2SiO_5 and Ce:Gd_2SiO_5

Fig. 3.4.2.1 shows the cathodoluminescent spectrum of the blue emitting cerium activated phosphor Ce:Y_2SiO_5. Since the spectrum of Ce:Y_2SiO_5 peaks at about 390 nm, much of its light output is not visible, reducing its efficiency. The similar phosphor Ce:Gd_2SiO_5 has a spectrum which peaks at 430 nm.

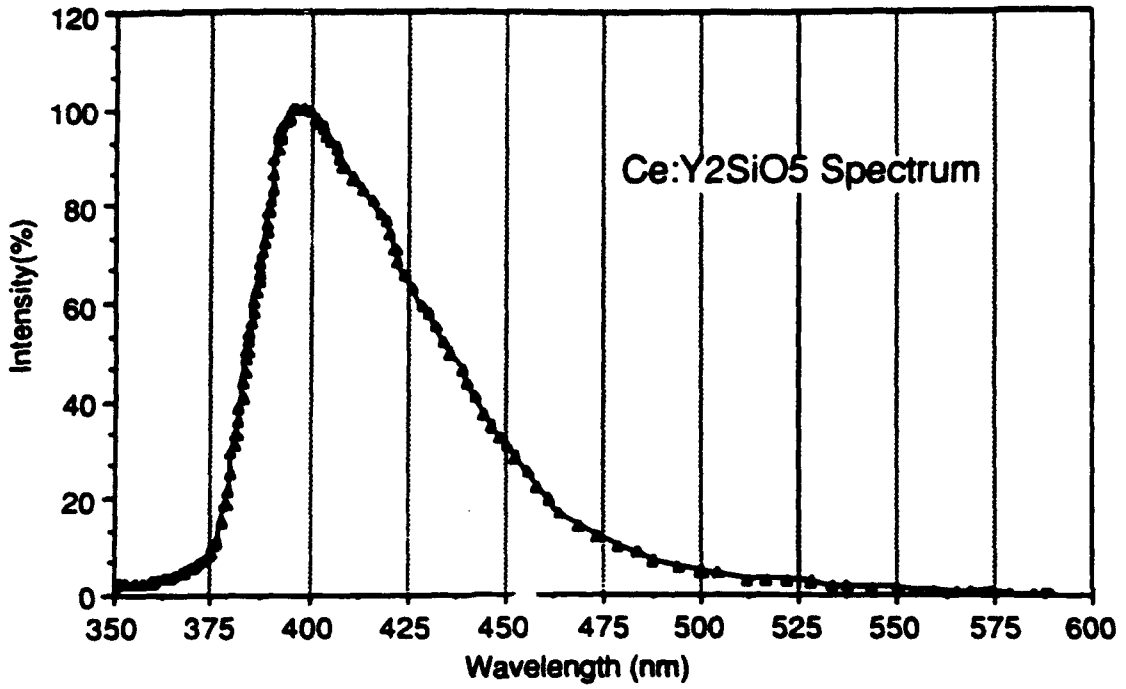

Fig. 3.4.2.1. Cathodoluminescent spectrum of the blue emitting cerium activated phosphor Ce:Y_2SiO_5.

4.0.0 SCALE-UP CONSIDERATIONS

Table 4.0.0.1 summarizes the actual performance of two inch Ce:YAG faceplates and the predicted performance of three and four inch faceplates.

Table 4.0.0.1. Performance data for Ce:YAG faceplates.

	Demonstrated (2")	Predicted (3")	Predicted (4")
Faceplate Luminance, fL	62,700	86,750	86,750
Faceplate Efficiency, L/W	4.84	4.84	4.84
Raster Size, in^2 (cm^2)	1 (6.45)	3.63 (23.4)	5.88 (37.9)
Beam Power, W	90	413	413
Beam Power Density, W/cm^2	14	18	10.9
Faceplate Output, L	435	2000	2000

4.1.0 Crystal Growth Process of Substrate Wafers

The Czochralski method has produced YAG crystal up to three inches in diameter. Experience indicates that four inch crystal is a possibility, but only by a flat interface technique pioneered at Allied-Signal. However, a considerable development effort would be required to attain a process for the Czochralski growth of four inch YAG.

The Heat Exchanger Method (HEM™) is being used for the commercial production of 10" diameter sapphire crystals of very high quality. The growth of YAG crystal to this diameter appears possible. These melting point of YAG (1950°C) is lower than that for Al_2O_3 (2040°C): therefore, current HEM™ furnaces are adequate for growing this crystal. In the case of sapphire (Al_2O_3) crystals grown by HEM™, the processing is carried out under vacuum; however, it is expected that even though the host phosphor materials may be stable under vacuum, it may be necessary to control the atmosphere during growth of doped crystals. The candidate phosphor materials are compatible with using a moybdenum crucible and graphite resistance heat zone of the HEM™ furnace so that these crystals can be grown with existing HEM™ furnaces. In the case of BEL, it would be necessary to set up additional safety procedures for handling BeO raw material and BEL crystals because of their toxic nature.

Crystal Systems Inc. (Dr. Chandra P. Khattak, 27 Congress Street, Salem, MA 01970, Telephone (508)-744-5059) is proposing a program for development of the HEM™ method for crystal growth of candidate phosphor materials. The first phase is a feasibility phase followed by the development phase. During the feasibility stage it is intended to develop procedures so that the growth characteristics of these materials can be established. Crucibles approximately two inches in diameter would be utilized for this effort. It is expected that single crystal material samples would be available for testing for high resolution, high brightness video projection CRT applications. Close cooperation would be maintained with the user so that optimization of this material for the application can be achieved. The problems involved with growth of larger crystals would also be identified during this phase. The development phase will be undertaken depending upon the results of the feasibility phase.

Crystal Systems Inc. expects that the feasibility phase could be completed in approximately a six-month time frame. The cost of their effort would be $50,000 per candidate phosphor material. This cost does not include the raw materials, installation of additional safety features required for beryllium crystal growth, or crystal characterization.

4.2.0 Optical Fabrication

Since the semiconductor industry is now fabricating wafers up to ten and twelve inches in diameter, it is concluded that wafer fabrication will not constrain the development of large diameter single crystal faceplates.

4.3.0 Liquid Phase Epitaxy

Liquid phase epitaxy is routinely carried out for wafers up to three inches in diameter in the preparation of magneto-optical materials. These wafers, however, are thin (0.020 inch) compared with YAG faceplate wafers (0.125 inch). Generally, a slower withdrawal rate from the epitaxy furnace is required for these thick wafers. Liquid phase epitaxy has been demonstrated on four-inch diameter by 0.020 inch thick wafers. There appears to be no fundamental size limitation for the liquid phase epitaxy process.

4.4.0 Photoreticulation

Since the semiconductor industry is now fabricating wafers up to ten and twelve inches in diameter, it is concluded that this processing step will not constrain the development of large diameter single crystal faceplates.

5.0.0 COST ESTIMATES

The following cost estimates for the production of 100 and 200 faceplates per year are calculated on the basis of minimal dedicated facilities being constructed to accomplish each step necessary for the production of faceplates at these quantities. At the 100 and 200 faceplate per year levels, such minimal facilities would still be significantly under-utilized, and the cost per faceplate is high. Section 5.5.0 below contains estimates of faceplate cost with the assumption of 100% utilization of facilities. These costs for 100% utilization will be lower that those which can be anticipated from tolling these steps to outside vendors, perhaps by as much as 25%.

5.1.0 Crystal Growth Process of Substrate Wafers

The following table is an estimate of cost per wafer of substrate wafer growth for three inch and four inch diameter wafers at a 100 and 200 wafer per year production level. Note that the facility is not fully utilized at even the 200/year level.

Cost of YAG Substrate Wafer Crystal Growth at 100% and 80% Yield for Dedicated Facility (maximum facility utilization at 400 faceplates/year)

	Three-Inch Wafers		Four-Inch Wafers	
	100/year	200/year	100/year	200/year
Capital Equipment (5 yr. amort.)	500	250	700	350
Laboratory Facility	600	300	600	300
Materials	150	150	300	300
Fabrication & Maintenance	35	35	50	50
Labor & Employee Overhead	175	175	225	225
Electrical Power	25	25	30	30
Environmental/Toxic Disposal	20	20	30	30
Cost per Wafer at 100% Yield	1505	955	1935	1285
Cost per Wafer at 80% Yield	**1881.25**	**1193.75**	**2418.75**	**1606.25**

5.2.0 Fabrication

The following table is an estimate of cost per wafer of substrate wafer polishing for three inch and four inch diameter wafers at a 100 and 200 wafer per year production level. Note that the facility is not fully utilized at even the 200/year level.

Cost of Wafer Polishing at 100% and 80% Yield for Dedicated Facility (maximum facility utilization at 800 faceplates/year)

	Three-Inch Wafers		Four-Inch Wafers	
	100/year	200/year	100/year	200/year
Capital Equipment (5 yr. amort.)	400	200	450	225
Laboratory Facility	600	300	600	300
Supplies	20	20	25	25
Maintenance	5	5	5	5
Labor & Employee Overhead	50	50	50	50
Environmental/Toxic Disposal	10	10	15	15
Cost per Wafer at 100% Yield	1085	585	1145	620
Cost per Wafer at 80% Yield	**1356.25**	**731.25**	**1431.25**	**775**

5.3.0 Liquid Phase Epitaxy

The following table is an estimate of cost per wafer of phosphor epitaxy for three inch and four inch diameter wafers at a 100 and 200 wafer per year production level.

Cost of Unreticulated Epitaxial Phosphor Faceplates at 100% and 50% Yield for Dedicated Facility (maximum facility utilization at 200 faceplates/year)

	Three-Inch Wafers		Four-Inch Wafers	
	100/year	200/year	100/year	200/year
Capital Equipment (5 yr. amort.)	600	300	750	375
Laboratory Facility	600	300	600	300
Materials (less substrate wafer)	160	180	220	245
Fabrication & Maintenance	15	15	20	20
Substrate Wafer	1115	1115	1485	1485
Labor & Employee Overhead	175	175	225	225
Electrical Power	40	20	60	30
Environmental/Toxic Disposal	20	15	25	20
Cost per Wafer at 100% Yield	2725	2120	3385	2700
Cost per Wafer at 50% Yield	**5450**	**4240**	**6770**	**5400**

5.4.0 Photoreticulation

The following table is an estimate of cost per wafer of wafer reticulation for three inch and four inch diameter wafers at a 100 and 200 wafer per year production level. Note that the facility is not fully utilized at even the 200/year level.

Cost of Faceplate Reticulation at 100% and 80% Yield for Dedicated Facility (maximum facility utilization at 1000 faceplates/year)

	Three-Inch Wafers		Four-Inch Wafers	
	100/year	200/year	100/year	200/year
Capital Equipment (5 yr. amort.)	1150	575	1150	575
Laboratory Facility	800	400	800	400
Supplies (Chemicals, Photomasks)	400	200	450	225
Labor & Employee Overhead	60	60	75	75
Environmental/Toxic Disposal	20	15	25	20
Cost per Wafer at 100% Yield	2430	1250	2500	1295
Cost per Wafer at 80% Yield	**3037.5**	**1562.5**	**3125**	**1618.75**

5.5.0 Cost Summary

The following table is an estimate of cost per wafer of fully processed faceplates of three inch and four inch diameter at a 100 and 200 wafer per year production level. Note that these cost include idle equipment/workspace expenses at even the 200/year level.

Summary Costs of Epitaxial Phosphor Faceplates for Dedicated Facility

	Three-Inch Wafers		Four-Inch Wafers	
	100/year	200/year	100/year	200/year
Cost per Unreticulated Faceplate	**5450**	**4240**	**6770**	**5400**
Cost of Reticulation	3037.5	1562.5	3125	1618.75
Cost per Reticulated Faceplate	**8487.5**	**5802.5**	**9895**	**7018.75**

The following table is an estimate of cost per wafer of fully processed faceplates of three inch and four inch diameter at a 100% utilization of facilities.

Summary Costs of Epitaxial Phosphor Faceplates for 100% Facility Utilization

	Three Inch	Four Inch
YAG Wafer Crystal Growth	850	1200
YAG Wafer Polishing	265	285
Bare YAG Wafer Ready for Epitaxy	1115	1485
Epitaxial Phosphor Faceplate (Unreticulated)	4240	5400
Photoreticulation	600	650
Reticulated Epitaxial Phosphor Faceplate	4840	6050

6.0.0 RECOMMENDATIONS AND CONCLUSIONS

Ce:YAG epitaxial phosphor faceplates are capable of 2000 lumens light output in either their reticulated or facet-textured form in a 2.75-inch diagonal raster. Higher light outputs can be obtained from larger diameter faceplates, but the largest available YAG crystals are presently three-inches in diameter. Single crystals of YAG greater than three inches in diameter can be obtained only after a further development of either the Czochralski or HEM™ techniques.

Wafer flatness is a requirement for photolithographic reticulation over a large diameter faceplate. Epitaxy requires a surface which is free of even the smallest scratch or defect. Thus, polishing of YAG wafers to higher flatness and perfection would be a suitable area for research.

The reticulation process involves etching in hot phosphoric acid. A rapid etching rate has to be used to effect the reticulation before the etching mask is dissolved. This technique is marginally successful, and defects are introduced into the faceplate as the mask is undercut in some areas. Further research on alternative masking materials and etching methods is necessary.

Reticulation is most effective when there is a minimum in the ratio of the mesa top to bottom area, but this pointed reticulation gives "ghost" images of the raster in the six-fold symmetry of the reticulation. This "ghosting" effect must still be quantified.

Ce:$Gd_3Al_5O_{12}$ (Ce:GdAG, red), Ce:$Y_3Al_5O_{12}$ (Ce:YAG, green), and Ce:$La_2Be_2O_5$ (Ce:BEL, blue), appear to be an appropriate trio of epitaxial phosphors for a high intensity color projection display. Ce:BEL has not as yet been bonded to a CRT neck assembly, so that its suitability as a faceplate material is still unknown. Research on such bonding would be appropriate.

The growth of large crystals of $Gd_3Al_5O_{12}$ as substrates for epitaxial red phosphor faceplates would be a suitable area for research.

Further research on alternative masking materials and etching methods, and quantification of the reticulation "ghosting effect, is also required.

Ce:$Gd_3Al_5O_{12}$ (Ce:GdAG, red), Ce:$Y_3Al_5O_{12}$ (Ce:YAG, green), and Ce:$La_2Be_2O_5$ (Ce:BEL, blue), appear to be an appropriate trio of epitaxial phosphors for a high intensity color projection display. The growth of large crystals of $Gd_3Al_5O_{12}$ as substrates for epitaxial red phosphor faceplates would be a suitable area for research.

The HEM™ method seems to be the most appropriate path to large diameter crystals. This would require further development, as proposed by Crystal Systems, Inc.

Prepared for:

TRIDENT INTERNATIONAL, INC.
Orlando, Florida

Final Report

THE STUDY OF THE PERFORMANCE OF A YAG FACEPLATE

February 3, 1992

Prepared by:

Eric H. Ford

OPTICAL RESEARCH ASSOCIATES
550 N. Rosemead Boulevard
Pasadena, California 91107
(818) 795-9101

1.0 BACKGROUND

Trident International, Inc (TII) has funded Optical Research Associates (ORA) to undertake a study to determine the effects on the performance of a CRT of a change in faceplate material from a relatively low index of refraction glass (Nd = 1.537) to Yttrium Aluminum Garnet (YAG) crystal with relatively high index (1.832). The two primary goals of the study are to (1) evaluate the effect of anti-reflection coatings in reducing reflection losses at the glass boundaries and halation effects and (2) to determine the optimum index matching fluid and analyze its effectiveness in producing an optically coupled system. Since ORA's primary area of expertise is optical design and optical system engineering, and not coating design, ORA sub-contracted the services of Bruce Reinbolt of Santa Barbara Applied Optics (SBAO) to perform the coating portion of the study.

2.0 PROJECTION SYSTEM CHARACTERISTICS

Since the phosphor is deposited or grown directly on the faceplate material, it is in optical contact with the faceplate, eliminating most of the losses in injecting the emitted energy into the faceplate material. However, since the phosphor emits over a wide angular range, a significant portion of the energy can fall outside of the critical angle of the faceplate material. For the older faceplate materials (index = 1.537), the critical angle is 40.6° into air. Energy at angles greater than 40.6° is "waveguided" (totally internally reflected through multiple bounces) radially out to the edge of the faceplate and lost to the system.

CRT projection systems commonly are designed for *f* numbers approaching F/1.0, and possibly faster. In addition, due to the geometry of typical projection systems, the required field of view is often 25° -30° half-angle, with an aperture stop location central to the projection lens to reduce distortion and aid field correction. As a result, chief ray angles (the "central" ray of the optical bundle) are often steep at the focal plane (phosphor surface). It is normal for the chief ray angle at the faceplate to exceed the object field chief ray angle for air-coupled systems, and for optically coupled systems, for the chief ray angle to be nearly twice as steep as the object field chief ray angle. Thus, for CRT projection systems with a half field projection angle of 25°, the chief ray angle at the phosphor would be greater than 50°, if it were in air, and is reduced to between 30° and 40° in the faceplate material. To this must be added the angle due to the *f* number of the lens system, bringing the steepest ray angle to greater than 70° equivalent in air or nearly 40° in the faceplate glass.

From this quick analysis, it can be seen that the CRT projection system works at very steep angles, and that air-glass boundaries can have a profound effect on the system performance. It also indicates the reason why optically coupled or fluid coupled systems are in use for projection systems. Fluids are often used to cool the CRT faceplate when very high luminous output is required. In order to reduce the angles at which rays enter the faceplate-coolant-window assembly, the strongly negative, rearmost field lens is used as the window of the coolant chamber. The steepest bundles from the edge of the field are incident upon the curved front surface of the field lens at an incidence angle much closer to normal than is the case with a flat coolant window. This benefits the transfer of energy, as the fluid then reduces the index difference between the faceplate and the adjacent lens (no glass to air boundary).

Several effects take place at the boundary of the faceplate and coolant fluid which affect system performance. These are all related to the reflection and scattering losses at the interface. Energy scattered or reflected at the faceplate/coolant boundary are manifested as halation of the image or as contrast decrease due to broad angle scattering. Halation is probably due to the first reflection from the boundary to the phosphor surface and back to the boundary, where it is mostly transmitted as a defocused image of the source. Optimization of the characteristics of this boundary is discussed in section 5.0.

3.0 OPTICAL EFFECTS OF YAG FACEPLATES

When the index of the faceplate is increased from the original 1.537 to that of YAG (1.832), the critical angle becomes approximately 33°. This would imply that a YAG faceplate in air would tend to put out significantly less power than a lower index faceplate, since the angular distribution of the energy inside the faceplate is similar, but the part which can pass through into the air is limited to 33° instead of the 40°+ of the lower index faceplate. Stating it differently, for the same *f* number optical system, the solid angle in the faceplate is smaller for the higher index material, and therefore, a smaller cone of the emitted energy is injected into the optical system. The magnitude of this decrease in screen irradiance is $N1^2/N_2^2 \approx 0.70$, or a drop of 30%.

This would only hold true if the source in both faceplates were perfectly matched to the faceplate index, so that no boundary was encountered in passing from the phosphor into the faceplate. However, if a boundary (differential index) exists, then the difference in screen irradiance would not be seen, as the source output characteristics would be modified equivalently to the lens *f* number, cancelling the effect.

It would seem that this effect is independent of whether the lens system is optically coupled or not and this would indicate that the optimum faceplate material is the one with the lowest possible index, in order to maximize the collected energy.

The effectiveness of fluids in coupling the faceplate to the optical system is also dependent on the faceplate index, with higher index fluids required to efficiently couple higher index faceplates. This will be discussed in more depth later in this report.

4.0 PROJECTION LENS SYSTEMS

In order to evaluate the effects of the high index faceplate material on the optical system, ORA requested that TII supply a typical lens system from an existing projection system to use for the analysis. TII forwarded a patent supplied by US Precision Lens Corporation to be used for this purpose. TII expressed interest primarily in optically coupled systems, in which the CRT faceplate is coupled to the lens system through the use of a index matching fluid.

ORA used the patent (U.S. Patent 4,900,139, included as Appendix A) to generate models of lens systems for analysis. Two different configuration were modeled: one with an air gap between the field lens and the flat faceplate/coolant assembly, and the other with the field lens in optical contact (through a fluid) with the faceplate. Both lenses from the patent were poorly corrected from the patent data, but were reoptimized by releasing the aspheric coefficients and several variable airspaces to hold first order properties (focus and magnification).

Figure 1 shows the optically coupled model and Figure 2 shows a projection lens with a flat window on the coolant chamber and an air gap to the field lens. Correction is significantly better with the second, air-spaced design due to the fact that it has three aspheric, plastic elements and an additional degree of freedom in the bending of the field lens. However, both are representative of types of lenses used in fast CRT projection systems. Ray angles are steeper in the faceplate for the optically coupled system, but incidence angles are shallower at the coolant window interface. These designs are used in the analysis which follows.

5.0 ANALYSIS OF YAG FACEPLATE PERFORMANCE

In order to reduce reflection loss at the YAG faceplate fluid interface, two approaches were investigated. This involved (1) varying the refractive index of the coolant fluid, or (2) coating the faceplate with a matching layer. It will be seen that either adding a matching

layer or increasing the index of the cooling fluid can reduce the reflection losses to that of the current 1.537 index faceplate systems or better.

The spectral performance of the original faceplates are calculated, as well as the performance of the YAG faceplates with various index fluids and coatings. The nomenclature used is as shown below:

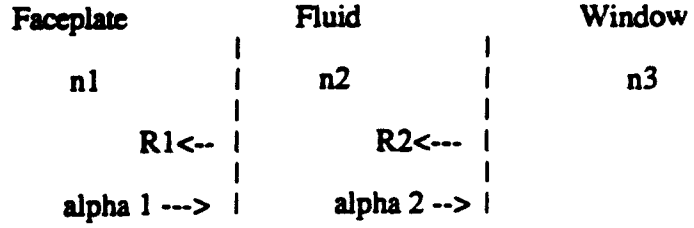

where R1 is the reflection at the faceplate/fluid boundary, and
R2 is the reflection at the fluid/window boundary.

The index of the current phosphor faceplate is 1.537 used with a fluid of index 1.41 and a front panel of 1.572. The reflections at the interfaces for this system are R1 = 0.2% and R2 = 0.3%. Changing the faceplate to YAG increases the index to about 1.83, which results in an R1 = 1.6%. By changing the index of the fluid, the value of R1 can be reduced as shown in Figure 3. An index of at least 1.6 would be required to restore the R1 values of the current system. The reflection losses for the YAG system become worse with angle as shown in Figure 4, but again can be improved with increasing fluid index. An alpha 1 of 33° was used as the incidence angle at the faceplate fluid interface based on information from Trident.

Since it may be difficult to attain an appropriate fluid with the proper index, the other option is to coat the faceplate with a single layer matching film. A film of index nf would be positioned as shown below:

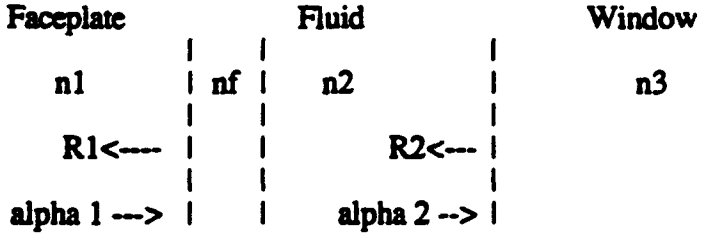

where nf is the matching single layer coating.

Choosing an index of approximately 1.6 will reduce the reflection at one wavelength as shown in Figure 5 and 6. The performance of a thin film interference coating varies as a function of wavelength, which is shown in Figure 7 for nf = 1.6 at 0 and 33° incidence on the YAG/film interface. A film of this type is normally deposited at temperatures of 200°C to 300°C to improve its durability. It would be more efficient to deposit this film prior to bonding the faceplate if processing conditions are not hostile to the coating. A possible candidate for the film would be Al203. There are other materials between 1.5 and 1.7 which may also be possibilities. For instance, the performance of SiO, which has an index of 1.7 and is very durable, is shown in Figure 8. This material may be even more appropriate for the optically coupled systems with steeper angles than those modeled here.

6.0 CHROMATIC FILTERS

An additional question was raised as to whether thin film spectral filters could be used to modify the performance of the YAG faceplate, shown in Figure 9 (provided by Trident via fax on 10/09/91), to an F-53 (green) or a P-22 (red). Figure 10 shows the spectral distribution of the the current, lower index faceplate, also provided by Trident (fax, 10/11/91).

It is possible to produce distributions similar to the P-23 (blue) in Figure 10 for the red and green filters. This would require that the spectral range performance for the green and red filters be defined with wavelength and transmittance tolerances for system-to-system variation. Filter glasses would, however, be the best choice for this application, as they would not suffer from the angular dependence of thin film filters. They would also be measurably less expensive to produce in the required 4 inch diameters than their thin film counterparts.

Using optical thin film filters, it is possible to divide and/or isolate certain portions of the YAG spectral response. Shown as sketched lines on the Figure 9 YAG spectral distribution curve are two edge filters. These are simple thin film designs, but they have several drawbacks in this application. The incidence angles on filters with current designs will range over at least 30°. The cut-off edge of any thin film filter shifts toward shorter wavelength as the angle increases, resulting in a color variation of the output. This phenomenon does not occur with filter glass.

The surface to be coated would be at least 4 inches in diameter, and if a narrow spectral spike is required, such as that shown in Figure 10 for the P-22 (red) band, with rigid spectral requirements, it would result in a low volume, low yield (expensive) part.

To reduce non-uniformity in the coating thickness, it is desirable that the filter be coated on a flat surface. If the optical design requires that the coating be placed on a strongly curved surface, cost can be expected to increase. Coating yields for multilayer filters are are typically lower than those for anti-reflection coatings.

7.0 CONCLUSIONS

ORA, with the help of Bruce Reinbolt of SBAO, has analyzed the characteristics of CRT faceplates to evaluate the effects of using a high index YAG material. Uncoated and with poorly index-matched fluids, reflection losses at the faceplate/fluid interface are nearly an order of magnitude greater than for current, low index faceplates.

From an optical performance viewpoint, low index faceplates may perform better than high index faceplates in energy collection, if the phosphor is index matched to the faceplate.

The halation effects that were seen in the original test plates were probably caused by the high reflection losses at the YAG/fluid (or YAG/air, if observed) interface. Reduction of this reflection can be accomplished by increasing the fluid index from 1.41 to between 1.58 and 1.75. It can also be improved by using the existing fluid if a film of index 1.5 to 1.7 is placed on the YAG faceplate. Implementing either of these solutions will increase the efficiency of the system to some degree by reducing reflection losses and decreasing halation effects.

Chromatic filtering of the spectral output of the phosphor is probably accomplished most effectively by filter glass materials, which are much less angularly sensitive than thin film filters.

FIGURE 1

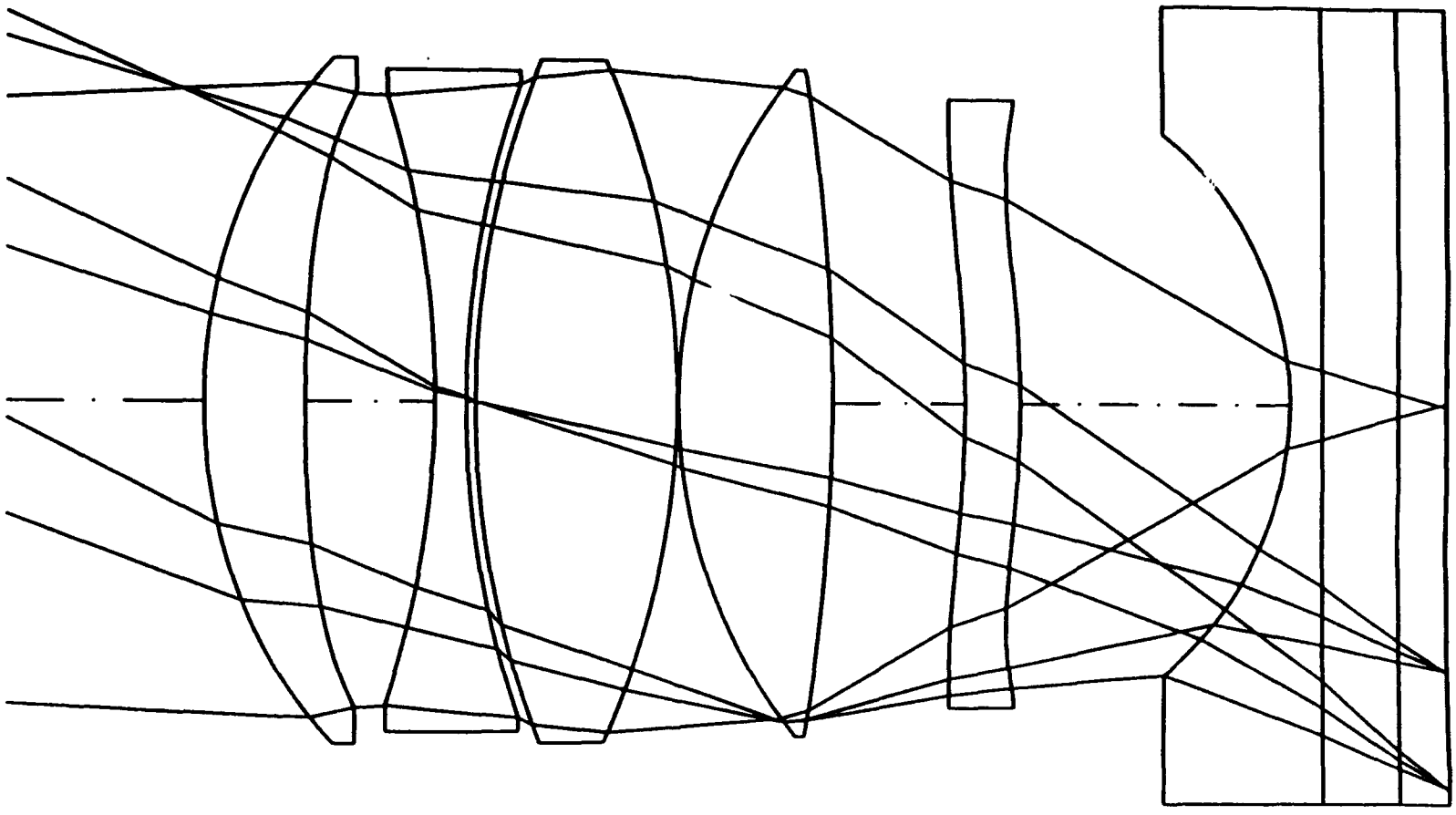

27.78 MM

Optically Coupled CRT Projection Lens

Position: 1
Scale: 0 30

ORA 3-Feb-92

FIGURE 2

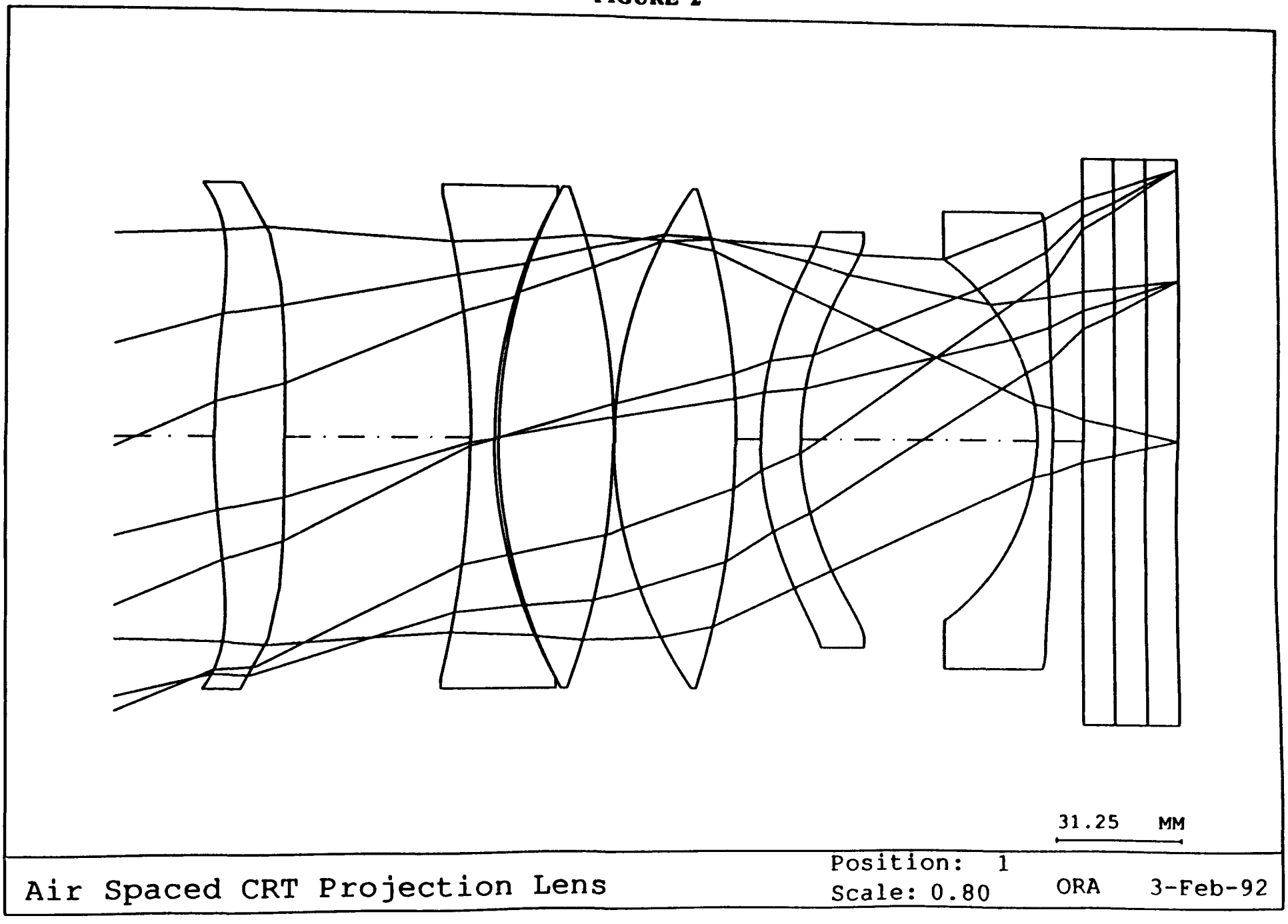
31.25 MM
Air Spaced CRT Projection Lens
Position: 1
Scale: 0.80
ORA
3-Feb-92

FIGURE 3

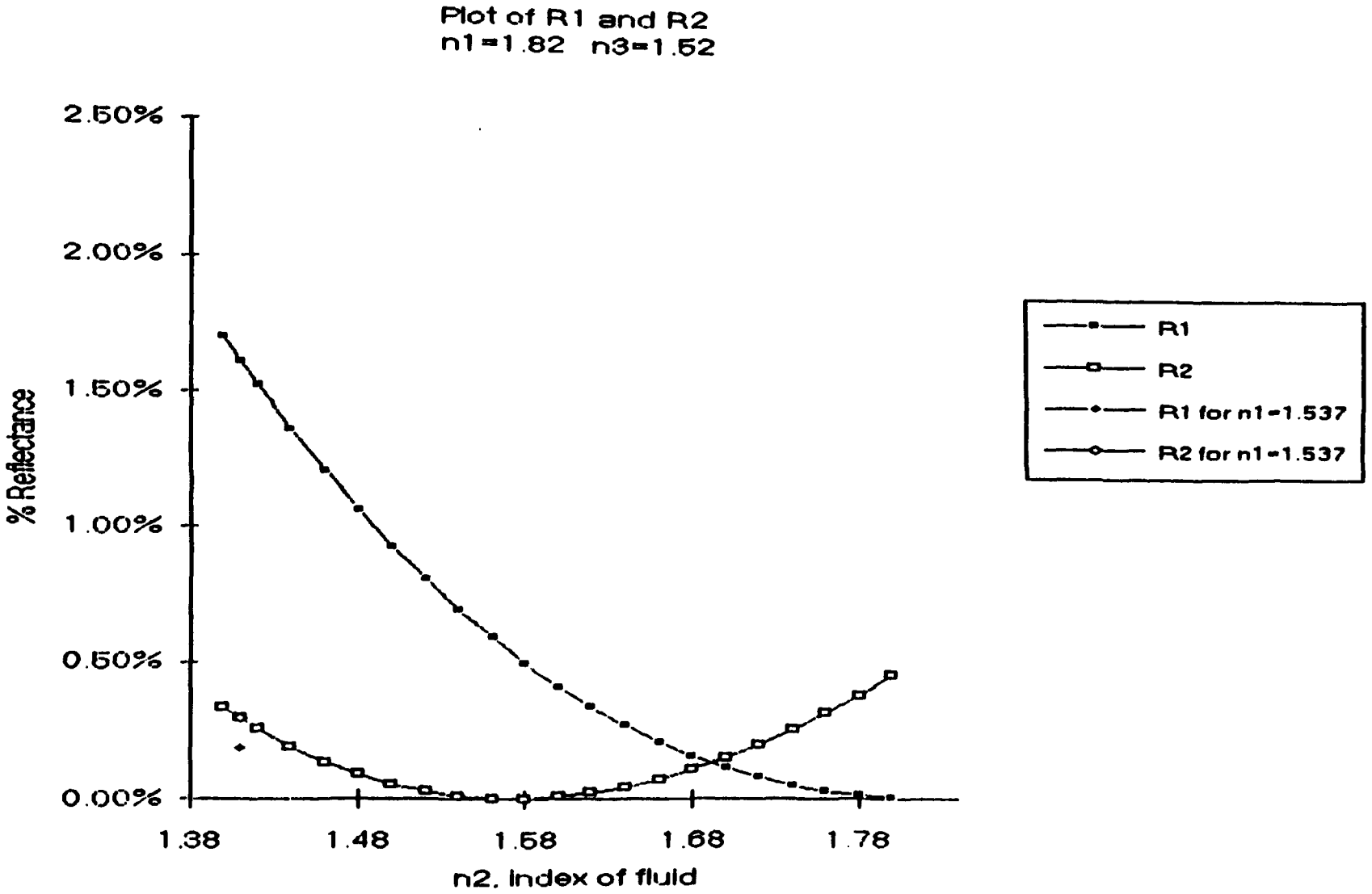
Plot of R1 and R2
n1=1.82 n3=1.52
2.50%
2.00%
1.50%
1.00%
0.50%
0.00%
% Reflectance
1.38
1.48
1.58
1.68
1.78
n2, Index of fluid
R1
R2
R1 for n1=1.537
R2 for n1=1.537

FIGURE 4

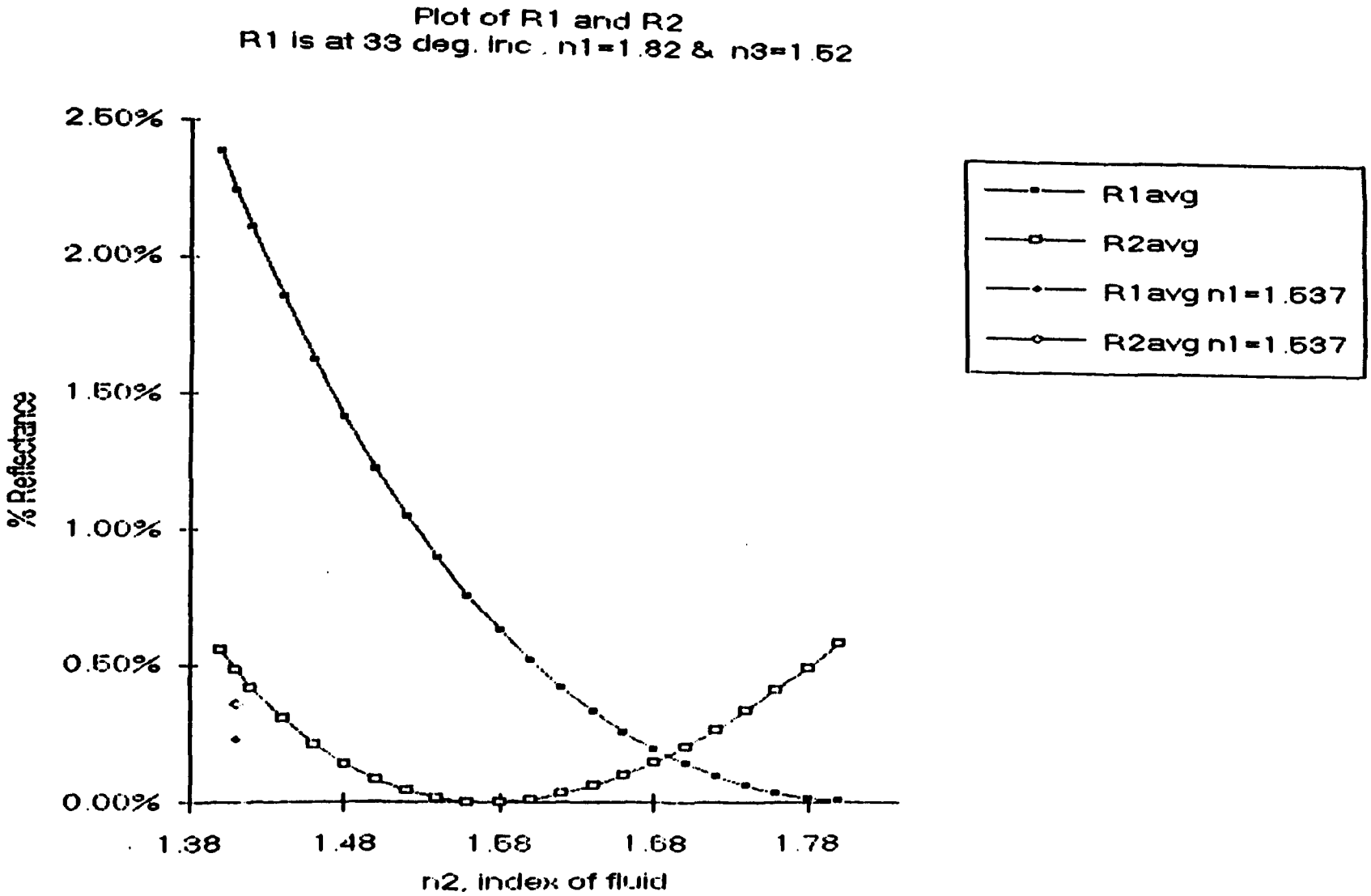
Plot of R1 and R2
R1 is at 33 deg. Inc . n1=1.82 & n3=1.52
2.50%
2.00%
1.50%
1.00%
0.50%
0.00%
% Reflectance
1.38
1.48
1.58
1.68
1.78
n2, index of fluid
R1avg
R2avg
R1avg n1=1.537
R2avg n1=1.537

FIGURE 5

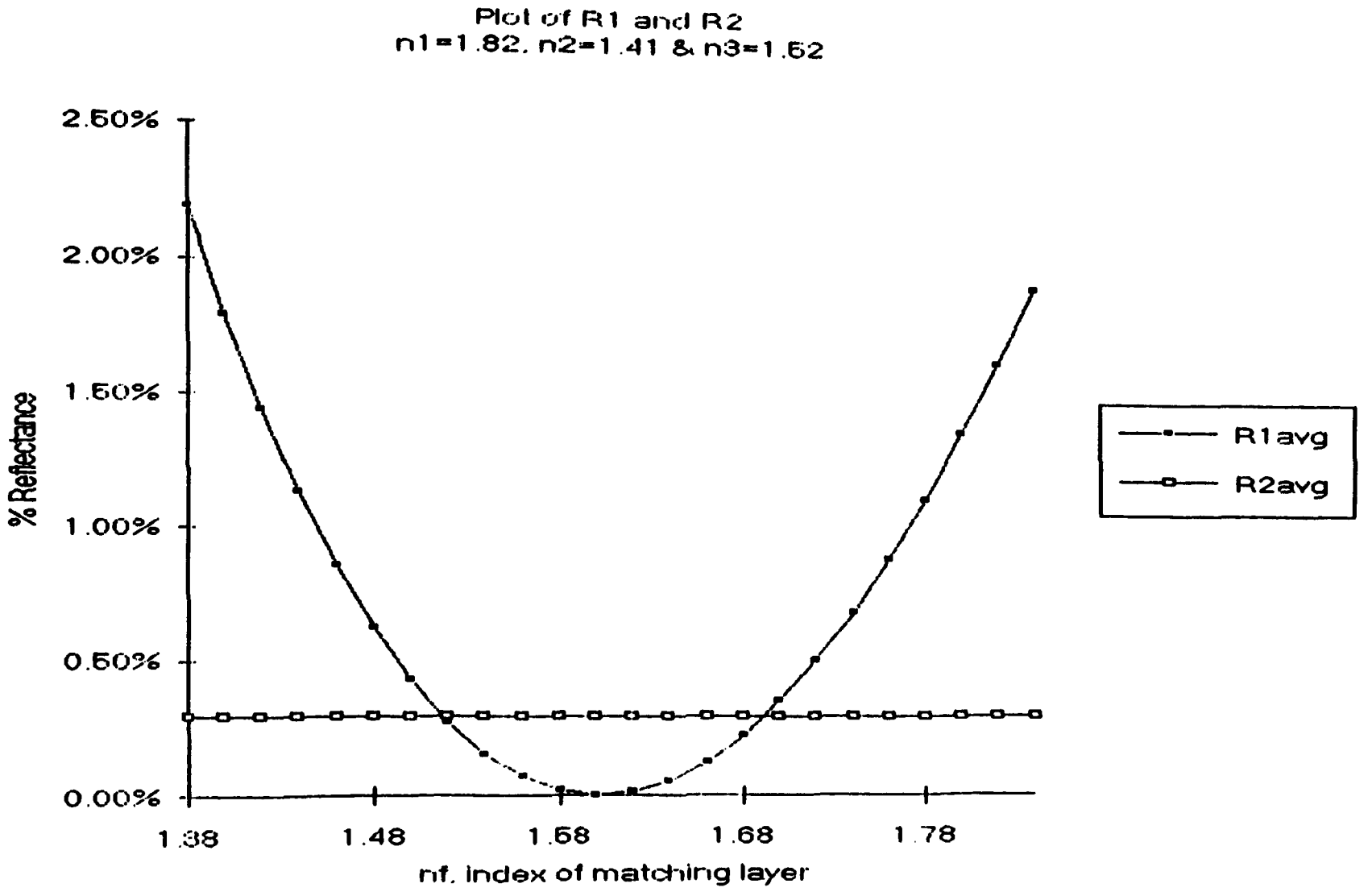
Plot of R1 and R2
n1=1.82, n2=1.41 & n3=1.62
2.50%
2.00%
1.50%
1.00%
0.50%
0.00%
% Reflectance
1.38
1.48
1.58
1.68
1.78
nf, index of matching layer
R1avg
R2avg

FIGURE 6

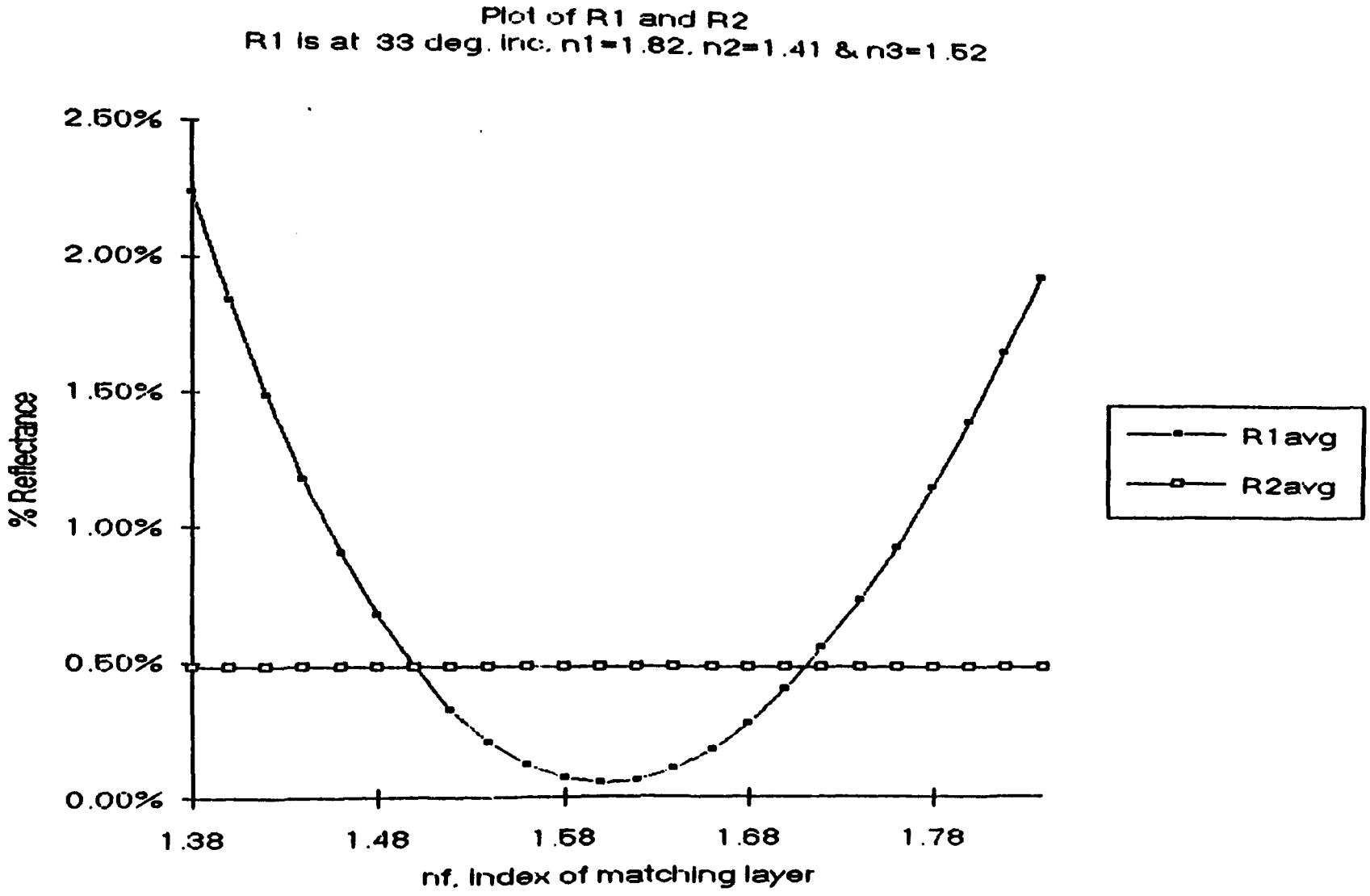
Plot of R1 and R2
R1 is at 33 deg. inc. n1=1.82, n2=1.41 & n3=1.52
2.50%
2.00%
1.50%
1.00%
0.50%
0.00%
% Reflectance
1.38
1.48
1.58
1.68
1.78
nf, Index of matching layer
R1avg
R2avg

FIGURE 7

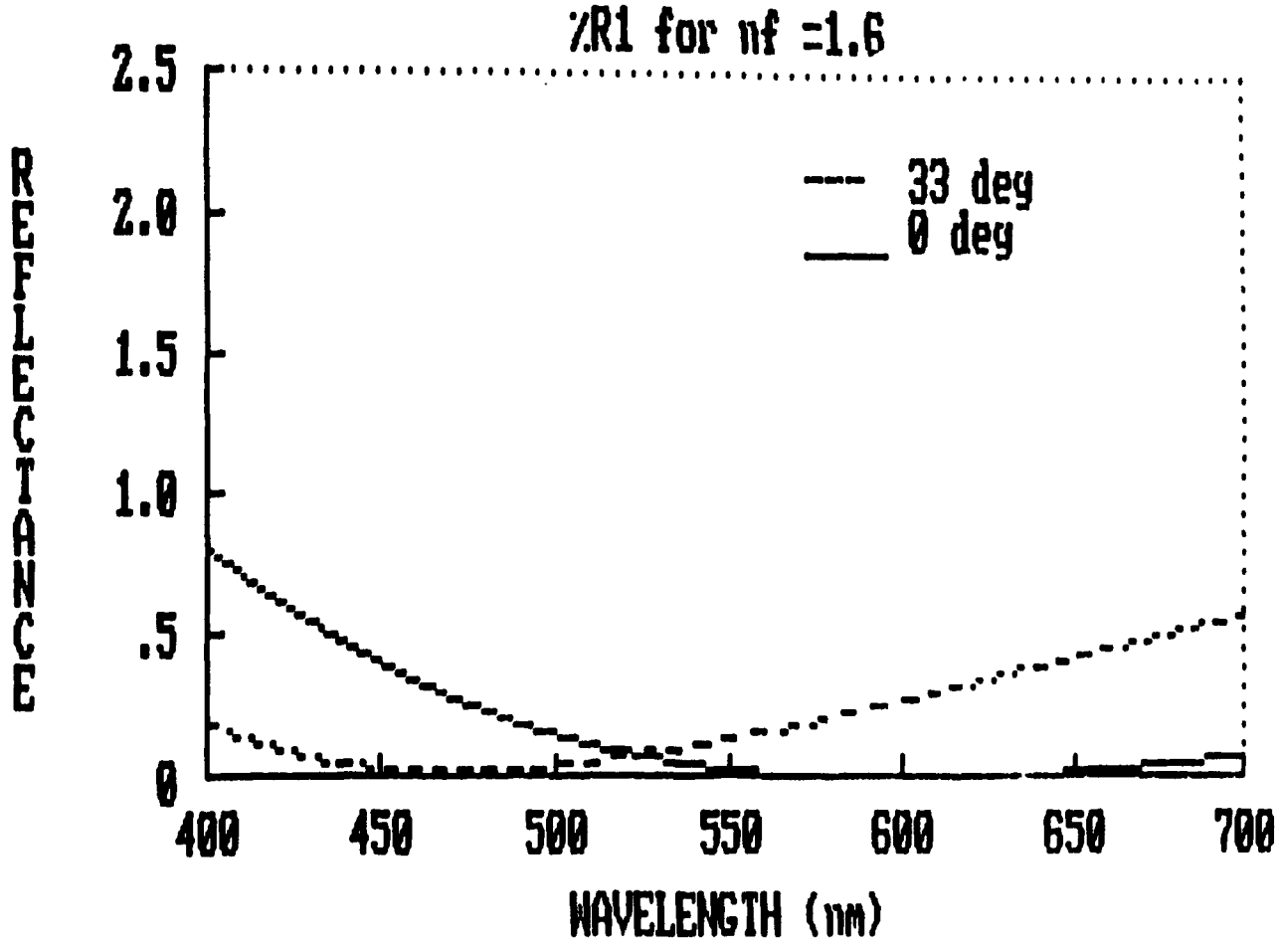
%R1 for nf =1.6
2.5
2.0
1.5
1.0
.5
0
REFLECTANCE
33 deg
0 deg
400
450
500
550
600
650
700
WAVELENGTH (nm)

FIGURE 8

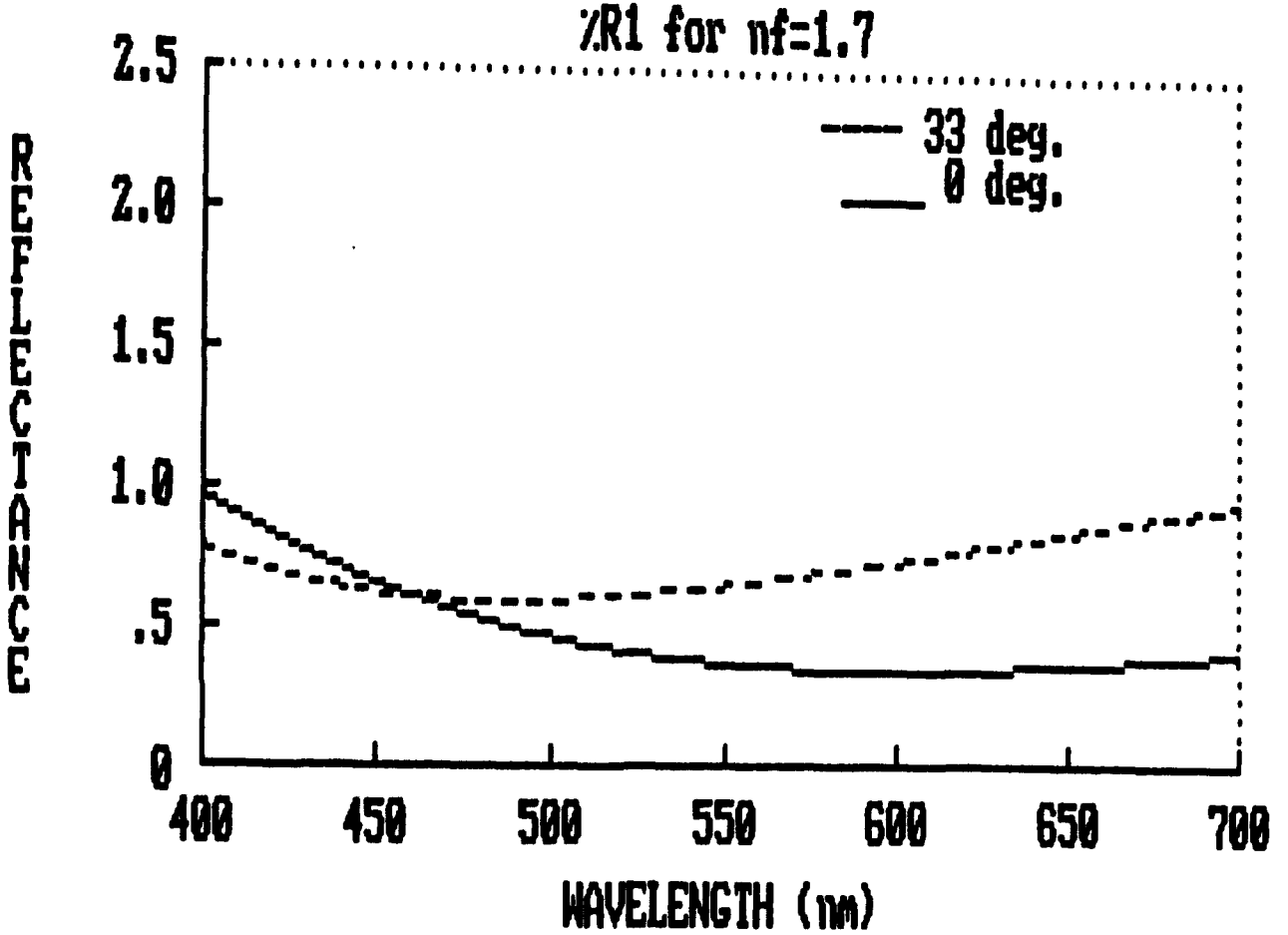
%R1 for nf=1.7
33 deg.
0 deg.
REFLECTANCE
2.5
2.0
1.5
1.0
.5
0
400
450
500
550
600
650
700
WAVELENGTH (nm)

FIGURE 9

01-D

Maximum Useful Screen H (mm)	V (mm)	B (mm)	Focus Type	Cathode	Screen Panel t (mm) (Nd=1.537)	Liquid t (mm) (Nd=1.41)	Front Panel t (mm) (Nd=1.572)
82	64	104	Electro Static	Oxide	4.0		
112	87	141.8	Electro Static	Oxide	5.75		
112	87	141.8	Electro Static	Oxide	5.75		
156	116	194.4	Electro Static	Oxide	7.0		
156	116	194.4	Magnetic	Impregnated	7.0		
82	64	104	Electro Static	Oxide	4.0	3.2	4.0
112	87	141.8	Electro Static	Oxide	5.75	5.0	5.75
112	87	141.8	Electro Static	Oxide	5.75	5.0	5.75
156	116	194.4	Electro Static	Oxide	7.0	4.3	7.0
156	116	194.4	Magnetic	Impregnated	7.0	4.3	7.0
82	64	104	Electro Static	Oxide	4.0	For 36" & 41" system	
112	87	141.8	Electro Static	Oxide	5.75	For 41" & 45" system	
112	87	141.8	Electro Static	Oxide	5.75	For 48" system	

Spectral Energy Distribution Curves

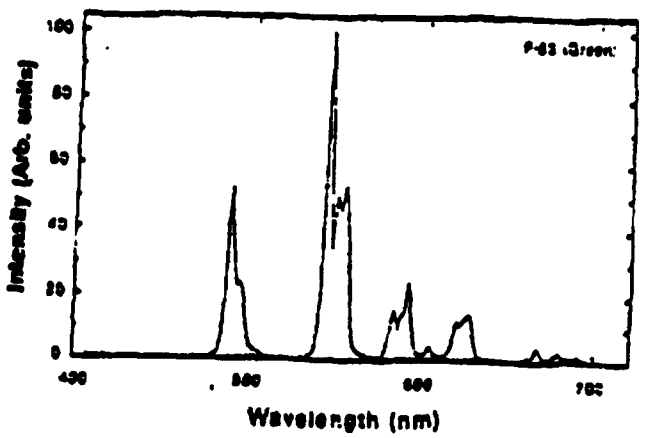

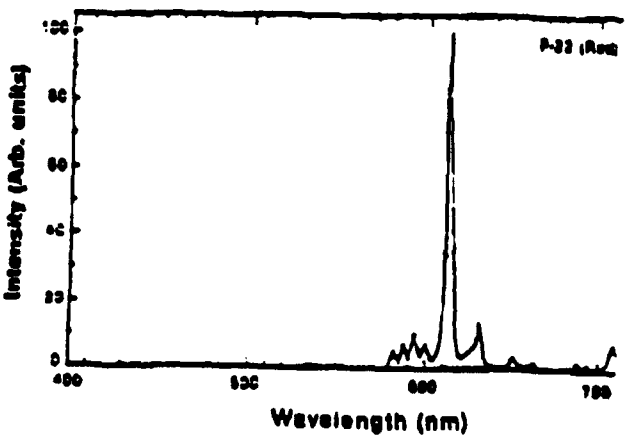

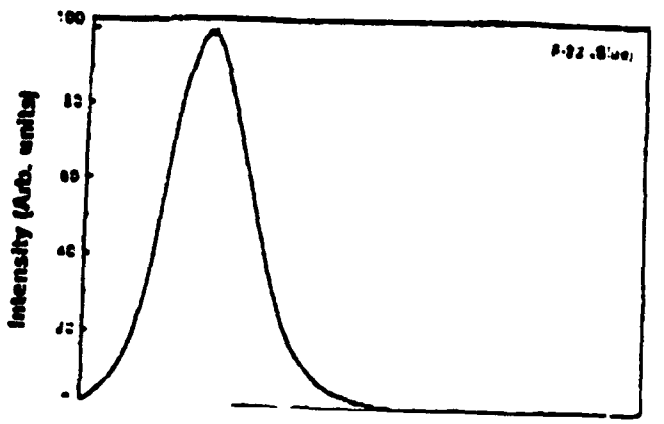

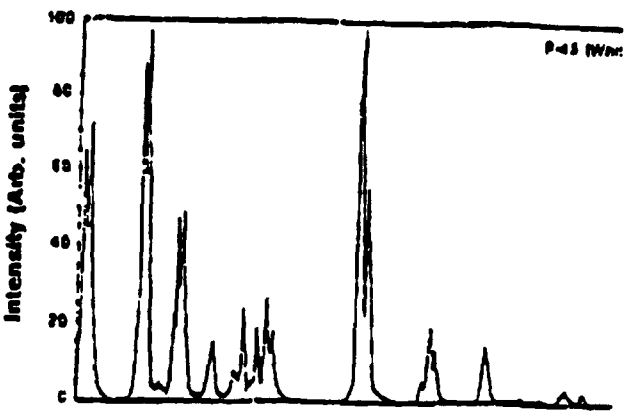

FIGURE 10

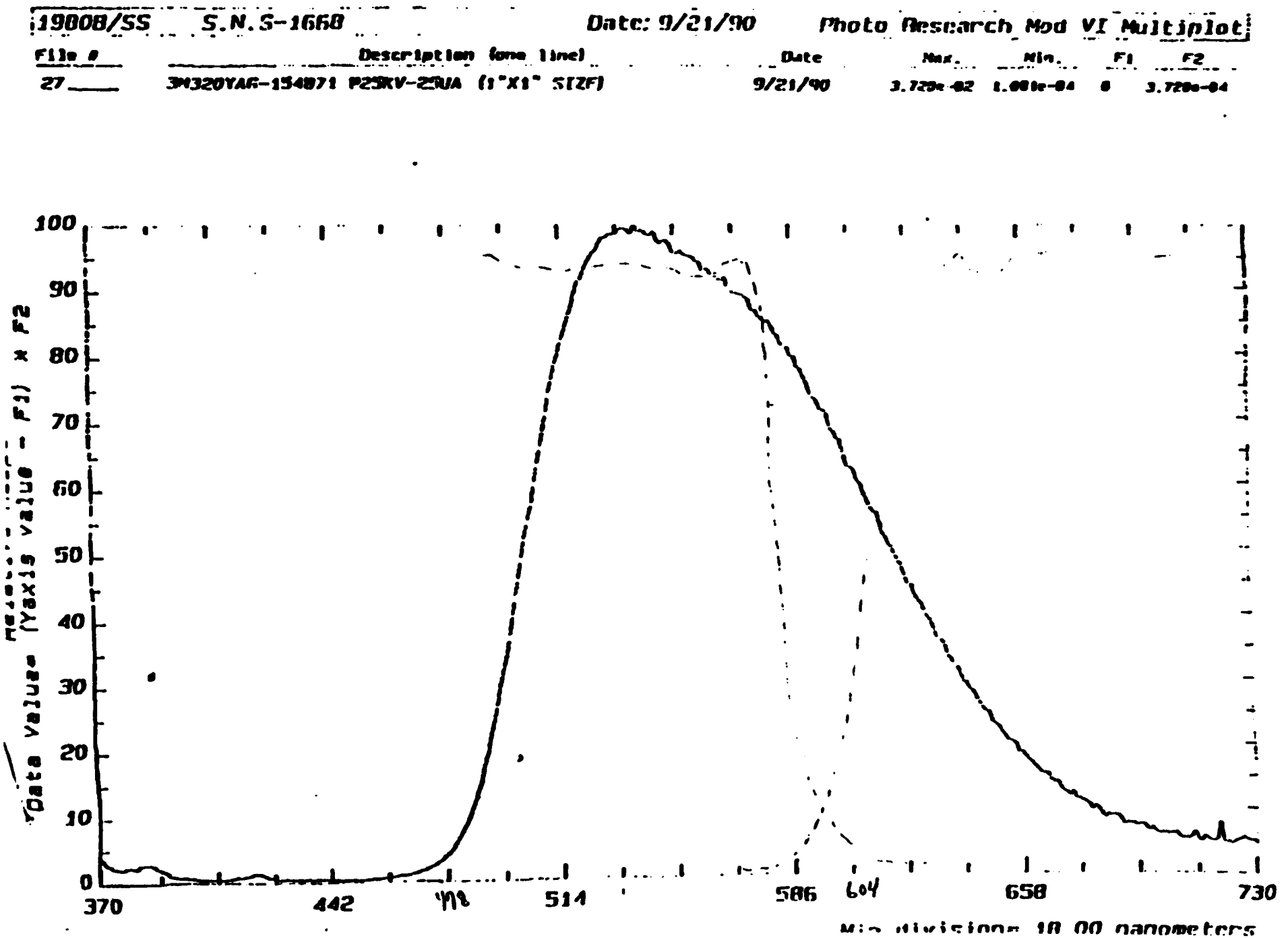
19008/SS S.N.S-1668 Date: 9/21/90 Photo Research Mod VI Multiplot
File # Description (one line) Date Max. Min. F1 F2
27 3M320YAG-154871 P25KV-25UA (1"X1" SIZE) 9/21/90 3.729e-02 1.081e-04 0 3.729e-04
Data Value (Yaxis value - F1) x F2
100
90
80
70
60
50
40
30
20
10
0
370
442
514
586
604
658
730
Min divisions 10.00 nanometers

APPENDIX A

Projection Lens Patent

United States Patent [19]

Kreitzer

[11] **Patent Number: 4,900,139**

[45] **Date of Patent: Feb. 13, 1990**

[54] **COLOR CORRECTED PROJECTION LENS**

[75] **Inventor:** Melvyn H. Kreitzer, Cincinnati, Ohio

[73] **Assignee:** U. S. Precision Lens, Inc., Cincinnati, Ohio

[21] **Appl. No.:** 266,234

[22] **Filed:** Oct. 28, 1988

Related U.S. Application Data

[63] Continuation of Ser. No. 48,026, May 11, 1987, abandoned.

[51] **Int. Cl.**[4] G02B 13/18; G02B 9/00; G02B 3/00

[52] **U.S. Cl.** 350/432; 350/463; 350/412

[58] **Field of Search** 350/412, 432, 463, 465

[56] **References Cited**

U.S. PATENT DOCUMENTS

3,446,547	5/1969	Jeffree	350/465
4,620,773	11/1986	Fukuda	350/432
4,682,862	7/1987	Moskovich	350/432
4,776,681	10/1988	Moskovich	350/432
4,810,075	3/1989	Fukuda	350/432
4,824,224	4/1989	Fukuda et al.	350/432

FOREIGN PATENT DOCUMENTS

0198016	11/1983	Japan	350/432

Primary Examiner—Bruce Y. Arnold
Assistant Examiner—Ronald M. Kachmarik
Attorney, Agent, or Firm—Robert H. Montgomery

[57] **ABSTRACT**

A lens comprising from the image side a first lens unit which is a positive element with at least one aspheric surface; a three element lens unit consisting of a biconcave element, a biconvex element and another positive component, in that order; a third lens unit having a strongly concave image side surface and which serves as a field flattener and to correct the Petzval sum of the lens.

59 Claims, 2 Drawing Sheets

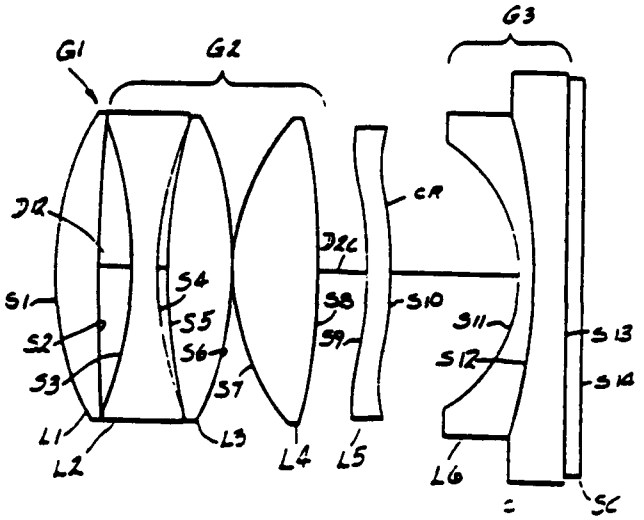

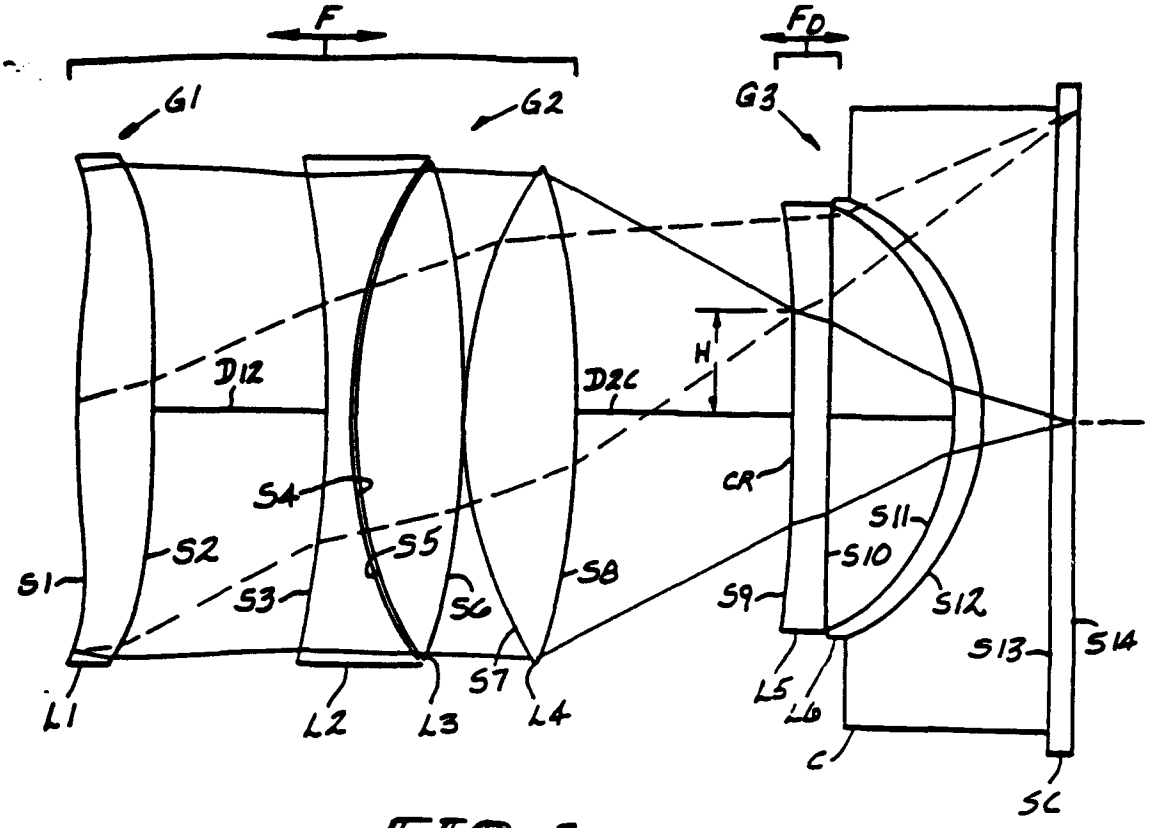
F
FD
G1
G2
G3
D12
D2C
H
S1
S2
S3
S4
S5
S6
S7
S8
S9
S10
S11
S12
S13
S14
CR
L1
L2
L3
L4
L5
L6
C
SC

FIG-1

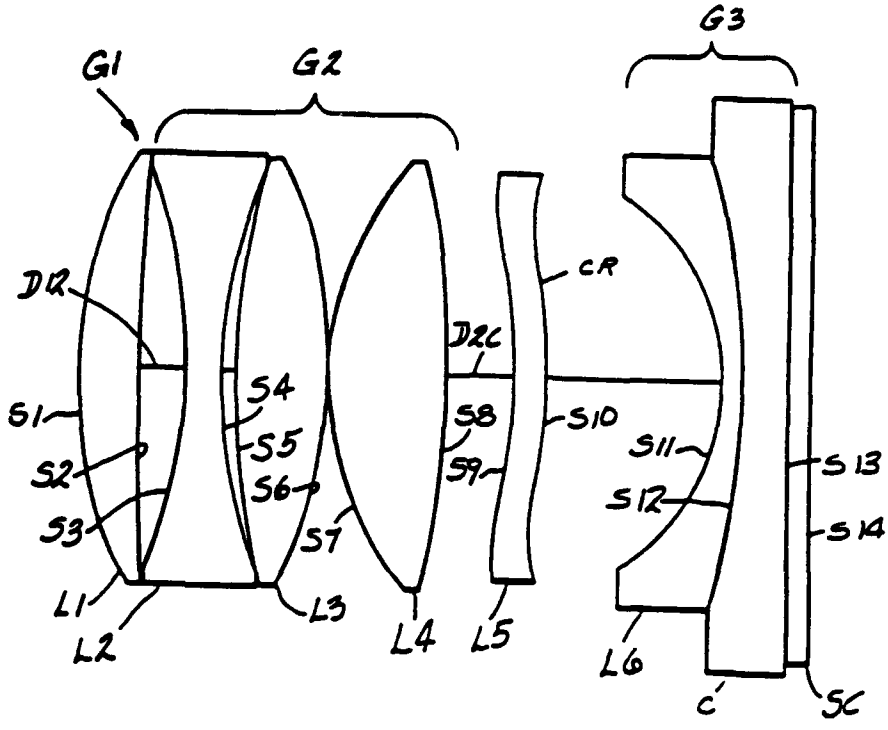
G1
G2
G3
D1
D2C
CR
S1
S2
S3
S4
S5
S6
S7
S8
S9
S10
S11
S12
S13
S14
L1
L2
L3
L4
L5
L6
C
SC

FIG-2

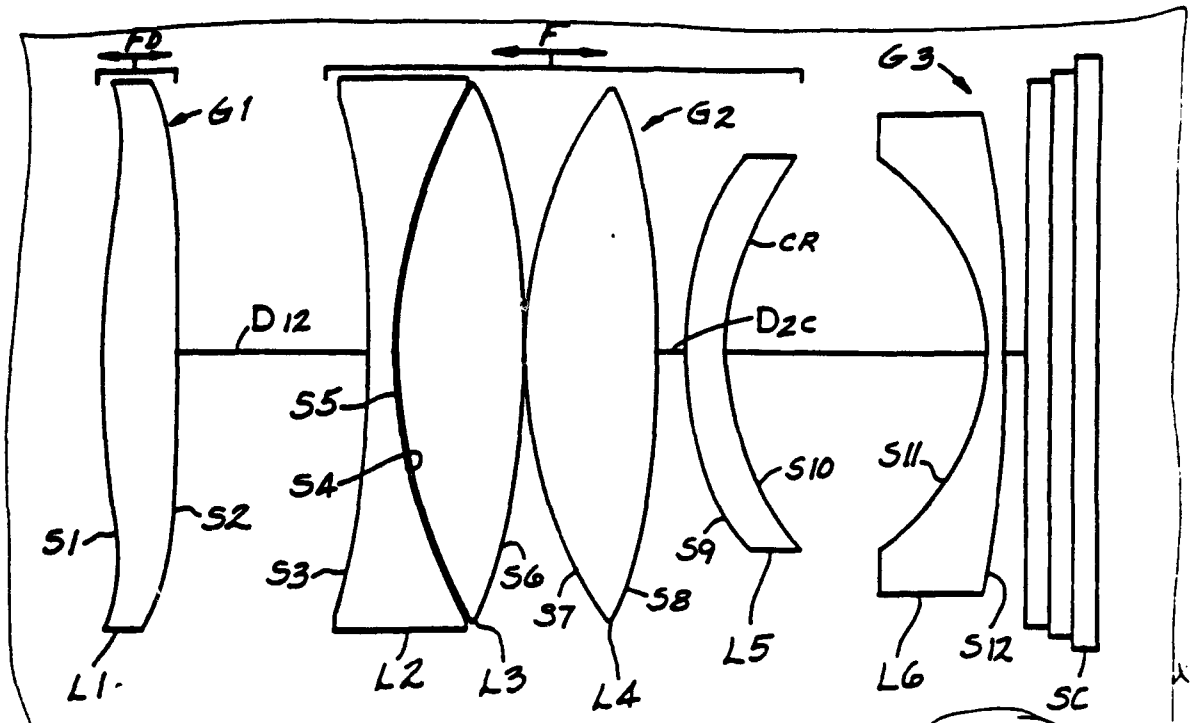
FD
F
G1
G2
G3
CR
D12
D2C
S5
S4
S10
S11
S1
S2
S9
S3
S6
S7
S8
L5
L1
L2
L3
L4
L6
S12
SC

FIG-3

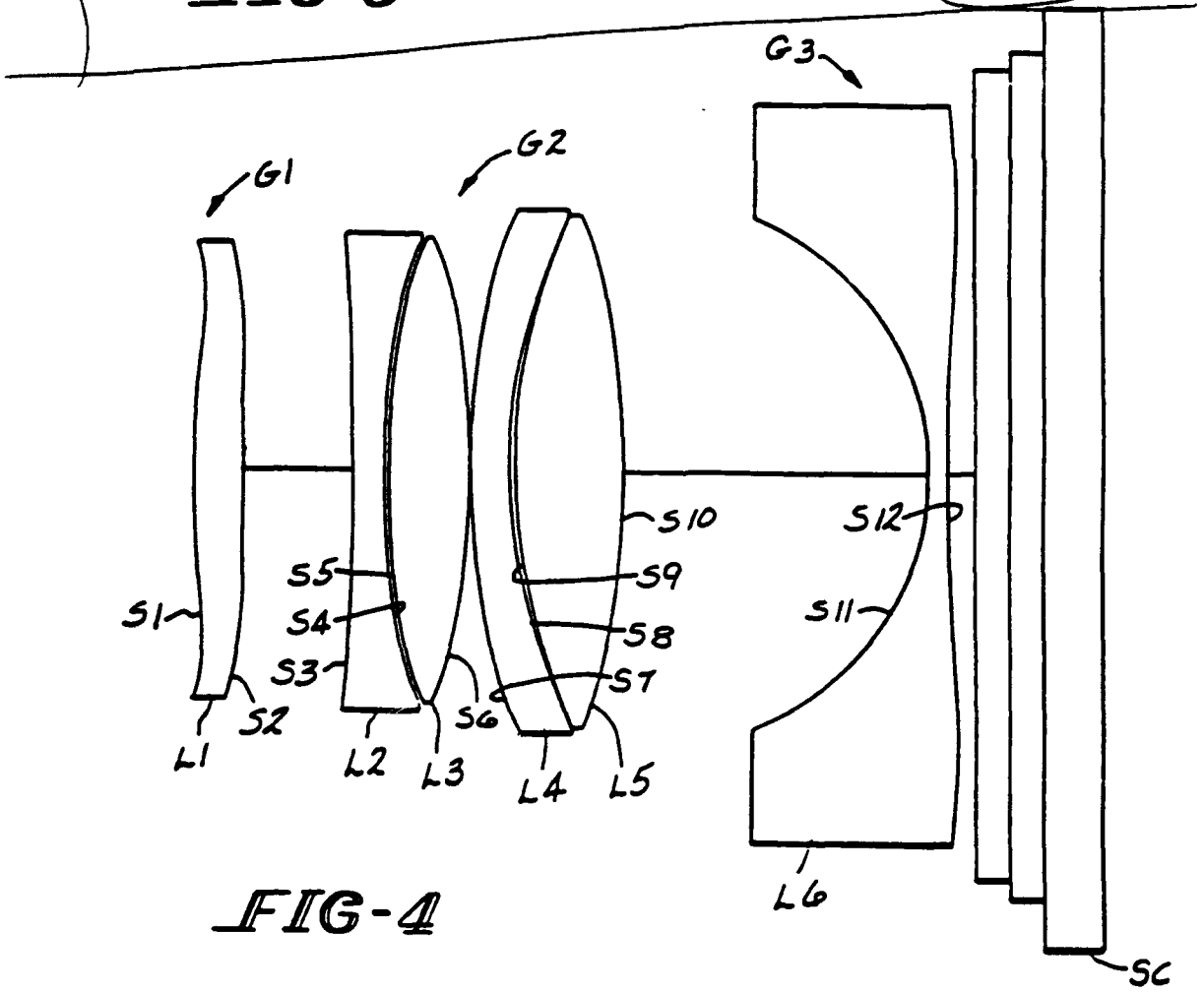
HD6
G3
G1
G2
S10
S12
S5
S9
S1
S4
S8
S11
S3
S7
S2
S6
L1
L2
L3
L4
L5
L6
SC

FIG-4

COLOR CORRECTED PROJECTION LENS

RELATED APPLICATION

This is a continuation of application Ser. No. 07/048,026 filed May 11, 1987 now abandoned.

FIELD OF THE INVENTION

This invention relates to projection lenses for cathode ray tubes and, more particularly, relates to such lenses which are color corrected.

BACKGROUND OF THE INVENTION

In projection television systems, it is common practice to utilize three cathode ray tubes (CRT's) of different colors, namely, red, blue and green. Utilizing three monochromatic CRT's does not require a color corrected lens for normal usage. Examples of such lenses are shown in U.S. Pat. Nos. 4,300,817, 4,348,081 and 4,526,442.

In practice, the phosphors of the three differently colored CRT's emit polychromatically with the green phosphor having significant side bands in blue and red. This chromatic spread can effect the image quality, particularly in situations where high resolution is of prime concern. Where there is to be a data display or large magnification, this color spread manifests itself as lowered image contrast and visible color fringing.

The degree of color correction required in the lenses for these applications depends on the intended application of the lenses.

In general, for lower resolution systems, such as for the projection of typical broadcast television, good color optical performance out to three cycles per millimeter as measured by the modulation transfer function (MTF) is adequate. In these cases, partial color correction may be adequate. For data display via red, green and blue inputs (RGB), and for high definition television, good performance out to ten cycles per millimeter, as measured by the MTF, may be required, and total color correction then becomes necessary.

The requirement for partial or total color correction always complicates an optical design problem. In projection television, it is of vital concern not to alleviate this difficulty by relaxing important system specification, such as field coverage, lens speed, and relative illumination. Additionally, it is often desirable that the lenses be capable of high performance over a significant range of magnifications. A typical front projection requirement might be from a magnification of 10× to 60×. This further complicates the optical design.

Accordingly, the present invention provides a new and improved projection lens for a cathode ray tube of high definition while maintaining a wide field angle and large relative aperture. The invention also provides a CRT projection lens that maintains a high level of image quality over a wide range of magnifications, for example, 10× to 60× or greater.

SUMMARY OF THE INVENTION

Briefly stated, a lens embodying the invention in one form thereof consists from the image side a first lens unit which is a positive element with at least one aspheric surface; a three element lens unit consisting of a biconcave element, a biconvex element and another positive component, in that order; a third lens unit having a strongly concave image side surface and which serves as a field flattener and to correct the Petzval sum of the lens; and a weak power corrector lens element having at least one aspheric surface that significantly improves the higher order sagittal flare aberration is positioned between the second and third lens units.

The first two elements of the second lens unit form a color correcting doublet of overall meniscus shape concave to the image side.

An object of this invention is to provide a new and improved color corrected lens for cathode ray tube projection which provides enhanced image quality while maintaining a large relative aperture and wide field.

Another object of this invention is to provide a new and improved color corrected lens for cathode ray tube projection which maintains enhanced image quality thoughout a wide range of magnifications.

The features of the invention which are believed to be novel are particularly pointed out and distinctly claimed in the concluding portion of the specification. The invention, however, together with further objects and advantages thereof, may best be appreciated by reference to the following detailed description taken in conjunction with the drawings.

BRIEF DESCRIPTION OF THE DRAWINGS

FIGS. 1–4 are schematic side elevations of lenses which may embody the invention.

DETAILED DESCRIPTION OF PREFERRED EMBODIMENTS OF THE INVENTION

Different projection lenses embodying the invention are set forth in Tables I-X and exemplified in the drawings.

In the drawings, the lens units are identified by the reference G followed by successive arabic numerals, except that a corrector lens unit is designated by the reference CR; lens elements are identified by the reference L followed by successive arabic numerals from the image to the object end. Surfaces of the lens elements are identified by the reference S followed by successive arabic numerals from the image to the object end. The reference SC denotes the screen of a cathode ray tube, while the reference C denotes a liquid optical coupler between the screen SC and the overall lens. In the embodiments of FIGS. 1 and 2, the coupler C contributes optical power as hereinafter explained.

In all disclosed embodiments of the invention, the first lens unit G1 comprises an element L1 of positive power and has at least one aspheric surface defined by the equation:

$$x = \frac{Cy^2}{1 + [1 - (1 + K)C^2y^2]^{\frac{1}{2}}} + Dy^4 + Ey^6 + Fy^8 + Gy^{10} + Hy^{12} + Iy^{14}$$

where x is the surface sag at a semi-aperture distance y from the axis A of the lens. C is the curvature of a lens surface at the optical axis A equal to the reciprocal of the radius at the optical axis. K is a conic constant and D, E, F, G, H and I are aspheric coefficients of correspondingly fourth through fourteenth order.

Reference is now made to FIG. 1, which discloses a lens embodying the invention. The lens of FIG. 1 comprises three lens units, G1, G2, and G3, as seen from the image side or the projection screen (not shown). Lens unit G1 consists of a single element L1 having two

aspheric surfaces. Lens unit G2 consists of a color correcting doublet L2 and L3 of weak total optical power which is closely spaced to a biconvex element L4. Lens unit G3 comprises an element having a concave image side surface, and a liquid coupler which optically couples the lens to the faceplate CS of a cathode ray tube. The construction of the coupler is disclosed and claimed in co-pending U.S. application Ser. No. 820,266 filed Jan. 17, 1986. The coupler C comprises a housing which defines a peripheral wall which is sealed against CRT faceplate CS. The housing has a window at the other side which is closed by a meniscus element L6 having a strongly concave image side surface. Lens unit G3 provides correction for field curvature and contributes to reduction of Petzval sum. Coupler C is filled with a liquid having an index of refraction close to the index of refraction of element L6 and the CRT faceplate. Thus, surface S12 of element L6 does not have to be highly finished. The material of element L6 may be a plastic material such as acrylic or, as specified in Table I, may be glass having spherical surfaces. Element L5 is a corrector, which is positioned between lens units G2 and G3 and as exemplified in Table I, has two aspheric surfaces.

Corrector element L5 is positioned with respect to lens unit G2 such that the marginal axial rays OA intersect surface S9 thereof at a height substantially less than the clear aperture of the lens, while allowing the dimension above the height H to be configured to correct for aberrations due to off-axis rays. In FIG. 1, the marginal axial rays AR are indicated in full line, while the off-axis rays OA are indicated in short broken line. The corrector element L5 is configured and spaced from lens unit G2 to permit the central portion thereof up to the height H to be utilized to aid in correction of aperture dependent aberrations and for this reason, L5 should be within a distance D_{2C}/F_0 where D_{2C} is the axial spacing between lens unit G2 and corrector element L5, and F_0 is the equivalent focal length (EFL) of the lens.

In all cases, The corrector lens unit CR where used is shaped to contribute to correction of spherical aberration in the center and to contribute to correction of off-axis aberrations toward the ends. These off-axis aberrations are sagittal oblique spherical, coma and astigmatism.

Lenses as shown in FIG. 1 are described in the prescriptions of Tables I and II. The lens of Table III has the same form but is not optically coupled to the CRT screen SC.

Lenses as shown in FIG. 2 are described in the prescriptions of Tables IV, V, VI, VII and VIII. In the lenses of Tables VI and VII the coupler C has no optical power.

Lenses as shown in FIG. 3 are described in the prescriptions of Tables IX and X. These lenses are air spaced from the CRT screen SC. The screen SC is shown as comprising two outer plates with a coolant therebetween.

A lens as shown in FIG. 4 is described in the prescription of Table XI. Here, there is no corrector CR, and the second biconvex element of the second lens unit is split into two elements.

In the following tables, the lens elements are identified from the image end to the object end by the reference L followed successively by an arabic numeral. Lens surfaces are identified by the reference S followed by an arabic numeral successively from the image to the object end. The index of refraction of each lens element is given under the heading N_D. The dispersion of each lens element as measured by its Abbe number is given by V_D. EFL is the equivalent focal length of the lens and the semi-field angle is set forth. F/No. is the relative aperture of the lens, and the aperture stop is indicated in relation to a surface. The aspheric surfaces of the lens elements are in accordance with the coefficients set forth in the foregoing aspheric equation.

The following Tables also set forth the magnification (M) of the image as an inverse function of the object, and the diagonal of the CRT for which the lens is designed. The dimension for the diagonal is for the phosphor raster of the CRT screen. The raster may vary for different CRT's having a nominal diagonal.

TABLE I

LENS		SURFACE RADII (mm)	AXIAL DISTANCE BETWEEN SURFACES (mm)	N_D	V_D
	S1	283.571			
L1			21.700	1.491	57.2
	S2	−1056.263			
			49.800		
	S3	−329.708			
L2			7.400	1.689	31.16
	S4	137.721			
			0.750		
	S5	142.546			
L3			30.000	1.456	91.25
	S6	−277.752			
			0.250		
	S7	133.119			
L4			32.400	1.517	64.17
	S8	−253.947			
			62.100		
	S9	−1569.033			
L5			10.000	1.491	57.2
	S10	3665.023			
			36.420		
	S11	−69.434			
L6			8.000	1.517	64.17
	S12	−70.013			
C			18.000	1.410	55.0
	S13	Plane			

f/No = 1.2 CRT Diagonal = 161 mm
EFL = 109.0 mm Magnification = −0.0610
Semi-field = 24° Aperture stop is 0.00 mm after S9
Aspheric Surfaces S1, S2, S9, S10

	S1	S2	S9
D	-0.2310×10^{-8}	-0.1901×10^{-8}	-0.2135×10^{-8}
E	-0.3115×10^{-10}	-0.2372×10^{-10}	-0.3129×10^{-10}
F	0.1117×10^{-14}	0.1940×10^{-14}	-0.1604×10^{-13}
G	-0.4454×10^{-18}	-0.3978×10^{-18}	0.2514×10^{-18}
H	0.7641×10^{-22}	0.6081×10^{-22}	0.2123×10^{-20}
I	-0.3878×10^{-26}	-0.3494×10^{-26}	-0.2004×10^{-24}

	S10
D	0.1728×10^{-8}
E	-0.6890×10^{-10}
F	0.1558×10^{-14}
G	0.1647×10^{-17}
H	0.1056×10^{-20}
I	-0.1015×10^{-24}

TABLE II

LENS		SURFACE RADII (mm)	AXIAL DISTANCE BETWEEN SURFACE (mm)	N_D	V_D
	S1	195.212			
L1			17.300	1.491	57.2
	S2	−1341.860			
			43.340		
	S3	−255.343			
L2			5.890	1.689	31.16

TABLE II-continued

	S4	123.557	1.030		
	S5	131.043			
L3			28.640	1.589	61.25
	S6	−177.946	0.200		
	S7	109.648			
L4			30.280	1.517	64.20
	S8	−205.352	D8		
	S9	−127.299			
L5			7.961	1.491	57.2
	S10	−211.498	D10		
	S11	−58.675			
L6			6.000	1.526	60.03
	S12	−60.201			
C			7.000		
	S13	Plano			

f/No = 1.1 CRT Diagonal = 124 mm
EFL = 135.0 mm Aperture stop is 0.00 mm after S5
Semi-field = 23°
Aspheric Surfaces S1, S2, S9, S10

	S1	S2	S9
D	-0.3078×10^{-9}	-0.2154×10^{-9}	0.1118×10^{-9}
E	-0.8541×10^{-13}	-0.7388×10^{-13}	-0.2040×10^{-13}
F	0.4895×10^{-14}	0.8120×10^{-14}	-0.1373×10^{-13}
G	-0.4066×10^{-17}	-0.3506×10^{-17}	0.4412×10^{-18}
H	0.8618×10^{-21}	0.7248×10^{-21}	0.1932×10^{-21}
I	-0.6304×10^{-25}	-0.5796×10^{-25}	-0.7326×10^{-26}

	S10	Focusing Data EFL (mm)	D8 (mm)	D10 (mm)	M
D	0.1483×10^{-5}				
E	-0.3031×10^{-9}	130.3	44.87	39.69	−.0992
F	-0.8927×10^{-14}	135.0	48.22	30.09	−.0500
G	-0.3316×10^{-18}	138.2	51.78	22.12	−.0165
H	0.3663×10^{-19}				
I	-0.8052×10^{-23}				

TABLE III

LENS		SURFACE RADII (mm)	AXIAL DISTANCE BETWEEN SURFACES (mm)	N_d	V_d
	S1	258.727			
L1			21.700	1.491	57.2
	S2	−1207.846			
	S3	−329.768	47.750		
L2			7.400	1.673	32.17
	S4	137.720			
	S5	142.596	0.740		
L3			30.000	1.589	61.26
	S6	−277.752			
	S7	133.119	0.250		
L4			32.400	1.517	64.20
	S8	−253.948			
	S9	396.343	57.490		
L5			10.00	1.491	57.2
	S10	479.403			
	S11	−69.734	31.400		
L6			4.760	1.491	57.2
	S12	Plano			

f/No. = 1.2 CRT Diagonal = 131.8 mm
EFL = 168. mm Magnification = −.0314
Semi-field = 24° Aperture stop is 22.5 mm after S5
Aspheric Surfaces S1, S2, S9, S10

	S1	S2	S9
D	-0.2401×10^{-9}	-0.1956×10^{-9}	0.2561×10^{-9}
E	-0.2852×10^{-10}	-0.2302×10^{-10}	-0.4838×10^{-10}
F	-0.8694×10^{-15}	0.1560×10^{-14}	0.4407×10^{-15}

TABLE III-continued

G	-0.1963×10^{-17}	-0.8864×10^{-17}	0.2010×10^{-17}
H	0.4700×10^{-22}	0.1240×10^{-21}	0.1876×10^{-21}
I	-0.3071×10^{-26}	-0.8422×10^{-26}	-0.4864×10^{-26}

S7

D	0.4413×10^{-7}
E	-0.1300×10^{-11}
F	0.1100×10^{-14}
G	-0.6116×10^{-19}
H	0.2027×10^{-23}
I	-0.2456×10^{-28}

TABLE IV

LENS		SURFACE RADII (mm)	AXIAL DISTANCE BETWEEN SURFACES (mm)	N_d	V_d
	S1	64.117			
L1			10.000	1.491	57.2
	S2	454.506	7.933		
	S3	−88.724			
L2			6.000	1.620	36.3
	S4	88.724	2.290		
	S5	133.595			
L3			15.000	1.517	64.2
	S6	−61.130	0.100		
	S7	52.655			
L4			20.000	1.517	64.2
	S8	−145.278	11.189		
	S9	−61.119			
L5			6.000	1.491	57.20
	S10	−65.972	29.963		
	L11	−35.209			
L6			3.200	1.620	36.30
	S12	−125.000			
C			7.530	1.410	60.00
	S13	Plano			

f/No = 1.0 CRT Diagonal = 86.5 mm
EFL = 67.5 mm Aperture stop is 11.25 mm after S5
Semi-field = 29°
Aspheric Surfaces S1, S9, S10

	S1	S9	S10
D	-0.1074×10^{-5}	0.1299×10^{-5}	0.2701×10^{-5}
E	-0.1105×10^{-9}	0.1361×10^{-9}	0.2393×10^{-9}
F	0.8360×10^{-12}	0.1851×10^{-11}	0.1398×10^{-11}
G	-0.1195×10^{-14}	0.6225×10^{-15}	0.9554×10^{-15}
H	0.6780×10^{-18}	-0.3643×10^{-17}	-0.2834×10^{-17}
I	-0.2118×10^{-21}	0.1561×10^{-20}	0.1139×10^{-20}

Focusing Data EFL (mm)	D10 (mm)	M
67.94	29.55	−.0831
67.46	29.96	−.0935

TABLE V

LENS		SURFACE RADII (mm)	AXIAL DISTANCE BETWEEN SURFACES (mm)	N_d	V_d
	S1	76.197			
L1			13.000	1.491	57.2
	S2	−472.688	10.334		
	S3	−81.639			
L2			4.000	1.620	36.30
	S4	90.843	0.066		
	S5	91.468			
L3			21.100	1.517	64.17
	S6	−91.468			

TABLE V-continued

			0.130			
L4	S9	84.109	19.200	1.589	61.27	
	S9	−120.724	12.300			
L5	S9	−80.743	6.140	1.491	57.2	
	S10	−105.033	D10			
L6	S11	−40.818	4.000	1.491	57.2	
C	S12	−44.007	3.000	1.443	50.0	
	S13	Plano				

f/No = 1.0 CRT Diagonal = 121.0
EFL = 77.2 mm Aperture stop is 6.33 mm after S5
Semi-field = 33°
Aspheric Surfaces S1, S2, S9, S10, S11

	S1	S2	S9
D	−0.6915 × 10⁻⁷	−0.3031 × 10⁻⁷	0.3387 × 10⁻⁷
E	−0.3240 × 10⁻⁹	−0.1899 × 10⁻⁹	−0.1011 × 10⁻⁹
F	−0.1245 × 10⁻¹²	0.0000 × 10⁻¹⁰	−0.1141 × 10⁻¹²
G	−0.3111 × 10⁻¹⁶	0.0000 × 10⁻¹⁰	0.1345 × 10⁻¹⁵
H	0.4997 × 10⁻¹⁹	0.0000 × 10⁻¹⁰	−0.2782 × 10⁻¹⁹
I	−0.2346 × 10⁻²²	0.0000 × 10⁻¹⁰	0.9852 × 10⁻²²

	S10	S11
D	0.3964 × 10⁻⁷	−0.6488 × 10⁻⁷
E	0.4331 × 10⁻⁹	0.1265 × 10⁻⁹
F	−0.5884 × 10⁻¹³	0.1142 × 10⁻¹²
G	0.3546 × 10⁻¹⁵	0.2181 × 10⁻¹⁶
H	−0.7876 × 10⁻¹⁹	0.2972 × 10⁻¹⁹
I	−0.6164 × 10⁻²²	−0.1388 × 10⁻²²

Focusing Data

EFL(mm)	D10 (mm)	M
78.25	34.06	−.0844
77.16	35.29	−.1170
77.95	34.40	−.1000

TABLE VI

LENS		SURFACE RADII (mm)	AXIAL DISTANCE BETWEEN SURFACES (mm)	N_d	V_d
L1	S1	89.851	16.000	1.491	57.2
	S2	452.287	15.205		
L2	S3	−141.472	5.000	1.620	36.30
	S4	111.221	1.200		
L3	S5	113.348	32.900	1.517	64.20
	S6	−113.348	0.200		
L4	S7	84.350	25.000	1.517	64.20
	S8	−1933.295	21.747		
L5	S9	−205.505	9.000	1.491	57.2
	S10	−112.793	D10		
L6	S11	−57.034	5.500	1.620	36.30
	S12	plano			

f/No = 1.0
EFL = 105.0
Semi-field = 30°
Aperture stop is 6.50 mm after S5
Aspheric Surfaces S1, S2, S9, S10

	S1	S2	S9
D	−0.1719 × 10⁻⁹	0.2117 × 10⁻⁹	0.2250 × 10⁻⁹
E	−0.2179 × 10⁻⁹	−0.4171 × 10⁻¹⁰	0.4005 × 10⁻⁹

TABLE VI-continued

F	0.1418 × 10⁻¹³	0.6046 × 10⁻¹³	−0.2752 × 10⁻¹³
G	−0.6256 × 10⁻¹⁷	0.1555 × 10⁻¹⁶	0.6675 × 10⁻¹⁷
H	0.1324 × 10⁻¹⁹	−0.1450 × 10⁻¹⁹	−0.1324 × 10⁻¹⁹
I	−0.6000 × 10⁻²⁴	0.3482 × 10⁻²³	−0.1624 × 10⁻²³

	S10	Focusing Da EFL(mm)	D(mm)	M
D	0.7114 × 10⁻⁷			
E	0.4129 × 10⁻⁹	105.1	40.42	−.1[illegible]
F	0.6262 × 10⁻¹³	106.3	39.83	−.12[illegible]
G	0.1164 × 10⁻¹⁵	107.2	39.33	−.1[illegible]
H	0.3025 × 10⁻¹⁹			
I	−0.8300 × 10⁻²³			

TABLE VII

LENS		SURFACE RADII (mm)	AXIAL DISTANCE BETWEEN SURFACES (mm)	N_d	V_d
L1	S1	90.401	17.0[illegible]	1.491	57.2
	S2	551.910	15.03[illegible]		
L2	S3	−148.320	6.00[illegible]	1.62[illegible]	36.3
	S4	100.940	0.50[illegible]		
L3	S5	102.822	30.00[illegible]	1.51[illegible]	64.2
	S6	−134.365	0.20[illegible]		
L4	S7	85.055	24.50[illegible]	1.51[illegible]	64.2
	S8	−309.659	25.36[illegible]		
L5	S9	−155.451	9.00[illegible]	1.491	57.2
	S10	−112.107	D10		
L6	S11	−57.391	4.000	1.620	36.4
	S12	plano			

f/No = 1.0 CRT Diagonal = 122 mm
EFL = 104.7 mm Aperture stop is 9.40 mm after S5
Semi-field = 28°
Aspheric Surfaces S1, S2, S9, S10

	S1	S2	S9
D	−0.2255 × 10⁻⁹	0.1469 × 10⁻⁹	0.2639 × 10⁻⁹
E	−0.1505 × 10⁻⁹	−0.1695 × 10⁻¹⁰	0.4973 × 10⁻⁹
F	0.7536 × 10⁻¹³	0.3153 × 10⁻¹³	−0.8879 × 10⁻¹³
G	−0.3857 × 10⁻¹⁶	0.5873 × 10⁻¹⁷	0.4487 × 10⁻¹⁶
H	0.9174 × 10⁻²⁰	−0.7355 × 10⁻²⁰	−0.1095 × 10⁻¹⁹
I	−0.1059 × 10⁻²³	0.1920 × 10⁻²³	−0.1734 × 10⁻²³
K	1.326		

	S10	Focusing Data EFL (mm)	D10 (mm)	M
D	0.8827 × 10⁻⁹			
E	0.4826 × 10⁻⁹	104.8	36.40	−.116
F	0.6637 × 10⁻¹⁴	105.7	35.55	−.096
G	−0.8763 × 10⁻¹⁷	103.6	37.30	−.123
H	0.2104 × 10⁻¹⁹			
I	−0.6838 × 10⁻²³			

TABLE VIII

LENS		SURFACE RADII (mm)	AXIAL DISTANCE BETWEEN SURFACES (mm)	N_d	V_d
L1	S1	79.527	14.000	1.491	57.2
	S2	380.482	14.450		
L2	S3	−116.430	4.500	1.620	36.4

TABLE VIII-continued

	S4	93.7[illegible]			
			0.10		
	S5	93.126			
L3			31.0[illegible]	1.51[illegible]	[illegible]
	S6	−93.12[illegible]			
			0.200		
	S7	73.00[illegible]			
L4			20.000	1.51[illegible]	[illegible]
	S8	−[illegible]06.2[illegible]			
			16.870		
	S9	−94.045			
L5			8.000	1.491	57.2
	S10	−83.071			
			D10		
	S11	−53.241			
L6			5.75	1.620	36.4
	S12	−130.000			
C			8.000	1.435	50.0
	S13	Plano			

f/No = 1.2 CRT Diagonal = 126.6 mm
EFL = 96.[illegible] Aperture stop is 0.20 mm after S5
Semi-field = 28°
Aspheric Surfaces S1, S2, S9, S10

	S1	S2	S9
D	−0.2013 × 10[illegible]	0.2b03 × 10[illegible]	0.9194 × 10[illegible]
E	−0.4457 × 10[illegible]	−0.1816 × 10[illegible]	0.9549 × 10[illegible]
F	0.314[illegible] × 10[illegible]	0.1593 × 10[illegible]	−0.2721 × 10[illegible]
G	−0.1513 × 10[illegible]	0.4[illegible] × 10[illegible]	0.1107 × 10[illegible]
H	0.3487 × 10[illegible]	−0.6[illegible] × 10[illegible]	−0.4843 × 10[illegible]
I	−0.2575 × 10[illegible]	0.1777 × 10[illegible]	0.5510 × 10[illegible]
K	1.326		

	S10	Focusing Data EFL (mm)	D10 (mm)	M
D	0.1532 × 10[illegible]			
E	0.8778 × 10[illegible]	96.87	45.21	−.109
F	0.3840 × 10[illegible]	95.96	46.12	−.123
G	−0.9903 × 10[illegible]	98.07	44.05	−.092
H	0.6608 × 10[illegible]			
I	−0.1801 × 10[illegible]			

TABLE IX

LENS		SURFACE RADII (mm)	AXIAL DISTANCE BETWEEN SURFACES (mm)	N_d	V_d
	S1	178.554			
L1			13.000	1.491	57.2
	S2	2078.521			
			D2		
	S3	−255.343			
L2			5.890	1.689	31.2
	S4	123.551			
			1.030		
	S5	131.041			
L3			28.640	1.589	61.3
	S6	−177.989			
			0.200		
	S7	109.648			
L4			30.280	1.517	64.2
	S8	−205.352			
			0.210		
	S9	100.488			
L5			8.830	1.491	57.2
	S10	92.312			
			70.634		
	S11	−50.216			
L6			4.000	1.491	57.2
	S12	−368.024			
			D12		
	S13	Plano			

f/No = 1.1 CRT Diagonal = 124 mm
EFL = 134.3 mm Aperture stop is 0.00 mm after S5
Semi-field = 23°
Aspheric Surfaces S1, S2, S9, S10, S11, S12

	S1	S2	S9

TABLE IX-continued

D	−0.13[illegible] × 10[illegible]	0.[illegible] × 10[illegible]	[illegible]
E	0.2185 × 10[illegible]	−0.3[illegible] × 10[illegible]	0.120[illegible] × 10[illegible]
F	−0.9[illegible] × 10[illegible]	−0.1[illegible] × 10[illegible]	−0.[illegible] × 10[illegible]
G	−0.3269 × 10[illegible]	−0.[illegible] × 10[illegible]	[illegible] × 10[illegible]
H	−0.1[illegible] × 10[illegible]	−0.4[illegible] × 10[illegible]	[illegible] × 10[illegible]
I	0.2055 × 10[illegible]	0.[illegible] × 10[illegible]	[illegible] × 10[illegible]

	S11	S1[illegible]	S[illegible]
D	0.4[illegible] × 10[illegible]	0.[illegible] × 10[illegible]	[illegible] × 10[illegible]
E	−0.1594 × 10[illegible]	0.[illegible] × 10[illegible]	−0.[illegible] × 10[illegible]
F	0.1444 × 10[illegible]	0.4[illegible] × 10[illegible]	[illegible] × 10[illegible]
G	−0.1501 × 10[illegible]	0.[illegible] × 10[illegible]	[illegible] × 10[illegible]
H	0.[illegible] × 10[illegible]	−0.45[illegible] × 10[illegible]	[illegible] × 10[illegible]
I	−0.1204 × 10[illegible]	0.[illegible] × 10[illegible]	−0.[illegible] × 10[illegible]

Focusing Data EFL (mm)	D2 (mm)	D12 (mm)	M
135.[illegible]	50.[illegible]	[illegible]	−.[illegible]
134.[illegible]	46.[illegible]	4.[illegible]	−.05[illegible]
133.[illegible]	43.[illegible]	[illegible]	−.[illegible]

TABLE X

LENS		SURFACE RADII (mm)	AXIAL DISTANCE BETWEEN DISTANCES (mm)	N_d	V_d
	S1	164.[illegible]			
L1			1[illegible]	1.[illegible]	[illegible]
	S2	−4893.612			
			D2		
	S3	−255.343			
L2			5.[illegible]	1.[illegible]	[illegible]
	S4	123.551			
			1.03[illegible]		
	S5	131.041			
L3			28.6[illegible]	1.5[illegible]	61.[illegible]
	S6	−177.989			
			0.20[illegible]		
	S7	109.648			
L4			30.280	1.517	64.2
	S8	−205.352			
			0.20[illegible]		
	S9	78.134			
L5			10.0[illegible]	1.491	57.2
	S10	67.399			
			60.21[illegible]		
	S11	−48.559			
L6			4.000	1.491	57.2
	S12	−252.989			
			1.302		
	S13	Plano			
			D12		

f/No = 1.1 CRT Diagonal = 124 mm
EFL = 135.7 mm Aperture stop is 0.00 mm after S5
Semi-field = 23°
Aspheric Surfaces S1, S2, S9, S10, S11, S12

	S1	S2	S9
D	−0.2911 × 10[illegible]	−0.1945 × 10[illegible]	−0.3015 × 10[illegible]
E	−0.7792 × 10[illegible]	−0.5934 × 10[illegible]	0.8356 × 10[illegible]
F	0.7366 × 10[illegible]	0.7111 × 10[illegible]	−0.1079 × 10[illegible]
G	−0.4384 × 10[illegible]	−0.3414 × 10[illegible]	0.4778 × 10[illegible]
H	0.7916 × 10[illegible]	0.7097 × 10[illegible]	−0.1167 × 10[illegible]
I	−0.3500 × 10[illegible]	−0.4415 × 10[illegible]	−0.8726 × 10[illegible]

	S10	S11	S12
D	0.2618 × 10[illegible]	0.1161 × 10[illegible]	0.[illegible] × 10[illegible]
E	−0.3268 × 10[illegible]	−0.6628 × 10[illegible]	−0.5860 × 10[illegible]
F	0.9906 × 10[illegible]	0.4292 × 10[illegible]	0.2597 × 10[illegible]
G	−0.1459 × 10[illegible]	0.9961 × 10[illegible]	−0.4923 × 10[illegible]
H	0.7475 × 10[illegible]	−0.59[illegible] × 10[illegible]	0.1168 × 10[illegible]
I	−0.1894 × 10[illegible]	0.1511 × 10[illegible]	0.633[illegible] × 10[illegible]

Focusing Data EFL (mm)	D2 (mm)	D12 (mm)	M
135.71	48.71	11.73	−.1000
134.97	44.80	5.42	−.0500

TABLE X-continued

134.36	41.5	1.30	−.0167

TABLE XI

LENS		SURFACE RADII (mm)	AXIAL DISTANCE BETWEEN SURFACES (mm)	N_d	V_d
	S1	100.333			
L1			9.000	1.491	57.2
	S2	−14321.009			
			20.1000		
	S3	−600.536			
L2			6.000	1.785	25.7
	S4	132.672			
			0.080		
	S5	134.262			
L3			15.350	1.589	61.3
	S6	−132.733			
			0.200		
	S7	171.212			
L4			7.000	1.491	57.2
	S8	100.514			
			1.200		
	S9	111.206			
L5			19.450	1.589	61.3
	S10	−142.661			
			55.750		
	S11	−68.462			
L6			4.000	1.491	57.2
	S12	269.671			

f/No = 1.4 CRT Diagonal = 125.8 mm
EFL = 111.6 Magnification = .0263
Semi-field = 34° Aperture stop is 5.05 mm after S5
Aspheric Surfaces S1, S2, S7, S8, S11, S12

	S1	S2	S7
D	-0.9964×10^{-6}	-0.3034×10^{-6}	0.6027×10^{-6}
E	-0.4344×10^{-9}	-0.3497×10^{-9}	-0.1651×10^{-10}
F	-0.1037×10^{-12}	-0.3718×10^{-13}	0.5166×10^{-14}
G	0.1695×10^{-16}	-0.1261×10^{-16}	-0.6497×10^{-17}
H	0.1831×10^{-19}	0.2801×10^{-19}	0.6405×10^{-21}
I	0.2021×10^{-23}	-0.1241×10^{-23}	-0.7613×10^{-24}

	S8	S11	S12
D	0.1130×10^{-6}	-0.3187×10^{-5}	-0.8632×10^{-6}
E	0.3713×10^{-12}	0.2489×10^{-9}	0.1616×10^{-9}
F	-0.1677×10^{-13}	-0.2606×10^{-12}	-0.1755×10^{-13}
G	-0.8127×10^{-18}	0.1321×10^{-15}	0.2955×10^{-17}
H	0.6405×10^{-21}	0.7036×10^{-19}	0.1630×10^{-21}
I	-0.9106×10^{-24}	-0.4831×10^{-22}	-0.1388×10^{-24}

Table XII sets forth the powers K_{G1}, K_{G2}, K_{G3}, and K_{CR} of the lens units of each of the examples as a ratio of the power of the overall lens.

TABLE XII

TABLE	K_{G1}/K_O	K_{G2}/K_O	K_{G3}/K_O	K_{CR}/K_O
I	.373	.949	−1.032	−.068
II	.392	1.000	−1.149	−.203
III	.387	.948	−1.189	.124
IV	.452	.838	−1.021	−.011
V	.574	.838	−.838	−.108
VI	.479	.755	−.838	−.212
VII	.488	.803	−1.080	.139
VIII	.478	.789	−.975	.083
IX	.340	1.000	−1.149	−.004
X	.377	.947	−1.099	−.095
XI	.355	1.009	−1.013	— —

It will be seen that the corrector element CR has little optical power. Its primary purpose is to provide aspheric surfaces for correction of aberrations.

In all embodiments, except that of Table XI, all elements of lens unit G2 are glass with spherical surfaces, and thus avoid focus drift with temperature.

In the examples of Tables IV-VIII the optical power of the first lens unit K_1/K_0 is greater than 0.4. This is permissable in view of the spacing D_{12}/F_0 which is less than 0.2. Thus the spacing D_{12}/F_0 will be a function of the axial optical power of the first lens unit. The lesser the optical power of the first lens unit, the greater the spacing D_{12}/F_0 may be.

The optical power of the doublet consisting of L2 and L3 is all embodiments is very weak.

The axial spacing between L3 and the power element L4 is very small, less than one tenth of one per cent of the EFL of the lens.

The power of the corrector element CR as a ratio to the power of the lens is weak and

$$0.1 > K_{CR}/K_0\ 0.3$$

Thus any change in index of refraction of the corrector element due to temperature does not adversly affect the focus of the lens.

Table XIII sets forth the spacing of element L1 and L2, D_{12}/F_0, and also the spacing of the corrector element from the second lens unit D_{2C}/F_0, together with the ratio of the powers of L2 and L3 to the power of the lens.

TABLE XIII

TABLE	D_{12}/F	D_{2C}/F	K_{L2}/K	[illegible]
I	.264	.245	−1.194	[illegible]
II	.314	.367	−1.133	[illegible]
III	.264	.342	−1.180	[illegible]
IV	.117	.100	−.962	[illegible]
V	.134	.160	−.962	[illegible]
VI	.148	.207	−.990	[illegible]
VII	.151	.242	−1.031	[illegible]
VIII	.147	.175	1.127	[illegible]
IX	.321	— —	−1.127	[illegible]
X	.302	.050	−1.133	[illegible]
XI	.161	−.13	−.817	[illegible]

The color correcting doublet of the second lens unit is designed to provide the necessary color correction without introducing uncorrectable aberrations. The lenses of Tables I, II, II, VII and VIII provide modulation transfer functions of ten cycles/millimeter over most of the field. In these examples, the absolute optical power of the biconcave element L2 and the first biconvex element L3 are greater than the optical power of the overall lens.

The lens of Table XI provides an MTF of 6.3 cycles/-millimeter and the embodiments of Tables IV-VIII provide 5.0 cycles/millimeter.

The lens of Table XI and FIG. 4 utilizes a two element power component L4 and L5 where L4 is acrylic and has two aspheric surfaces, and has an axial power which is about 21% of L5. The EFL's of the lenses as set forth in the prescriptions may vary as the lens is focused for various projection distances and magnifications.

The lenses of Tables I and III are designed for front projection at predetermined distances and provide image/object magnifications of 16.4× and 31.5× respectively.

The lens of Table II is also designed for front projection and has a range of magnifications 10× to 60×. To focus for varying image distances elements L1-L5 move in the same direction with the corrector L5 moving differentially to correct for aberrations introduced by movement of lens units G1 and G2. In FIG. 1, the focusing movement of elements L1-L4 is shown by the

arrow F and the focusing movement of element L5 is shown by the arrow F_1.

The lenses of Tables IX and X are also designed and have magnifications of 10× to 60×. Here elements L1-L5 move axially for focusing with L1 moving differentially at a lesser rate. This differential movement corrects for aberrations introduced by the focusing movement of elements L1-L5. In FIG. 3, the focusing movement of elements L2-L5 is shown by the arrow F while the differential movement of element L1 is shown by the arrow F_D.

The lenses of Table IV-VIII are designed for rear projection and in some cases are provided with focusing capability dependent on the magnification required for the size of the viewing screen. That is, the same lens may be used for a forty or fifty inch diagonal viewing screen.

The lens of Table XI does not use a corrector element CR as shown in the other embodiments, but does include a weak meniscus L4 having two aspheric surfaces as a part of the second lens unit G2.

It may thus be seen that the objects of the invention set forth as well as those made apparent from the foregoing description are efficiently attained. While preferred embodiments of the invention have been set forth for purposes of disclosure, modification of the disclosed embodiments of the invention as well as other embodiments thereof may occur to those skilled in the art. Accordingly, the appended claims are intended to cover all of the embodiments of the invention and modifications to the disclosed embodiments which do not depart from the spirit and scope of the invention.

Having described the invention, what is claimed is:

1. A projection lens for use in combination with a cathode ray tube where the projection lens is closely coupled to the cathode ray tube, said lens comprising from the image end a first lens unit of positive optical power having at least one aspheric surface and contributing to correction of aperture dependent aberrations, a second lens unit providing a majority of the positive power of said lens, and a third lens unit having a strongly concave image side surface which provides correction for field curvature and Petzval sum of other units of said lens, said second lens unit consisting from the image end of a biconcave element, a biconvex element and a positive component, said biconcave element and said biconvex element forming a color correcting doublet and being of overall meniscus shape concave to the image end, said color correcting doublet being axially spaced from said positive component a distance less than 0.01 of the equivalent focal length of said lens.

2. The lens of claim 1 where said doublet is axially spaced from said first lens unit at least 0.1 of the equivalent focal length of said lens.

3. The lens of claim 1 further including a corrector lens unit of weak optical power having two aspheric surfaces positioned between said second and third lens units, said corrector lens unit being axially spaced from said second lens unit a distance

$$0.4 > D_{2C}/F_O > 0.15$$

where D_{2C} is the axial spacing distance between said second lens unit and said corrector element and F_O is the equivalent focal length of said lens.

4. The lens of claim 3 where said lens has a variable magnification, said first and said second lens units move axially in fixed relation to focus said lens and said corrector lens unit moves axially in the same direction but at a differential rate.

5. The lens of claim 3 where said element of said first lens unit has two aspheric surfaces.

6. The lens of claim 3 where the axial marginal rays traced from the long conjugate intersect a surface of said corrector lens unit substantially below the clear aperture of said image side surface.

7. The lens of claim 1 where said element of said first lens unit has two aspheric surfaces.

8. The lens of claim 1 where said first and second lens units move axially in the same direction at differential rates to vary the focus of said lens.

9. The lens of claim 8 where the axial spacing between said first lens unit and said second lens unit is

$$0.4 > D_{12}/F_O > 0.1$$

where D_{12} is the distance between the first and second lens units and F_O is the equivalent focal length of said lens.

10. The lens of claim 1 where said positive lens component is also biconvex.

11. The lens of claim 1 where all elements of said second lens unit have spherical surfaces.

12. The lens of claim 1 wherein said corrector lens has two aspheric surfaces, said corrector lens unit being axially spaced from said second lens unit a distance

$$0.4 > D_{2C}/F_O > 0.15$$

where D_{2C} is the axial distance between said biconvex element and said biconvex lens and F_O is the equivalent foal length of said lens.

13. A projection lens for use in combination with a cathode ray tube where the projection lens is closely coupled to the cathode ray tube, said lens comprising from the image end a first lens unit of positive optical power having at least one aspheric surface and contributing to correction of aperture dependent aberrations, a second lens unit providing a majority of the positive power of said lens, and a third lens unit having a strongly concave image side surface which provides correction for field curvature and Petzval sum of other units of said lens, said second lens unit consisting from the image end of a biconcave element, a biconvex element and a positive component, said biconcave element and said first biconvex element forming a color correcting doublet and being of overall meniscus shape concave to the image end, said positive component comprising two elements, one of said elements of said positive component having two aspheric surfaces and being of meniscus shape.

14. The lens of claim 13 where said doublet is spaced from said first lens unit at least 0.1 of the focal length of said lens.

15. A projection lens for use in combination with a cathode ray tube where the projection lens is closely coupled to the cathode ray tube, said lens comprising from the image end a first lens unit of positive optical power having at least one aspheric surface and contributing to correction of aperture dependent aberrations, said first lens unit consisting of a single element, a second lens unit providing a majority of the positive power of said lens, and a third lens unit having a strongly concave image side surface which provides correction for field curvature and Petzval sum of other units of said lens, said second lens unit comprising from the image

end a biconcave element, a biconvex element and a positive element, said biconcave element and said biconvex element forming a color correcting doublet and being of overall meniscus shape concave to the image end, and a corrector lens unit of weak optical power having at least one aspheric surface positioned between said second and third lens units, said corrector lens unit being axially spaced from said second lens unit a distance

$$0.4 > D_{2C}/F_0 > 0.1$$

where D_{2C} is the axial spacing distance between said second lens unit and said corrector element and F0 is the equivalent focal length of said lens

16. The lens of claim 15 where said element of said first lens unit has two aspheric surfaces.

17. The lens of claim 15 where said lens has a variable magnification, said first and said second lens units move axially in fixed relation to focus said lens and said corrector lens element moves axially in the same direction but at a differential rate.

18. The lens of claim 15 where said first and second lens units move axially in the same direction at differential rates to vary the focus of said lens

19. The lens of claim 15 where said positive element is also biconvex.

20. The lens of claim 15 where all elements of said second lens unit have spherical surfaces.

21. The lens of claim 15 where the axial marginal rays traced from the long conjugate intersect the image side surface of said corrector lens unit substantially below the clear aperture of said image side surface.

22. A projection lens for use in combination with a cathode ray tube where the projection lens is closely coupled to the cathode ray tube, said lens comprising from the image end a first lens unit of postive optical power having at least one aspheric surface and contributing to correction of aperture dependent aberrations, a second lens unit providing a majority of the positive power of said lens, and a third lens unit having a strongly concave image side surface which provides correction for field curvature and Petzval sum of the other units of said lens, said second lens unit comprising from the image end a biconcave element, a biconvex element and a positive lens element, said biconcave element and said biconvex element forming a color correcting doublet and being of overall meniscus shape concave to the image end, a corrector lens unit positioned between said second and third lens units, said lens having a variable focus and said first lens unit, said second lens unit, and said corrector lens unit being movable axially in the same direction to change the focus of said lens, one of said first lens unit and said corrector lens unit moving differentially with respect to the other movable lens units.

23. The lens of claim 22 where said biconcave element has an absolute optical power greater than the power of said lens.

24. The lens of claim 22 where said first lens unit consists of a single element having two aspheric surfaces.

25. The lens of claim 22 where the axial spacing between said first lens unit and said second lens unit is

$$0.4 > D_{12}/F_0 > 0.1$$

where D_{12} is the distance between the first and second lens units and F_0 is the equivalent focal length of said lens

26. The lens of claim 22 where said positive component is also biconvex

27. The lens of claim 22 where all elements of said second lens unit have spherical surfaces

28. The lens of claim 22 where said first lens unit moves differentially

29. The lens of claim 22 where said corrector lens unit moves differentially

30. A projection lens for use in combination with a cathode ray tube where the projection lens is closely coupled to the cathode ray tube, said lens comprising from the image end a first lens unit of positive optical power having at least one aspheric surface and contributing to correction of aperture dependent aberrations, a second lens unit providing a majority of the positive power of said lens, and a third lens unit having a strongly concave image side surface which provides correction for field curvature and Petzval sum of other units of said lens, said second lens unit comprising from the image end a biconcave element, a biconvex element and a positive element, said biconcave element and said biconvex element forming a color correcting doublet and being of overall meniscus shape concave to the image end, and a corrector lens unit of weak optical power having at least one aspheric surface positioned between said second and third lens units, said corrector lens unit being axially spaced from said second lens unit a distance

$$0.4 > D_{2C}/F_0 > 0.15$$

where D_{2C} is the axial spacing distance between said second lens unit and said corrector element and F_0 is the equivalent focal length of said lens.

31. The lens of claim 30 where said first lens unit consists of a single element having two aspheric surfaces.

32. The lens of claim 30 where said positive element is also biconvex.

33. The lens of claim 30 where all elements of said second lens unit have spherical surfaces.

34. A projection lens for use in combination with a cathode ray tube where the projection lens is closely coupled to the cathode ray tube, said lens comprising from the image end a first lens unit of weak optical power having at least one aspheric surface and contributing to correction of aperture dependent aberrations, a second lens unit providing a majority of the positive power of said lens, said second lens unit being spaced from said first lens unit at least 0.1 of the equivalent focal length of the lens, and a third lens unit having a strongly concave image side surface which provides correction for field curvature and Petzval sum of other units of said lens, said second lens unit comprising from the image end a biconcave element, a biconvex element and a positive element, said biconcave element and said biconvex element forming a color correcting doublet and being of overall meniscus shape concave to the image end, and a corrector lens unit of weak optical power positioned between said second and third lens, said corrector lens unit having at least one aspheric surface, the configuration and the positioning of said corrector lens element from said second lens unit being such that the axial marginal rays from said second lens unit as traced from the long conjugate intersect a sur-

face of said corrector lens unit at a height H from the optical axis of said lens that is less than the clear aperture of said surface of said corrector lens unit, said corrector lens surface being configured to contribute to correction of aperture dependent aberrations within said height H, said surface of said corrector lens beyond said height H being configured to contribute to correction of aberrations due to off-axis rays

35. The lens of claim 34 wherein said positive element of said second lens unit is biconvex.

36. The lens of claim 34 where said corrector lens unit consists of a single element.

37. The lens of claim 34 where all elements of said second lens unit have spherical surfaces.

38. A projection lens for use in combination with a cathode ray tube where the projection lens is closely coupled to the cathode ray tube, said lens comprising from the image end a first lens unit of positive optical power having at least one aspheric surface and contributing to correction of aperture dependent aberrations, said first lens unit comprising a front meniscus element convex toward the image end, a second lens unit providing a majority of the positive power of said lens, said second lens unit being spaced from said meniscus element at least 0.1 of the equivalent focal length of the lens, and a third lens unit having a strongly concave image side surface which provides correction for field curvature and Petzval sum of other units of said lens, said second lens unit consisting from the image end of a biconcave element, a biconvex element and a positive element, said biconcave element and said biconvex element forming a color correcting doublet and being of overall meniscus shape concave to the image end, and a corrector lens unit of weak optical power positioned between said second and third lens, the configuration and the positioning of said corrector lens element from said second lens unit being such that the axial marginal rays from said second lens unit as traced from the long conjugate intersect a surface of said corrector lens unit at a height H from the optical axis of said lens that is less than the clear aperture of said surface of said corrector lens unit, said corrector lens surface being configured to contribute to correction of aperture dependent aberrations within said height H, said surface of said corrector lens beyond said height H being configured to contribute to correction of aberrations due to off-axis rays.

39. The lens of claim 38 wherein said positive element of said second lens unit is biconvex.

40. The lens of claim 38 where said corrector lens unit consists of a single element.

41. A projection lens for use in combination with a cathode ray tube where the projection lens is closely coupled to the cathode ray tube, said lens comprising from the image end a first lens unit of weak positive optical power having at least one aspheric surface and contributing to correction of aperture dependent aberrations, a second lens unit providing a majority of the positive power of said lens, and a third lens unit having a strongly concave image side surface which provides correction for field curvature and Petzval sum of other units of said lens, said second lens unit comprising from the image end a biconcave element, a biconvex element and a positive element, said biconcave element and said biconvex element forming a color correcting doublet and being of overall meniscus shape concave to the image end, and a corrector lens unit of weak optical power positioned between said second and third lens, the configuration and the positioning of said corrector lens unit from said second lens unit being such that the axial marginal rays from said second lens unit as traced from the long conjugate intersect a surface of said corrector lens unit at a height H from the optical axis of said lens that is less than the clear aperture of said surface of said corrector lens unit, said corrector lens surface being configured to contribute to correction of aperture dependent aberrations within said height H, said surface of said corrector lens beyond said height H being configured to contribute to correction of aberrations due to off-axis rays

42. The lens of claim 41 wherein said positive element of said second lens unit is biconvex

43. The lens of claim 41 where said corrector lens unit consists of a single element

44. The lens of claim 41 where said biconcave element has an absolute optical power greater than the power of said lens and said biconvex element has an optical power greater than the optical power of said lens

45. The lens of claim 41 where said biconcave element has an absolute optical power greater than the power of said lens

46. The lens of claim 41 where all elements of said second lens unit have spherical surfaces

47. The lens of claim 41 where said color correcting doublet is of weak negative optical power

48. The lens of claim 41 where the absolute optical power of said biconcave element is greater than the optical power of said biconvex element

49. The lens of claim 41 where said lens has a variable magnification, said first and said second lens units move axially in fixed relation to focus said lens and said corrector lens element moves axially in the same direction but at a differential rate.

50. The lens of claim 41 where said first and second lens units move axially in the same direction at differential rates to vary the focus of said lens

51. A projection lens system for use in combination with a cathode ray tube comprising:

(a) a first lens at the image end of said lens system wherein the surface of said first lens on the image side is convex to the image on the axis of said first lens and is concave to the image at and near the clear aperture of said first lens and the other surface of said first lens is concave to the image.

(b) a second lens adapted to be closely coupled to a cathode ray tube, said second lens having a concave image side surface;

(c) a color correcting doublet located between said first and second lenses, said color correcting doublet being comprised of a biconcave lens and a biconvex lens;

(d) a biconvex lens located between said color correcting doublet and said second lens; and

(e) a corrector lens located between said biconvex lens and said second lens, said corrector lens being shaped and positioned to contribute to correction of spherical aberrations in the central portion thereof and to contribute to the correction of aberrations due to off axis rays beyond said central portion.

52. The lens of claim 51 where both elements of said color correcting doublet and said biconvex lens are glass having spheric surfaces.

53. The lens of claim 51 where said color correcting doublet is of weak negative optical power.

54. The lens of claim 51 where said doublet is spaced from said first lens unit at least 0.1 of the equivalent focal length of said lens

55. The lens of claim 51 where said first lens has two aspheric surfaces.

56. The lens of claim 51 where said color correcting doublet is axially spaced from said biconvex element no more than 0.01 of the equivalent focal length of said lens.

57. The lens of claim 51 where said doublet is concave to the images.

58. A projection lens system for use in combination with a cathode ray tube comprising

(a) a first lens at the image end of said lens system wherein the surface of said first lens on the image side is convex to the image on the axis of said first lens and is concave to the image at and near the clear aperture of said first lens and the other surface of said first lens is concave to the image.

(b) a second lens adapted to be closely coupled to the cathode ray tube, said second lens having a concave image side aspheric surface.

(c) a color correcting doublet located between said first and second lenses, the color correcting doublet being comprised of a biconcave lens and a biconvex lens.

(d) a biconvex lens located between said color correcting doublet and said biconvex lens; and

(e) a meniscus lens convex to the image located between said doublet and said biconvex lens.

59. The lens system of claim 58 wherein both surfaces of said second lens are aspheric.

* * * * *

HUGHES

HUGHES DISPLAY PRODUCTS
A subsidiary of Hughes Aircraft Company

FACSIMILE LEAD PAGE

TO: Thomas St. John

FROM: Chuck Martino

COMPANY: Trident International

DIRECT DIAL: (606) 243-5519
FAX: (606) 243-5555

FAX NO.: 407-282-3343

DATE: February 13, 1992

NUMBER OF PAGES (INCLUDING COVER PAGE)

SUBJECT: Estimation of Costs for the Development of YAG CRTs

In Reply Refer to 92AM085:

Following our telephone conversation, we are attaching the first breakdown of tasks and estimated costs to develop YAG faceplate CRT's with delivery of 5 samples as described in the paragraph "Goal".

These costs are a first estimate which may be subject to revision up or down according to our findings. We have thought it much safer to attack the basic CRT envelope problems prior to making sample tubes.

Sincerely yours,

André Martin
Manager, Color Programs

1501 Newtown Rd., Lexington, KY 40511
(606) 243-5500 • FAX (606) 243-5555

TRIDENT DEVELOPMENT PROGRAM
(ROM PRICING)

GOAL: Manufacture five (5) sample tubes with YAG or BEL faceplates supplied by Trident International.

3 - 3" CRT's with YAG green faceplate
1 - 1.5" CRT with YAG red faceplate
1 - 3/4" CRT with BEL faceplate

Development Program Projected:

Because of the nature of the faceplates, whose expansion coefficients are 75.10^{-7} for YAG and 80.10^{-7} for BEL, the color television $94X^{10-7}$ expansion standard frit sealing materials and glass cannot be used. As these tubes have to be operated at 35 KV 4mA beam current, 140 watts have to be dissipated in the faceplate. The faceplate to bulb frit seal, if not properly cooled, may develop a conductive path through the seal. Breakdown will occur with the corresponding loss of vacuum in the tube. Another difficulty lies in the anode to faceplate contact, because of the nature of the materials required to make a glass to metal seal, and of the 4mA current. Last thing is the graded glass seals needed to accommodate a glass neck whose expansion coefficient is in the 90.10^{-7} range.

All these problems need to find a solution before even a CRT is built. We hence propose the following program.

1. Study of a frit material compatible with the materials of funnel and faceplate.

   Manufacture of full size samples for high temperature high voltage testing.

   This study has to be made in close touch with Trident for the cooling system to be used.

2. Anode contact development

   This will require experimentation of various metal glass seals and of faceplate to anode contact, with temperature testing.

3. When 1 and 2 are complete, start the manufacture of ten (10) bulbs with the final configuration decided.

4. Using part of these 10 bulbs, build first 3 3" YAG faceplate. CRT's seal.

5. Make guns and seal, exhaust and test 3 each, 3" YAG CRT's.

6. Make the same steps than 4 and 5 for the 1.5" YAG red tube.

7. Make the same steps than 4 and 5 for the 3/4" BEL CRT.

Budgetary Costs, Estimated:

1	$ 23,000	8 Weeks
2	13,000	+ 3
3	12,000	(10 X 1200) + 3
4	8,100	(3 X 2700) + 2
5	11,000	+ 3
6	5,000	+ 3
7	4,000	+ 3
	$ 76,100	25 Weeks

Optical Research Associates

550 NORTH ROSEMEAD BOULEVARD
PASADENA, CALIFORNIA 91107
TELEPHONE (818) 795-9101
FAX (818) 795-9102

February 3, 1992

Mr. Tom St. John
TRIDENT INTERNATIONAL, INC
Central Florida Research Park
3280 Progress Drive
Orlando, FL 32826

Subject: Final Report for the Study of the Performance of a YAG Faceplate.

Reference: Trident International, Inc. Purchase Order 9159, Fax Copy Received 11/15/91.

Dear Tom:

Enclosed is the final report on the YAG Faceplate Study. I am still investigating the source coupling efficiency as a function of faceplate index, and will forward any new information that I can find. At this point in time, a majority of our engineers take the position that the phosphor index of refraction is the determining factor, and that if the same phosphor is used for both faceplates, the same brightness will be observed.

If I can confirm the source issue either way, I will contact you. I have enjoyed the opportunity to help in your CRT faceplate development project. If the opportunity comes to develop a new CRT projection lens design, we would be pleased to help. If you have any questions or suggestion, please feel free to contact me.

This completes Optical Research Associates' efforts on the Referenced purchase order.

Sincerely,

OPTICAL RESEARCH ASSOCIATES

Eric H. Ford, Director
of Optical Engineering Services

EHF:cmn:R04:fed ex

cc: B. Reinbolt/SBAO
K. Thompson/ORA

enc: Final Report